

# Emerging quantum computing algorithms for quantum chemistry

Mario Motta<sup>\*</sup> and Julia E. Rice<sup>†</sup>

*IBM Quantum, IBM Research-Almaden, San Jose, CA 95120, USA*

Digital quantum computers provide a computational framework for solving the Schrödinger equation for a variety of many-particle systems. Quantum computing algorithms for the quantum simulation of these systems have recently witnessed remarkable growth, notwithstanding the limitations of existing quantum hardware, especially as a tool for electronic structure computations in molecules. In this review, we provide a self-contained introduction to emerging algorithms for the simulation of Hamiltonian dynamics and eigenstates, with emphasis on their applications to the electronic structure in molecular systems. Theoretical foundations and implementation details of the method are discussed, and their strengths, limitations, and recent advances are presented.

## CONTENTS

I. Introduction	2
II. Computer simulations in chemistry	2
A. Digital quantum computers	4
1. Universality and limitations of digital quantum computers	6
2. Quantum computational complexity	6
III. Some important problems in computational chemistry	7
A. Electronic structure	7
1. Basis sets	8
2. Classical algorithms and open problems	8
B. Electronic dynamics	10
C. Molecular vibrations	10
D. Chemical reactions	11
IV. Quantum algorithms for chemistry	12
A. Mappings to qubits	12
1. Fermions in second quantization	12
2. Bosons in second quantization	14
3. Alternative approaches	14
B. Simulation of Hamiltonian dynamics	15
1. Product formula algorithms	15
2. Quantum walks	16
3. The linear combination of unitary operators: LCU lemma	17
4. LCU based algorithms	18
5. Quantum signal processing and qubitization	19
6. Applications of Hamiltonian dynamics, and open problems	20
C. Simulation of Hamiltonian eigenstates	22
1. Variational quantum algorithms	23
2. The variational quantum eigensolver	23
3. Variational quantum simulation	25
4. Quantum diagonalization algorithms	25
5. Applications of variational algorithms, and open problems	27
V. Error mitigation techniques for near-term quantum devices	27
VI. Conclusion and Outlook	30
Acknowledgment	31
A. Glossary	31
References	31

<sup>\*</sup> corresponding author, e-mail: mario.motta@ibm.com

<sup>†</sup> corresponding author, e-mail: jrice@us.ibm.com

## I. INTRODUCTION

Determining the quantum-mechanical behavior of many interacting particles, by means of accurate and predictive computations, is a problem of conceptual and technological relevance [1]. An important area within the quantum-mechanical many-body problem is represented by molecular chemistry which, over the last few decades, has been addressed using numerical methods, and designed and implemented for a variety of computational platforms [2–4].

More recently, digital quantum computers have been proposed as an alternative and complementary approach to the numerical computation of molecular properties [5–7]. Molecular chemistry has been identified as an application for a digital quantum computer. This is because a digital quantum computer can serve as a quantum simulator [8] of a molecule, i.e. a controllable quantum system that can be used to study certain properties of a molecule. We will focus on Hamiltonian dynamics, in particular, since at the current state of knowledge, it can be simulated with lower scaling on a digital quantum computer than on a conventional computer [5, 6].

The idea of a quantum simulator is conceptually interesting and appealing, and the manufacturing, control and operation of quantum-mechanical devices is one of the most outstanding open problems in physics. On the other hand, a mutual disconnect exists between the quantum chemistry and quantum information science communities, which represents a significant barrier to progress. A shared terminology, a rigorous assessment of the potential impact of quantum computers on practical applications, including a careful identification of areas where quantum technologies can be relevant, and an appreciation of the subtle complications of quantum chemical research, are necessary for quantum information scientists to conduct research in the quantum simulation of chemistry. On the other hand, a robust understanding of quantum information science, quantum computational complexity, quantum simulation algorithms, and of the nature and peculiarities of quantum devices are necessary for chemists to contribute to the design and implementation of algorithms for the quantum simulation of chemistry.

In this work, we aim at bridging the gap between the quantum chemistry and quantum computation communities, by examining prospects for quantum computation in molecular chemistry. We review two important classes of quantum algorithms, one for the simulation of Hamiltonian dynamics and the other for the heuristic simulation of Hamiltonian eigenfunctions. We analyze their advantages and disadvantages, suggesting opportunities for future developments and synergistic research.

We begin by presenting the concept of simulation and its relevance in quantum chemistry in Section II. We then proceed to describe the concept of a digital quantum computer, providing a high level view to help understand how it can be used as a simulator of a quantum system, and focus on strengths and weaknesses of such an approach.

Several important concepts pertaining to the quantum simulation of chemical systems are then presented in Section IV. Emphasis will be placed on the requirements and challenges posed by the adoption of these algorithms in the study of molecular properties.

A discussion about the nature and decoherence phenomena occurring on quantum hardware follows, with the purpose of describing error mitigation and correction techniques for today’s quantum hardware. Such techniques are a requirement for meaningful calculations on the hardware in the near-term.

Conclusions are drawn in the last section, highlighting the need of synergistic investigations by quantum information and quantum chemistry scientists to understand and overcome the subtle complications of research at the interface between these two fields. In this context, we will discuss chemical applications that can be targeted to assess and monitor the performance of quantum algorithms and hardware, and opportunities to work collaboratively to improve their performance towards relevant investigations of chemical systems.

Note that in Table III, the acronyms used throughout this work are listed, together with their explicit meaning.

## II. COMPUTER SIMULATIONS IN CHEMISTRY

Our understanding of the properties of molecular systems often comes from experiments [9, 10]. A prominent class of experiments is represented by spectroscopic investigations, sketched in Fig. 1a. In spectroscopic investigations, electromagnetic radiation is applied to a molecule, and the scattering or absorption of the radiation is measured. These experimental techniques probe different aspects of the structure of molecules by observing their response to applied electromagnetic fields. For example, infrared and visible-ultraviolet radiation are used to probe ro-vibrational and electronic excitations, respectively [11, 12]; nuclear magnetic-resonance spectroscopy to perform *in situ* identification and concentrations for target chemicals in complex mixtures [13]; linear and non-linear optics to probe the polarization of molecules in the presence of external electric fields [9].

Spectroscopic investigations are not the only kinds of experiments performed to understand molecular systems. Another important class of experiments is represented by chemical reaction rate measurements, in which reactants are prepared under suitable experimental conditions, and indicators of chemical compositions, such as electrical conductivity, are measured as a function of time, to reveal the evolution of the amount of reactants in the system [14]. Such

chemical processes can be very complicated to model, because obtaining accurate rate constants involves description of a delicate balance of competing phenomena at the molecular level. These include description of conformers within  $k_B T$  of the lowest energy conformer, effects of solvation, temperature and pressure, to name but a few. Even within the Born-Oppenheimer approximation at zero Kelvin, this results in potentially very large numbers of intermediates, and reaction paths, as in catalytic and metabolic pathways.

Although experiments differ from each other due to a large number of crucially important technical aspects, a recurring theme can be recognized, which is schematically depicted in Fig. 1a and in the first row of Fig. 1b. A chemical sample is prepared in a suitable quantum state, often at thermal equilibrium at a finite inverse temperature  $\beta$ . It is then coupled with an external probe, such as a classical external field, or beam of impinging quantum particles, or a change in a chemical or physical environment, where it evolves under the action of such an external perturbation, and is subsequently measured.

The structure sketched in Fig. 1 is found not only in experiments, but also in the theory of quantum mechanics: an initial preparation is described by wavefunction or density operators in a Hilbert space, the coupling to a probe by a unitary transformation or a more general quantum operation, and a final measurement by a Hermitian operator or a more general operator-valued measure. The same structure informs quantum computations, which can thus be used to simulate the properties of a quantum system. The relationship between the phases of an experiment, the postulates of quantum mechanics, and the structure of a quantum computation provides a useful high-level framework to recognize the purpose and limitations of quantum computation.

One of the goals of computer simulations in chemistry is to explain and predict the outcome of experiments conducted in laboratories. Over the last few decades, molecular electronic structure theory has developed to a stage where computational chemistry practitioners can work alongside experimental collaborators to interpret experimental results and to work as a team to design new molecular systems. Notwithstanding this progress, the electronic structure of molecules and materials still presents many mysterious aspects, and methodological developments towards greater accuracy, predictive power, and access to larger systems are to this day highly investigated research activities.

In the 1980s, the seminal work of several scientists led to the conception of innovative computational devices, now termed digital (or universal) quantum computers [5–7]. At this point, it is worth remarking that the term "classical" refers to conventional (not quantum) computers. It by no means implies that "classical" is a past era, and in fact, as discussed in the remainder of this work, the best of computations will likely be based on a hybrid approach, where classical and quantum co-processors are used in synergy.

In the context of chemistry, digital quantum computers are used as digital quantum simulators [8]. By the term **quantum simulator**, we denote a controllable quantum system used to simulate the behavior of another quantum system. A **digital (or universal) quantum simulator** is a quantum simulator that can be programmed to execute any unitary transformation [8, 15]. The term "simulator" can be a source of confusion. While the quantum computing literature calls a classical computer emulating the behavior of a quantum system a simulator, in quantum information science the term refers to an actual quantum system (e.g. an electric circuit with superconducting elements or an array of ions confined and suspended in free space using electromagnetic fields) used to execute an algorithm and simulate the behavior of another quantum system (e.g. a molecule). We will be using the latter definition in this article.

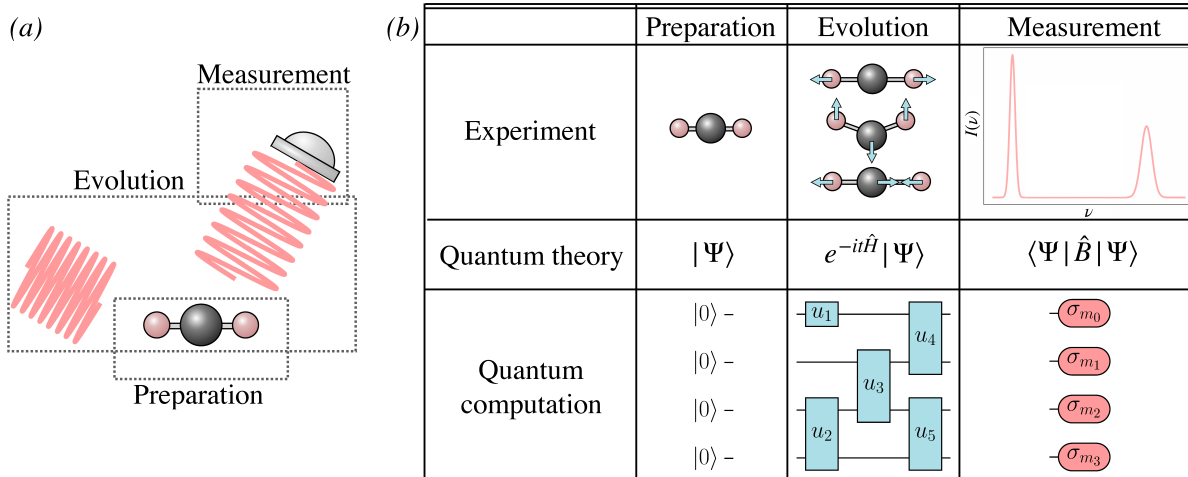


FIG. 1. a) Schematic representation of infrared spectroscopy experiment on the carbon dioxide molecule. b) Analogous phases of both experiment (top row), quantum theory (middle row) and quantum simulations (bottom row).

The basic idea of quantum simulation is represented schematically in Fig. 2. We require that wavefunctions in the Hilbert space of the system under study and the simulator can be connected by a one-to-one correspondence  $\hat{F}$ , as exemplified in Section IV A 1. The simulator can then be initialized in a state  $|\Psi'_i\rangle$ , corresponding to some initial preparation  $|\Psi_i\rangle$  of the system under study. The simulator can be manipulated with some quantum operation, such as a unitary transformation  $\hat{U}'$ , to reach a final state  $|\Psi'_f\rangle$ , corresponding to some state  $|\Psi_f\rangle$  of the system under study. The wavefunction  $|\Psi'_f\rangle$  has to be measured, to extract information about the state  $|\Psi_f\rangle$ .

It is important to emphasize that not all computational problems can be accelerated under a model of computation based on unitary transformations and quantum measurements. Thus one must carefully identify areas where the use of quantum simulators can be of actual relevance. For example, the assumption of controllability of the digital quantum simulators is crucial for the actual use of these devices to solve a computational problem. This issue will be reviewed in Section V, where the nature and decoherence phenomena occurring on near-term quantum hardware is discussed, and techniques for error mitigation and correction are presented. The main factors affecting the performance of quantum hardware are (i) the limited numbers of qubits that can be used for any one chemical problem, (ii) the limited qubit connectivity, and (iii) the various decoherence phenomena that limit the number of quantum operations that can be executed.

Similarly, the importance of preparation, transformation and measurement steps must be stressed here, because the success of a quantum simulation depends on the ability to perform certain operations efficiently on the quantum simulator, as well as to extract useful information from it. The inherent difficulty of computational problems is typically formalized in terms of the resources required by different models of computation to solve a given problem. For digital quantum computers, such a formalization is achieved by the theory of quantum computational complexity, reviewed in Section II A 2, which identifies the class of problems that are naturally tackled by a digital quantum simulator. This in turn requires introducing the model of a digital quantum computer and of the operations that can be performed on it, which is the goal of the next Section.

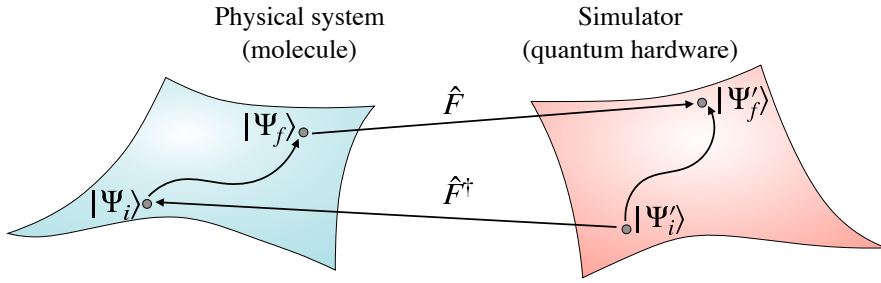


FIG. 2. Schematic representation of a quantum simulator. A one-to-one correspondence  $\hat{F}$  connects states and operations of a physical system (left, light blue manifold) with states and operations of a controllable quantum system (right, light red manifold) that serves as a simulator for the behavior of the physical system of interest.

### A. Digital quantum computers

The concept of a quantum computer can be represented by several equivalent models, each corresponding to a specific approach to the problem of executing computation on a device based on quantum mechanics. Such models include quantum Turing machines, circuits, random access machines and walks. In this work, we focus on what is arguably the most widely used model of quantum computation, the circuit model. It is worth emphasizing that the only educational platforms giving a robust understanding of quantum computation are dedicated textbooks covering the topic in depth and breadth. Interested readers are thus referred, for example, to the books by Nielsen and Chuang [16], Mermin [17], Kitaev et al [18], Benenti et al [19] and Popescu et al [20].

The circuit model of quantum computation is based on the notion of **qubit**. A qubit is a physical system whose states are described by unit vectors in a two-dimensional Hilbert space  $\mathcal{H} \simeq \mathbb{C}^2$ . A system of  $n$  qubits, also called an  $n$ -qubit **register**, has states described by unit vectors in the Hilbert space  $\mathcal{H}_n = \mathcal{H}^{\otimes n}$ . An orthonormal basis of the Hilbert space  $\mathcal{H}_n$  is given by the following vectors, called **computational basis states**,

$$|\mathbf{z}\rangle = \bigotimes_{\ell=0}^{n-1} |z_\ell\rangle = |z_{n-1} \dots z_0\rangle = |z\rangle \quad , \quad \mathbf{z} \in \{0,1\}^n \quad , \quad z = \sum_{\ell=0}^{n-1} z_\ell 2^\ell \in \{0 \dots 2^n - 1\} \quad . \quad (1)$$

Starting from a register of  $n$  qubits prepared in the state  $|0\rangle \in \mathcal{H}_n$ , a generic  $n$ -qubit state  $|\psi\rangle$  can be prepared applying single- and multi-qubit unitary transformations, or **gates**. Examples of single-qubit and two-qubit gates are

listed in Table I. In quantum computation, a role of particular importance is played by **Pauli operators**, defined as

$$\hat{\sigma}_{\mathbf{m}} = \hat{\sigma}_{m_{n-1}} \otimes \cdots \otimes \hat{\sigma}_{m_0} , \quad \hat{\sigma}_m \in \{\mathbb{1}, X, Y, Z\} , \quad (2)$$

where the single-qubit Pauli operators are illustrated in Table I.

Pauli operators are a basis for the space of linear operators on  $\mathcal{H}_n$ . Exponentials of Pauli operators can be represented as tensor products of  $Z$  operators,

$$\hat{R}_{\hat{\sigma}_{\mathbf{m}}}(\theta) = e^{-\frac{i\theta}{2}\hat{\sigma}_{\mathbf{m}}} = \hat{V}^\dagger e^{-\frac{i\theta}{2}Z \otimes \cdots \otimes Z} \hat{V} , \quad \hat{V} = \bigotimes_{\ell=0}^{n-1} \hat{A}_{m_\ell} , \quad \hat{A}_m^\dagger \hat{\sigma}_m \hat{A}_m = Z , \quad (3)$$

and then applied to a register of qubits as illustrated in Fig. 3a. Such a circuit contains ladders of CNOT gates that compute the total parity into the last qubit [21].

Two parameters, respectively called **width** and **depth**, are often used to characterize the cost of a quantum circuit. Width refers to the number of qubits that comprise the circuit (in Fig. 3a, width = 4). Depth refers to the number of layers of gates that cannot be executed at the same time (in Fig. 3a, depth = 9). Although width and depth are both limiting factors in the execution of quantum algorithms (large width corresponds to many qubits, and large depth to many operations in presence of decoherence), the latter is a major computational bottleneck on near-term devices. The error mitigation techniques presented in Section II are used to increase the width and depth of circuits that can be executed on near-term hardware.

Furthermore, Pauli operators are Hermitian, and thus can be measured. Since

$$\hat{\sigma}_{\mathbf{m}} = \hat{V}^\dagger (Z \otimes \cdots \otimes Z) \hat{V} = \sum_{\mathbf{z}} f(\mathbf{z}) \hat{V}^\dagger |\mathbf{z}\rangle \langle \mathbf{z}| \hat{V} , \quad f(\mathbf{z}) = \prod_{\ell=0}^{n-1} (-1)^{z_\ell} , \quad (4)$$

preparing a register of qubits in a state  $|\Psi\rangle$ , applying the transformation  $\hat{V}$  and measuring all qubits in the computational basis as shown in Fig. 3b yields a collection of samples, or "shots",  $\{\mathbf{z}_i\}_{i=1}^{n_s}$ , from which the expectation value  $\langle\Psi|\hat{\sigma}_{\mathbf{m}}|\Psi\rangle$  can be estimated as  $\mu \pm \sigma$  with  $\mu = n_s^{-1} \sum_i f(\mathbf{z}_i)$  and  $\sigma^2 = n_s^{-1} (1 - \mu^2)$ .

The presence of statistical uncertainties on measurement results is a basic but centrally important aspect of quantum computation: quantum algorithms must be understood and formulated in terms of random variables and stochastic

name	symbol	matrix	name	symbol	matrix	name	symbol	matrix
X rotation		$\begin{bmatrix} \cos(\theta) & -i\sin(\theta) \\ -i\sin(\theta) & \cos(\theta) \end{bmatrix}$	Y rotation		$\begin{bmatrix} \cos(\theta) & -\sin(\theta) \\ \sin(\theta) & \cos(\theta) \end{bmatrix}$	Z rotation		$\begin{bmatrix} e^{-i\theta} & 0 \\ 0 & e^{i\theta} \end{bmatrix}$
Pauli X		$\begin{bmatrix} 0 & 1 \\ 1 & 0 \end{bmatrix}$	Pauli Y		$\begin{bmatrix} 0 & -i \\ i & 0 \end{bmatrix}$	Pauli Z		$\begin{bmatrix} 1 & 0 \\ 0 & -1 \end{bmatrix}$
Hadamard		$\frac{1}{\sqrt{2}} \begin{bmatrix} 1 & 1 \\ 1 & -1 \end{bmatrix}$	S gate		$\begin{bmatrix} 1 & 0 \\ 0 & i \end{bmatrix}$	T gate		$\begin{bmatrix} 1 & 0 \\ 0 & e^{i\pi/4} \end{bmatrix}$
Z measurement		$p(z) =  \langle z \Psi\rangle ^2$	general measurement		$p(k) =  \langle \varphi_k \Psi\rangle ^2$	post-selection		$k = k_0$
CNOT		$\begin{bmatrix} 1 & 0 & 0 & 0 \\ 0 & 0 & 0 & 1 \\ 0 & 0 & 1 & 0 \\ 0 & 1 & 0 & 0 \end{bmatrix}$	controlled- $U$		$\begin{bmatrix} 1 & 0 & 0 & 0 \\ 0 & u_{00} & 0 & u_{10} \\ 0 & 0 & 1 & 0 \\ 0 & u_{10} & 0 & u_{11} \end{bmatrix}$	SWAP		$\begin{bmatrix} 1 & 0 & 0 & 0 \\ 0 & 0 & 1 & 0 \\ 0 & 1 & 0 & 0 \\ 0 & 0 & 0 & 1 \end{bmatrix}$

TABLE I. Examples of quantum gates and circuit elements. From top to bottom: single-qubit rotations (i.e. exponentials of single-qubit Pauli operators), for example  $R_x(\theta) = \exp(-i\theta X/2)$ . Single-qubit Pauli operators, which are equal to special single-qubit Pauli rotations up to a global phase, for example  $X = R_x(\pi/2)$ . Single-qubit operations in the Clifford group (Hadamard,  $S$  and  $T$  gates), which are equal to special single-qubit Pauli rotations up to a global phase, namely  $S = R_z(\pi/2)$ ,  $T = R_z(\pi/4)$  and  $H = \exp(-i\pi/2(X + Z))$ . Measurement of a single qubit in the computational basis, measurement of an observable  $B = \sum_k b_k |\varphi_k\rangle \langle \varphi_k|$ , and measurement of an observable with post-selection (retaining only one specific outcome  $k_0$ ). Two-qubit CNOT (controlled- $X$ ), cU (controlled- $U$ ) and SWAP gates. The CNOT gate is sometimes denoted  $\text{CNOT}_{ij}$ , where  $i$  and  $j$  are called the control and target qubit respectively, and applies an  $X$  transformation to its target qubit ( $\oplus$  symbol) if its control qubit ( $\bullet$  symbol) is in the state  $|1\rangle$ , the cU can be written as a product of up to two CNOT gates and four single-qubit gates, and the SWAP gate can be written as a product of three CNOT gates,  $\text{SWAP}_{ij} = \text{CNOT}_{ij} \text{CNOT}_{ji} \text{CNOT}_{ij}$ . Qubits are ordered from top to bottom, and matrix elements are defined as  $G_{zw} = \langle z|\hat{G}|w\rangle = \langle z_{n-1} \dots z_0 | \hat{G} | w_{n-1} \dots w_0 \rangle$ , with binary digits running from right to left as in Eq. (1).

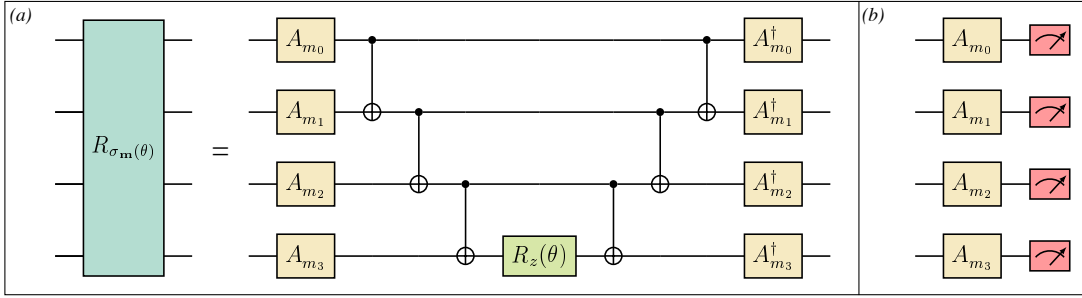


FIG. 3. Quantum circuits (a) to apply the exponential of a Pauli operator  $\otimes_{\ell=0}^3 \sigma_{m_\ell}$  and (b) to measure its expectation value. The single-qubit gates are  $A_X = H$ ,  $A_Y = HS$  and  $A_Z = I$ .

calculus, and their results accompanied with carefully estimated statistical uncertainties. These aspects cannot be overlooked in the design and implementation of quantum algorithms.

In the remainder of this work, we will call measurements and unitary transformations executed on a digital quantum computer **operations**, and use the term **gates** to denote unitary transformations only.

In this section, we provided a very concise presentation of the concepts of qubit, quantum gates and measurements, with the purpose of fixing notation and maintaining the remainder of the work self-contained. In the coming sections, we will show that suitable sets of single- and two-qubit gates are universal, i.e. they can be multiplied to yield a generic unitary transformation, and present strengths and limitations of quantum computation in the light of quantum complexity theory.

### 1. Universality and limitations of digital quantum computers

Informally, a set  $\mathcal{S}$  of quantum gates is called **universal** if any unitary transformation that can be applied on a quantum computer can be expressed as a product of a finite number of gates from  $\mathcal{S}$ . Any multi-qubit gate can be expressed as a product of single-qubit and CNOT operations only, and therefore  $\mathcal{S}_1 = \{\text{single-qubit gates, CNOT}\}$  is a universal set of quantum gates.

Since single-qubit operations have continuous parameters (corresponding to rotation angles), the set  $\mathcal{S}_1$  is not countable. However, it is known that the set  $G$  of single-qubit gates generated by  $\{\text{Had, S, T}\}$  is dense in  $SU(2)$  [16]. According to the Solovay-Kitaev theorem [16, 18, 22–24], for any  $\hat{U} \in SU(2)$  and any target accuracy  $\varepsilon$  there exists a sequence of  $\mathcal{O}(\log^c(1/\varepsilon))$  gates from the generating set of  $G$  that approximates  $\hat{U}$  within accuracy  $\varepsilon$  and  $c \simeq 4$ . Subsequent work has demonstrated [25, 26] that  $z$  rotations and generic single-qubit gates can be implemented with no more than  $3 \log(1/\varepsilon)$  and  $9 \log(1/\varepsilon)$  T and H gates respectively, which is asymptotically optimal, with a practical algorithm. Therefore, the countable set  $\mathcal{S}_2 = \{\text{Had, S, T, CNOT}\}$  is a universal set of quantum gates.

It should be noted, however, that a generic  $n$ -qubit unitary transformation is exactly represented with  $\mathcal{O}(4^n)$  single-qubit and CNOT gates [27–29], meaning that quantum computers are not guaranteed to give access to a generic  $n$ -qubit state with an amount of operations scaling polynomially with  $n$ . Furthermore, finding an **efficient** decomposition of a unitary transformation in terms of elementary quantum operations can itself be a challenging task [30].

Finally, the set  $\mathcal{C} = \{\text{Had, S, CNOT}\}$  generates the so-called **Clifford group** of unitary transformations, that map Pauli operators onto Pauli operators. An important theoretical result, the Gottesman-Knill theorem [31–33], states that quantum circuits using only (a) preparation of qubits in computational basis states, (b) application quantum gates from the Clifford group and (c) measurement of a single Pauli operator, can be efficiently simulated on a classical computer. Therefore, the entanglement that can be achieved with circuits of Clifford gates alone does not give any computational advantage over classical computers. Computational advantage is to be sought in circuits also containing  $T$  gates.

### 2. Quantum computational complexity

Solving a problem on a computational platform requires designing an algorithm, by which term we mean the application of a sequence of mathematical steps. Executing an algorithm requires a certain amount of resources, typically understood in terms of space (or memory) and time (or elementary operations). Computational complexity theory groups computational problems in complexity classes defined by their resource usage, and relates these classes

to each other. Quantum computational complexity theory is a branch of computational complexity theory that, loosely speaking, studies the difficulty of solving computational problems on quantum computers, formulates quantum complexity classes, and relates such quantum complexity classes with their classical counterparts [18, 34, 35]. Two important quantum complexity classes are BQP (bounded-error quantum polynomial time) and QMA (quantum Merlin-Arthur). Roughly speaking, BQP comprises problems that can be solved with polynomial space and time resources on a quantum computer. In the context of quantum simulation for quantum chemistry, the most important BQP problem is the simulation of **Hamiltonian dynamics** [5, 6, 36, 37]. QMA, on the other hand, comprises problems where putative solutions can be verified but not computed in polynomial time on a quantum computer. Producing a putative solution means executing a quantum circuit giving access to a wavefunction  $\Psi$ , and verifying a putative solution means executing a second quantum circuit to ensure that  $\Psi$  is actually a solution of the problem of interest. In the context of quantum simulation for quantum chemistry, the most important QMA problem is the simulation of **Hamiltonian eigenstates**, as discussed for example in [18, 38].

Current knowledge indicates that both the ground-state and the Hamiltonian dynamics problems are, in a worst-case scenario, exponentially expensive on a classical computer. The Hamiltonian dynamics problem is thus a relevant application for quantum algorithms, as it offers theoretical opportunities for better computational performance when tackled on a quantum computer. However, there are a number of practical considerations to take into account. For example, the statements of computational complexity theory refer to exact solutions of the problem at hand, and experience indicates that approximate methods can deliver accurate results for certain problems, which calls for a systematic characterization of quantum algorithms for chemistry in both accuracy and computational cost across a variety of chemical problems. Furthermore, quantum hardware has to reach a level of control and predictability compatible with large-scale quantum chemical simulations, which is one of the most important challenges confronting experimental physics and engineering.

The division between BQP and QMA problems will inform the remainder of the present work: in the next Section we will present some important problems in computational chemistry, highlighting those based on the simulation of Hamiltonian dynamics. We will then present quantum algorithms for the simulation of Hamiltonian dynamics, and heuristic algorithms for Hamiltonian eigenstate approximation.

### III. SOME IMPORTANT PROBLEMS IN COMPUTATIONAL CHEMISTRY

In this Section, we briefly review some problems studied in computational chemistry. While their extensive description is beyond the scope of the present review, we will attempt to highlight some technical challenges, through the lens of which the quantum algorithms presented in the forthcoming sections can be examined.

#### A. Electronic structure

The main objective of electronic structure in chemistry is to determine the ground and low-lying excited states of a system of interacting electrons. Often relativistic effects and the coupling between the dynamics of electrons and nuclei can be neglected, or treated separately. Within this approximation, the many-electron wavefunction can be found by solving the time-independent Schrödinger equation for the Born-Oppenheimer Hamiltonian [39, 40]

$$\hat{H}\Psi = \left[ \sum_{a < b}^{N_n} \frac{Z_a Z_b}{|\mathbf{R}_a - \mathbf{R}_b|} \right] \Psi - \frac{1}{2} \sum_{i=1}^N \frac{\partial^2 \Psi}{\partial \mathbf{r}_i^2} - \left[ \sum_{i=1}^N \sum_{a=1}^{N_n} \frac{Z_a}{|\mathbf{r}_i - \mathbf{R}_a|} \right] \Psi + \left[ \sum_{i < j}^N \frac{1}{|\mathbf{r}_i - \mathbf{r}_j|} \right] \Psi, \quad (5)$$

where  $\mathbf{r}_i$  is the position of electron  $i$ , and  $\mathbf{R}_a$  the position of nucleus  $a$ , having atomic number  $Z_a$ . The numbers of electrons and nuclei are  $N$  and  $N_n$ , respectively, nuclear positions are held fixed, and atomic units are used throughout.

Solving the time-independent Schrödinger equation is needed to access molecular properties including, and not limited to, energy differences (e.g. ionization potentials, electron affinities, singlet-triplet gaps, binding energies, deprotonation energies), energy gradients (e.g. forces and frequency-independent polarizabilities) and electrostatic properties (e.g. multipole moments and molecular electrostatic potentials).

The first step of any electronic structure simulation is to approximate Eq. (5) with a simpler Hamiltonian acting on a finite-dimensional Hilbert space. This is usually achieved by truncating the Hilbert space of a single electron to a finite set of orthonormal basis functions or spin-orbitals  $\{\varphi_p\}_{p=1}^M$ . Electronic structure simulations based on the first quantization formalism describe a system of  $N$  electrons in  $M$  spin-orbitals using the configuration interaction (CI)

representation

$$|\Psi\rangle = \sum_{i_1 < \dots < i_N}^M \psi_{i_1 \dots i_N} |i_1 \dots i_N\rangle , \quad (6)$$

where  $|i_1 \dots i_N\rangle$  is the Slater determinant where orbitals  $i_1 \dots i_N$  are occupied.

Electronic structure simulations based on the second quantization formalism, on the other hand, operate in the Fock space of electrons in  $M$  spin-orbitals, and represent the Hamiltonian as

$$\hat{H} = \sum_{a < b}^{N_n} \frac{Z_a Z_b}{|\mathbf{R}_a - \mathbf{R}_b|} + \sum_{pr} h_{pr} \hat{a}_p^\dagger \hat{a}_r + \sum_{prqs} \frac{(pr|qs)}{2} \hat{a}_p^\dagger \hat{a}_q^\dagger \hat{a}_s \hat{a}_r , \quad (7)$$

where  $\hat{a}_p^\dagger, \hat{a}_r$  are fermionic creation and annihilation operators associated to spin-orbitals  $\varphi_p, \varphi_r$  respectively.

### 1. Basis sets

Choosing a finite set of spin-orbitals  $\{\varphi_p\}_{p=1}^M$  balances two concerns: the need of representing electronic states and operators with as few orbitals as possible, and the need for obtaining accurate results. Gaussian bases are most commonly employed in molecular simulations due to their compactness, while plane waves are most often used in the simulation of crystalline solids. In order to get quantitatively accurate results, very large one-electron basis sets have to be used, in either case.

Since, as we shall see, the number  $M$  of orbitals translates into the number of qubits needed to perform a simulation (see Section IV A 1) and near-term hardware is limited in the number and quality of qubits (see Section V), most quantum computing simulations so far have been limited to  $M \simeq 10$  orbitals. Theoretical and computational chemists can help the field of quantum computation by integrating techniques (e.g. optimized orbitals [41], perturbative treatments [42], explicit electronic correlation [43]) to account for more orbitals without extra qubits and gates.

Furthermore, most quantum algorithms have so far been tested and characterized using sets of  $M \simeq 10$  orbitals (corresponding to small active spaces or minimal bases). While the results of such investigations have often indicated high accuracy when compared to classical methods with the same basis sets, it is in many cases uncertain whether known algorithms are useful when larger bases are used. Thus, another area of research where theoretical and computational chemists can offer insight and help is the systematic extension and benchmark of quantum algorithms beyond the small basis sets investigated so far.

### 2. Classical algorithms and open problems

The main obstacle to the investigation of electronic structure is that, in general, the computational cost of finding the exact eigenfunctions of Eq. (5) grows combinatorially with the size of the studied system [44, 45]. This limitation has so far precluded exact studies for all but the smallest systems and motivated the development of approximate methods. At a high level, those methods can be distinguished by general categories such as wavefunction, embedding, and diagrammatic (or Green's function).

*a. Wavefunction methods* formulate an Ansatz for an eigenstate, e.g. the ground state, and compute expectation values of observables and correlation functions with respect to that wavefunction. The nature of the underlying Ansatz is ultimately responsible for the accuracy and computational cost of a given method. For molecular systems, a hierarchy of quantum chemistry methods has been developed, which allow systematic improvement in accuracy, at increasing computational cost. These techniques typically have their starting point in the Hartree-Fock (HF) method, which approximates the ground state of a molecular Hamiltonian with the lowest-energy Slater determinant, and incorporate electronic correlation. For example, one of the most accurate methods is coupled-cluster with singles and doubles and perturbative estimate to the connected triples, CCSD(T) [2, 46, 47]. Other promising alternative approaches include tensor network methods [48–52], which represent electronic wavefunctions as contractions between tensors, and quantum Monte Carlo methods [53–59], which instead represent electronic properties as expectation values of carefully designed random variables.

*b. Density functional (DFT) methods* The most widely used methods are mean field in nature and are based on the density [60, 61], making them less expensive than wavefunction methods. DFT methods are based on an approximation to the Hamiltonian rather than an approximation to the wavefunction and there is no hierarchy of functionals as there is in wavefunction methods [62]. Nevertheless, density functional methods are standard tools for electronic structure calculations in many areas across multiple disciplines, with sophisticated computer software packages available due to their significantly lower cost.

c. *Embedding methods* evaluate the properties of a large system by partitioning it within a given basis (e.g. the spatial or energy basis) into a collection of fragments, embedded in a self-consistently determined environment [63–67]. These methods combine two different types of quantum calculations: high-level calculations on fragments, and low-level calculations on the environment surrounding fragments. The accuracy of an embedding method is determined by a combination of several factors including: the size of the fragments, the accuracy in the treatment of the embedded fragments and environment, and the convergence of the self-consistency feedback loops between fragments and their environment.

d. *Diagrammatic methods* evaluate, either deterministically or stochastically, a subset of the terms in the diagrammatic interaction expansion [68–73] of a quantity such as the Green's function, the self-energy, or the ground-state energy. These methods are often based on the Feynman diagrammatic technique formulated in terms of self-consistent propagators and bare or renormalized interactions, at finite or zero temperature, and their accuracy and computational cost is determined by several factors, including the subsets of diagrams or series terms that are included in the calculation.

These methodologies tend to be most accurate for problems where a single electronic configuration dominates the representation Eq. (6) of the ground-state wavefunction, the so-called single-reference problems, exemplified by the ground states of many simple molecules at equilibrium. In many molecular excited states, along bond stretching, and in transition metal systems, multiple electronic configurations contribute to the ground-state wavefunction, as illustrated in Fig. (4)a, leading to multi-reference quantum chemistry problems.

Despite remarkable progress in the extension of quantum chemistry methods to multi-reference situations, the accuracy attainable for molecules with more than a few atoms is considerably lower than in the single-reference case. Some important examples of multi-reference quantum chemical problems are sketched in Fig. (4)b. Transition metal atoms, oxides, and dimers pose formidable challenges to even remarkably accurate many-body methods, as they feature multiple bonds, each with a weak binding energy, and potential energy surfaces resulting from the interplay between **static and dynamical** electronic correlation [74–79]. Full configuration interaction (FCI) methods can describe such an interplay but systems that can be studied with FCI methods are arguably small [80, 81]. Coupled binuclear copper centers are present in the active sites of some very common metalloenzymes found in living organisms. The correct theoretical description of the interconversion between the two dominant structural isomers of the  $\text{Cu}_2\text{O}_2^{2+}$  core is key to the ability of these metalloenzymes to reversibly bind to molecular oxygen, and is challenging since it also requires a method that can provide a balanced description of static and dynamic electronic correlations [82–85].

The chemistry of other active sites, such as the  $\text{Mn}_3\text{CaO}_4$  cubane core of the oxygen-evolving complex of photosystem II, and the  $\text{Fe}_7\text{MoS}_9$  cofactor of nitrogenase, pose some of the most intricate multi-reference problems in the field of biochemistry. In particular with respect to their spectroscopic properties, such systems require a detailed characterization of the interplay between spin-coupling and electron delocalization between metal centers. [86–91].

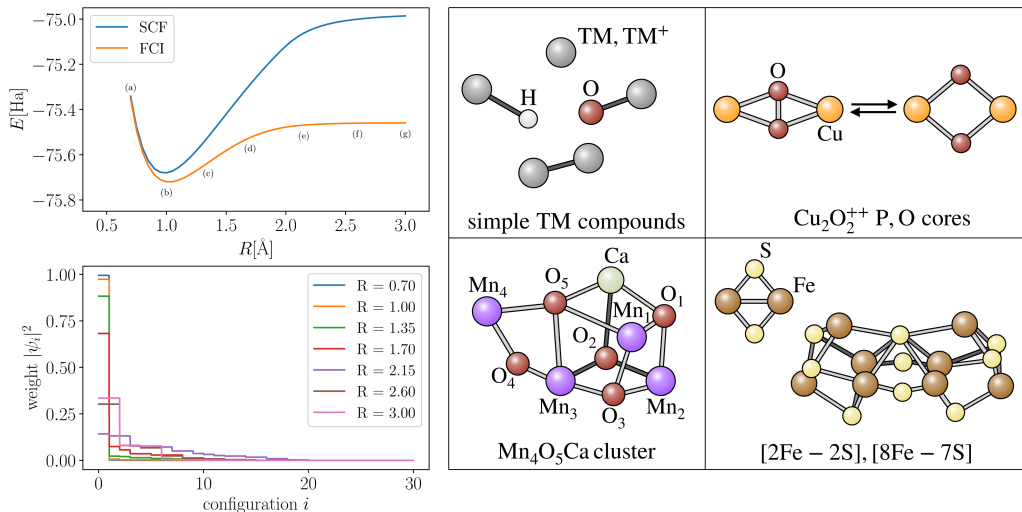


FIG. 4. Left: example of multi-reference character in the dissociation of  $\text{H}_2\text{O}$ . Right: transition metal (TM) compounds of relevance for fundamental chemistry and quantum computing research: TM atoms, ions, hydrides and oxides can constitute subjects of study for near-term quantum devices. Longer-term goals are the description of  $\text{CuO}$ ,  $\text{MnO}$  and  $\text{FeS}$  cores found in a variety of biological catalysts.

## B. Electronic dynamics

Many experiments conducted on molecules probe their dynamical, rather than equilibrium, properties. An important example are oscillator strengths

$$D_{0 \rightarrow f} \propto (E_f - E_0) \sum_{\alpha=x,y,z} |\langle \Psi_f | \hat{\mu}_\alpha | \Psi_0 \rangle|^2 , \quad (8)$$

where  $\Psi_0$  and  $\Psi_f$  are a ground and excited state of the electronic Hamiltonian, with energies  $E_0$  and  $E_f$  respectively, and  $\hat{\mu}_\alpha$  is the dipole moment along direction  $\alpha = x, y, z$ . Oscillator strengths exemplify properties, such as structure factors [92, 93], that are determined by excited electronic states through transition energies and matrix elements. A variety of algorithmic tools are available for the calculation of spectral functions and time-dependent properties on classical computers today, including time-dependent density functional theory, equation-of-motion coupled-cluster and diagrammatic theories [94, 95]. In some regimes (e.g. transitions to specific and structured excited states) dynamical properties such as oscillator strengths can be computed efficiently and accurately. On the other hand, there are computationally challenging regimes, where quantum algorithms can be relevant (e.g. congested spectra) owing to its ability to simulate time evolution.

In fact, oscillator strengths are straightforwardly obtained from dipole-dipole **structure factors**

$$S_{\mu_\alpha, \mu_\beta}(\omega) = \sum_l \langle \Psi_0 | \hat{\mu}_\alpha | \Psi_l \rangle \delta(\hbar\omega - (E_l - E_0)) \langle \Psi_l | \hat{\mu}_\beta | \Psi_0 \rangle , \quad (9)$$

as  $D_{0 \rightarrow f} = \sum_\alpha S_{\mu_\alpha, \mu_\alpha}(E_f - E_0)$ . Dipole-dipole structure factors are in turn the Fourier transform of the time-dependent dipole-dipole **correlation functions**,

$$C_{\mu_\alpha, \mu_\beta}(t) = \langle \Psi_0 | \hat{\mu}_\alpha e^{\frac{t}{i\hbar}(\hat{H}-E_0)} \hat{\mu}_\beta | \Psi_0 \rangle = \sum_f \langle \Psi_0 | \hat{\mu}_\alpha | \Psi_f \rangle e^{\frac{t}{i\hbar}(E_f - E_0)} \langle \Psi_f | \hat{\mu}_\beta | \Psi_0 \rangle , \quad (10)$$

and can be computed by simulating time evolution.

Another important and related research theme is the computation of **time- and frequency-dependent properties** (e.g. non-linear optical properties, electro-optical effects, circular dichroism). Similar to oscillator strengths, these properties are challenging to compute as they involve excited states, and are natural applications for quantum algorithms, as they can be computed by simulating time evolution.

Consider a system at equilibrium in the ground state  $\Psi_0$  of  $\hat{H}_S$  at time  $t = 0$ , and subject to a perturbation of the form  $\hat{V}(t) = \sum_k f_k(t) \hat{O}_k^\dagger$ . The expectation value of the operator  $\hat{O}_j$  at time  $t > 0$  is given by

$$O_j(t) = \langle \Psi(t) | \hat{O}_{j,S}(t) | \Psi(t) \rangle , \quad |\Psi(t)\rangle = \hat{U}(t) |\Psi_0\rangle , \quad \hat{U}(t) = \sum_{n=0}^{\infty} \int_0^t \frac{dt_1}{i\hbar} \dots \int_0^{t_{n-1}} \frac{dt_n}{i\hbar} \hat{V}_S(t_1) \dots \hat{V}_S(t_n) , \quad (11)$$

where  $\hat{V}_S(t) = e^{-\frac{t\hat{H}_S}{i\hbar}} \hat{V} e^{\frac{t\hat{H}_S}{i\hbar}}$ . The linear response approximation [96], valid for weak external perturbations, consists of truncating  $\hat{U}(t)$  and  $O_j(t)$  to first order in  $\hat{V}(t)$ , leading to the expression

$$O_j(t) = O_j(0) + \int_0^t \frac{dt'}{i\hbar} \sum_k f_k(t') \alpha_{jk}(t-t') , \quad \alpha_{jk}(t) = \langle \Psi_0 | [\hat{O}_{j,S}(t), \hat{O}_k^\dagger] | \Psi_0 \rangle , \quad (12)$$

where  $\alpha_{jk}(t)$  is the time-dependent polarizability of  $\hat{O}_j, \hat{O}_k$ .

Real-time correlation functions such as (10) and (12) are objects of central importance in many-particle physics, but naturally emerge in the framework of linear response theory, i.e. of weak external perturbation. Going beyond spectral properties, and probing the non-equilibrium real-time dynamics of chemical systems, is a research topic of increasing relevance, both because of experiments that can now probe quantum dynamics at atomic scales, and because of fundamental interest in studying the time-dependent behavior of many-particle systems.

## C. Molecular vibrations

The geometric structure of molecules is typically probed by gas-phase spectroscopic experiments, whose interpretation, for all but the smallest molecules, needs input from numerical simulations, due to many competing transitions

between states [97–99]. Numerical simulations of molecular rovibrational levels require solving the Schrödinger equation for the nuclei. Within the Born-Oppenheimer approximation, the nuclear Hamiltonian has the form

$$\hat{H}_{nuc} = -\frac{1}{2} \sum_{a=1}^{N_n} \frac{1}{M_a} \frac{\partial^2}{\partial \mathbf{R}_a^2} + V(\mathbf{R}_1 \dots \mathbf{R}_{N_n}), \quad (13)$$

where  $V$  denotes the ground-state potential energy surface of the electronic Hamiltonian Eq. (5) when nuclei have positions  $\{\mathbf{R}_a\}_{a=1}^{N_n}$ , and  $\{M_a\}_{a=1}^{N_n}$  are the nuclear masses, in atomic units. Solving the nuclear Schrödinger equation presents additional challenges: first of all, as the interaction among nuclei is mediated by electrons, the function  $V$  is not known a priori, and needs to be computed from quantum chemical calculations at fixed nuclear geometries as in Section III A, and then fitted to an appropriate functional form, which can be an expensive procedure [100, 101]. For certain problems, the harmonic oscillator approximation of  $V$  is appropriate, which is given by [100]

$$\hat{H}_{nuc} = \frac{1}{2} \sum_{\alpha\beta} (\hat{J}_\alpha - \hat{\pi}_\alpha) \mu_{\alpha\beta} (\hat{J}_\beta - \hat{\pi}_\beta) - \frac{1}{2} \sum_k \frac{\partial^2}{\partial Q_k^2} - \frac{1}{8} \sum_\alpha \mu_{\alpha\alpha} + V(\mathbf{Q}) \quad , \quad V(\mathbf{Q}) = \frac{\kappa}{2} \mathbf{Q}^2 . \quad (14)$$

In Eq. (14)  $\hat{J}_\alpha$  is the total angular momentum of a given cardinal direction ( $x$ ,  $y$ , or  $z$ ) denoted by  $\alpha$  or  $\beta$ ;  $\hat{\pi}_\alpha$  is the total vibrational angular momentum of the same direction;  $\mu_{\alpha\beta}$   $\mu_{\alpha\alpha}$  is the inverse of the moment of inertia tensor for the given geometric coordinate;  $Q_k$  is a single normal coordinate, and  $\mathbf{Q}$  is the set of all normal coordinates; and  $\kappa$  is a numerically determined spring constant.

Notwithstanding its simplicity (and usefulness in situations such as correction of binding energies for zero-point nuclear motion), the harmonic approximation Eq. (14) has several limitations. As a result of equal spacing of energy levels for a given normal mode, all transitions occur at the same frequency, and bond dissociation is not described. Improving over the harmonic approximation requires retaining higher-order or anharmonic terms in  $V$ , which poses additional challenges, especially a proper choice of curvilinear nuclear coordinates, and developing accurate solvers for the nuclear Schrödinger equation [100–105].

Computing solutions of the nuclear Schrödinger equation has many valuable applications, notably supporting the study of chemical processes occurring in atmospheric chemistry, and the identification of molecules in the interstellar medium and circumstellar envelopes [100, 101, 106–111].

#### D. Chemical reactions

Understanding the microscopic mechanisms underlying chemical reactions is another problem of central importance in chemistry. A particularly important goal is to calculate thermochemical quantities, such as reactant-product enthalpy and free energy differences, and activation energies.

A somewhat common misconception in the quantum computation community stems from the incorrect interpretation and use of the term "chemical accuracy". As the Arrhenius equation postulated that temperature dependence of the reaction rate constants is contained in an exponential factor of the form  $\exp(-\beta E_a)$ , where  $E_a$  is the activation energy, computed reaction rates differ by their experimental values by an order of magnitude at room temperature,  $\beta^{-1} \simeq 0.5922$  kcal/mol, when the energy difference  $E_a$  is biased by  $\Delta E \simeq 1.36$  kcal/mol. In the light of these considerations, the accuracy required to make realistic thermochemical predictions, called **chemical accuracy**, is generally considered to be 1 kcal/mol [112]. The term chemical accuracy refers to agreement between computed and experimental energy differences within 1 kcal/mol. Part of the quantum computing literature has used the term chemical accuracy to indicate agreement between computed and exact (i.e. FCI) total energies in a fixed basis set to within 1 kcal/mol, which we argue should instead be called **algorithmic accuracy**.

Determining the main features of the potential energy surface, i.e. the electronic energy as a function of nuclear positions, its minima and saddle points, is key to understanding chemical reactivity, product distributions, and reaction rates. On the other hand, several other factors affect chemical reactions. Potential energy surfaces are shaped by the presence and properties of solvents: indeed, it is known that solvents have the ability to modify the electron density, stabilizing transition states and intermediates and lowering activation barriers, e.g. [113, 114].

The systematic incorporation of **solvation effects**, within a hierarchy of implicit [115, 116], hybrid QM/MM where the solvent is treated with a force field (MM) [117, 118], and other multi-scale methods including embedding methods QM(active)/QM(surrounding) where the QM(active) refers to treatment of the most relevant part of the system with higher level quantum mechanics and QM(surrounding) refers to treatment of the surrounding by a lower level of quantum mechanics [115–118], is thus necessary to improve the description of chemical systems beyond gas-phase properties, and is especially important in the description of many chemical reactions, such as S<sub>N</sub>2 nucleophilic substitution reactions [113, 114].

Conformational effects are another important aspect of chemical reactivity, especially in molecular crystals. Molecular crystals have diverse applications in fields such as pharmaceuticals and organic electronics. The organic molecules comprising such crystals are bound by weak dispersion interactions, and as a result the same molecule may crystallize in several different solid forms, known as **polymorphs** [119–121]. The energy differences between polymorphs are typically within 0.5 kcal/mol or less and the structural differences between polymorphs govern their physical properties and functionality. These observations call for the accuracy of first-principles quantum mechanical approaches, the use and refinement of many-body dispersion methods, and efficient configuration space exploration, making the computational characterization of molecular crystals one of the most difficult and yet highly important in molecular chemistry [119, 122–124].

## IV. QUANTUM ALGORITHMS FOR CHEMISTRY

### A. Mappings to qubits

In this Section, techniques to map fermionic and bosonic degrees of freedom to qubits are presented. The second quantization formalism for fermions is discussed in Section IV A 1, its counterpart for bosons in Section IV A 2, and alternative approaches are briefly reviewed in Section IV A 3.

#### 1. Fermions in second quantization

The Fock space  $\mathcal{F}_-$  of fermions occupying  $M$  spin orbitals has the same dimension,  $2^M$ , of the Hilbert space of  $M$  qubits,  $\mathcal{H}^{\otimes M}$ . Therefore, it is possible to construct a one-to-one correspondence

$$\hat{F} : \mathcal{F}_- \rightarrow \mathcal{H}^{\otimes M}, |\Psi\rangle \mapsto \hat{F}|\Psi\rangle \equiv |\Psi'\rangle \quad (15)$$

to represent fermionic wavefunctions  $|\Psi\rangle$  and operators  $\hat{A}$  by qubit wavefunctions  $|\Psi'\rangle$  and operators  $\hat{B}' = \hat{F}\hat{B}\hat{F}^{-1}$  as in Fig. 2. There are combinatorially many ways to map a quantum system to a set of qubits [125, 126] and, since fermions exhibit non-locality of their state space, due to their antisymmetric exchange statistics, any representation of fermionic systems on collections of qubits must introduce non-local structures [127].

*a. Jordan-Wigner (JW) transformation.* The JW transformation [7, 128–130], maps electronic configurations with generic particle number onto computational basis states,

$$(\hat{a}_{M-1}^\dagger)^{x_{M-1}} \dots (\hat{a}_0^\dagger)^{x_0} |\emptyset\rangle \mapsto |\mathbf{x}\rangle, \quad (16)$$

and fermionic creation and annihilation operators ( $\hat{a}_k^\dagger$  and  $\hat{a}_k$  respectively) onto non-local qubit operators of the form

$$\hat{a}_k^\dagger \mapsto \frac{X_k - iY_k}{2} \otimes Z_{k-1} \otimes \dots \otimes Z_0 \equiv S_{+,k} Z_0^{k-1} \quad , \quad \hat{a}_k \mapsto \frac{X_k + iY_k}{2} Z_0^{k-1} \equiv S_{-,k} Z_0^{k-1}. \quad (17)$$

The non-locality of these operator is required to preserve canonical anticommutation relations between creation and destruction operators, and immediately translates to  $n$ -body fermionic operators. The main limitation of the Jordan-Wigner transformation is that, as a consequence of the non-locality of the operators  $Z_d^b$ , the number of qubit operations required to simulate a fermionic operator  $\hat{a}_k^\dagger$  scales as  $\mathcal{O}(M)$  [131, 132]. Such a limitation motivated the design of alternative transformations, such as the parity mapping described below. The JW transformation is exemplified in Fig. 5 using the hydrogen molecule in a minimal basis as an example. In this work, we follow the convention of mapping spin-up and spin-down orbitals to the first and the last  $M/2$  qubits respectively. It is worth emphasizing that, since the JW transformation operates in the Fock space, states with any particle number, spin, and point group symmetry can result.

*b. Parity transformation.* The operator  $Z_0^{k-1}$  computes the parity  $p_k = \sum_{j=0}^{k-1} x_j \bmod 2$  of the number of particles occupying orbitals up to  $k$ . The computation of parities can be achieved using only single-qubit  $Z$  operators using the following parity transformation,

$$(\hat{a}_{M-1}^\dagger)^{x_{M-1}} \dots (\hat{a}_0^\dagger)^{x_0} |\emptyset\rangle \mapsto |\mathbf{p}\rangle \quad , \quad \hat{a}_k^\dagger \mapsto X_{M-1} \otimes \dots \otimes X_{k+1} \otimes \frac{X_k - iY_k}{2} \equiv X_{k+1}^{M-1} \otimes S_{+,k}. \quad (18)$$

In the parity transformation, the calculation of parities is local but the change of occupation numbers brought by the application of a creation or destruction operator requires  $\mathcal{O}(M)$  single-qubit gates. The parity transformation,

therefore, does not improve the efficiency over that of the JW transformation, but naturally allows a reduction of two in the number of qubits, which is desirable when very small quantum computers are used [133]. The JW and parity transformations are exemplified in Fig. 5b,c. In JW representation, computational basis states  $|x_3, x_2, x_1, x_0\rangle$  encode occupations  $x_k$  of spin-orbitals; in parity representation, they encode parities  $|p_3, p_2, p_1, p_0\rangle$  with  $p_k = x_0 + \dots + x_k$ .

c. *Bravyi-Kitaev (BK) transformation.* This transformation balances the locality of the occupation numbers and that of parities, to achieve a mapping of fermionic creation and destruction operators onto  $\mathcal{O}(\log_2 M)$ -qubit operators [127]. It does so by mapping occupation number states onto suitably defined binary strings,

$$(\hat{a}_{M-1}^\dagger)^{x_{M-1}} \dots (\hat{a}_0^\dagger)^{x_0} \mapsto |\mathbf{b}\rangle, b_k = \sum_{j=0}^{M-1} A_{kj} x_j \bmod 2, \quad (19)$$

where the  $M \times M$  binary matrix  $A$  has the structure of a binary tree [21, 127]. Since it requires only  $\mathcal{O}(\log_2 M)$ -qubit operators, the BK transformations allows for more economical encoding of fermionic operators onto qubit operators, with reduced cost for both measurements and quantum circuits.

d. *Qubit reduction techniques.* Lowering the number of qubits required to encode fermionic degrees of freedom, for example leveraging Hamiltonian symmetries [133–135], is an active and valuable research direction [133, 136]. Since the Hilbert space of a single qubit is isomorphic to  $\mathbb{C}^2$  and operators acting on different qubits commute with each other, it is natural to consider Abelian symmetry groups isomorphic to  $\mathbb{Z}_2^{\times k}$ . Example of such symmetries are those generated by parities  $(-1)^{N_\uparrow}$  and  $(-1)^{N_\downarrow}$ , proper rotations  $C_2$ , plane reflections  $\sigma$  and inversion  $i$ . In the tapering algorithm [133], such symmetries are detected leveraging the formalism of stabilizer groups [137]: the Hamiltonian is

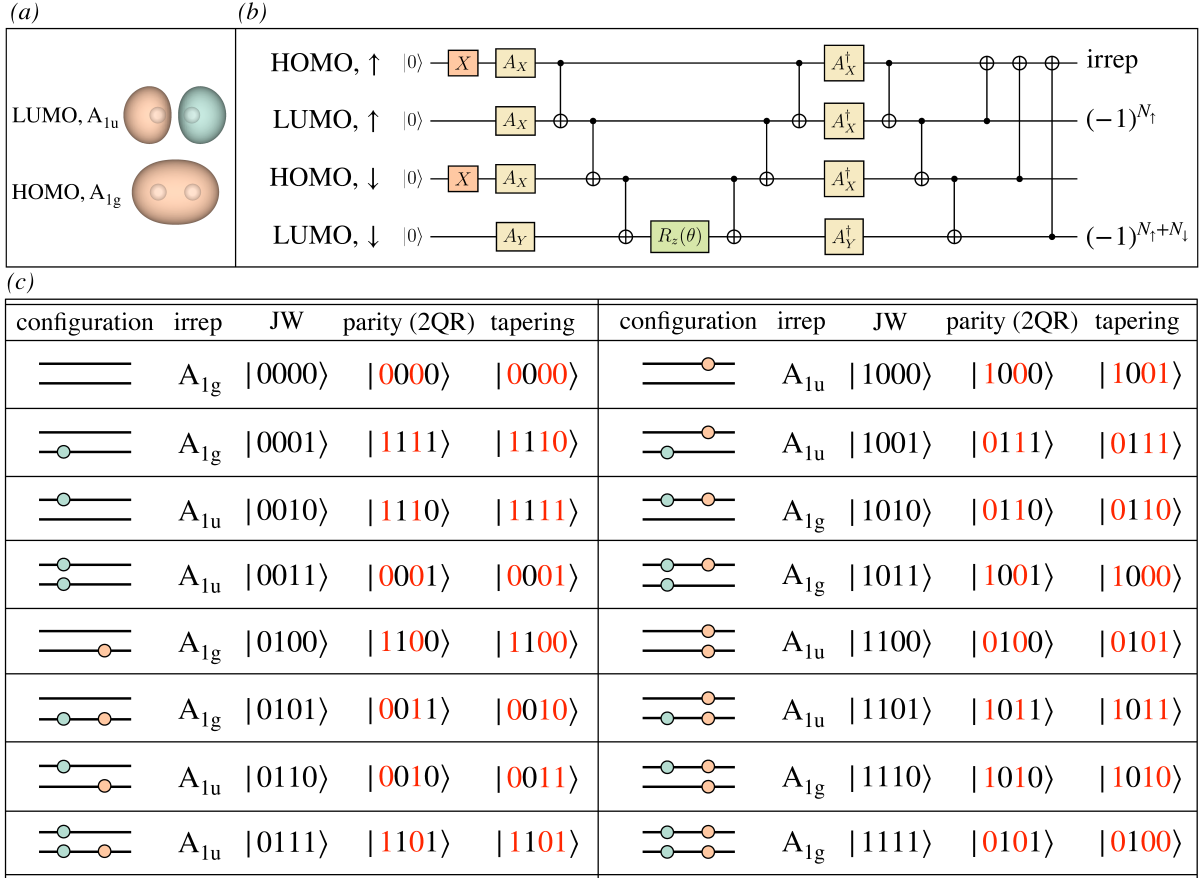


FIG. 5. Top: (a) molecular orbitals of the  $H_2$  molecule at equilibrium geometry using a minimal STO-6G basis; (b) quantum circuit to prepare the Hartree-Fock state ( $X$  gates) and a superposition of the Hartree-Fock and a doubly excited state  $\cos(\theta)|0101\rangle + \sin(\theta)|1010\rangle$  (exponential of the  $YXXX$  operator) in JW representation, to convert from JW to parity representation (subsequent 3 CNOT gates), and to compute the total irrep of the wavefunction (last 3 CNOT gates); (c) mapping of electronic configurations (horizontal black lines denote molecular orbitals and blue, orange circles denote spin-up, spin-down particles) in Jordan-Wigner representation and parity representation, and with tapering of the  $D_{2h}$  symmetry group. Red digits denote (left to right)  $(-1)^{N_\uparrow+N_\downarrow}$ ,  $(-1)^{N_\uparrow}$ , and the total irrep of the electronic configuration,  $x_1 + x_3 = p_0 + p_1 + p_2 + p_3 \bmod 2$ .

written as  $\hat{H} = \sum_j c_j P_j$ , where  $P_j$  denotes an  $M$ -qubit Pauli operator, and symmetry groups  $\mathcal{S}$  that (i) are Abelian subgroups of the  $M$ -qubit Pauli group, (ii)  $-I \notin \mathcal{S}$ , and (iii) every element of  $\mathcal{S}$  commutes with every Pauli operator  $P_j$  in the qubit representation of  $\hat{H}$  are considered. While such a restriction limits the generality of the formalism, it provides an efficient algorithm, based on linear algebra on the  $\mathbb{Z}_2$  field [133], to identify a set of generators  $\tau_1 \dots \tau_k$  for  $\mathcal{S}$ , and a Clifford transformation  $U$  such that  $\tau_i = U^\dagger Z_i U$  for all  $i = 1 \dots k$ . An  $M$ -qubit wavefunction  $\Psi$  is an eigenfunction of all symmetry operators with eigenvalues  $s_i$  if  $Z_i U |\Psi\rangle = s_i U |\Psi\rangle$ , i.e.  $U |\Psi\rangle = |\Phi_s\rangle \otimes |\mathbf{s}\rangle$ . One can thus search for eigenfunctions of the projections  $\hat{H}_{\mathbf{s}} = \text{Tr}_{1\dots k} [(\mathbb{1} \otimes |\mathbf{s}\rangle \langle \mathbf{s}|) U^\dagger H U]$  of  $\hat{H}$  on the irreducible representation of  $\mathcal{S}$  labeled by the eigenvalues  $\mathbf{s}$ .

The procedure is exemplified in Fig. 5b. At the end of the circuit, qubits 0,1 and 3 from above contain the irrep label and parities  $p_1, p_3$  respectively, so the calculation of the energy of the  $H_2$  molecule with the STO-6G basis using 4 qubits has resulted in the same energy but only using 1 qubit.

## 2. Bosons in second quantization

In the previous section, we showed how to map spin-1/2 fermions to qubits. For many problems, it is necessary to simulate  $d$ -level particles with  $d > 2$ , including bosonic elementary particles [138], spin- $s$  particles [139], vibrational modes [140] and electronic energy levels in molecules and quantum dots [141, 142]. Accordingly, several qubit-based quantum algorithms were recently developed for efficiently studying some of these systems, including nuclear degrees of freedom in molecules [143–147], the Holstein model [148, 149] and quantum optics [150, 151].

Mapping a  $d$ -level system to a set of qubits can be done in a variety of ways, and determining which encodings is optimal for a given problem has important practical implications. The standard binary mapping refers to the familiar base-two numbering system, such that an integer  $l = 0 \dots d - 1$ , corresponding to one of the  $d$  levels of the system, is represented as  $l = \sum_{i=0}^{n_q-1} x_i 2^i$ , with  $n_q = \lceil \log_2 d \rceil$ , and mapped on the binary string  $\mathbf{x}_l = (x_0 \dots x_{n_q-1})$ . This simple and natural mapping has been used for qubit-based quantum simulation of truncated bosonic degrees of freedom [143–151]. One mapping from classical information theory with particularly useful properties is called the Gray or the reflected binary code. Its defining feature is that the binary strings  $\mathbf{x}_{l+1}, \mathbf{x}_l$  encoding two consecutive integers  $l + 1, l$  have to differ by one digit only (i.e. the Hamming distance between the two bitstrings is 1). This encoding is especially favorable for tridiagonal operators with zero diagonals, and requires  $n_q = \lceil \log_2 d \rceil$  qubits. There exist encodings that make less efficient use of quantum resources, requiring more than  $\lceil \log_2 d \rceil$  qubits, but usually allow for fewer quantum operations. Among them one finds the unary encoding, using  $2^d$  qubits and mapping integers  $l$  onto binary strings  $(\mathbf{x}_l)_m = \delta_{lm}$ . Previous proposals for digital quantum simulation of bosonic degrees of freedom have used the unary encoding. The standard binary, Gray and unary codes are described in detail and compared in the literature [152, 153]. The most efficient encoding choice is often significantly dependent on the application at hand, due to the complicated and delicate interplay between Hamming distances, sparsity patterns, bosonic truncation, and other properties of the Hamiltonian and other operators, and it is sensitive to the number  $d$  of levels of the system [143–151].

## 3. Alternative approaches

For local Hamiltonians in one spatial dimension, the JW transformation allows mapping of a local theory of fermions onto a local theory of spins. In higher dimensions, however, the JW transformation gives rise to non-local coupling between spins. The possibility of reducing this non-local coupling has been explored by many authors, including Bravyi and Kitaev [127]. Similar ideas were explored by Ball [154] and Cirac and Verstraete [155]. The latter, in particular, achieved a mapping between local Fermi and local qubit Hamiltonians by introducing extra degrees of freedom in the form of Majorana fermions, which interact locally with the original ones. Other approaches have included the use of Fenwick trees [156] and graph theoretical tools [157].

Generalizations of the tapering qubit reduction formalism to more general discrete and continuous symmetries is known [134, 135], and symmetries have been recognised as an important ingredient in the implementation of error correction algorithms [158, 159]. Recently, techniques reducing the number of qubits by half focusing on the seniority-zero sector of the Hilbert space and partitioning an electronic system into classically correlated spin-up and spin-down sectors have also been proposed [160, 161]. As illustrated by the many different techniques referred to above, this continues to remain an important research direction for a variety of reasons: first, qubit reduction techniques allow for the simulation of problems with less quantum resources and thus to make use of near-term hardware; furthermore, they help enforce exact properties of electronic wavefunctions (e.g. particle number and spin conservation and, in presence of molecular point-group symmetries, labeling ground and excited states by irreducible representations).

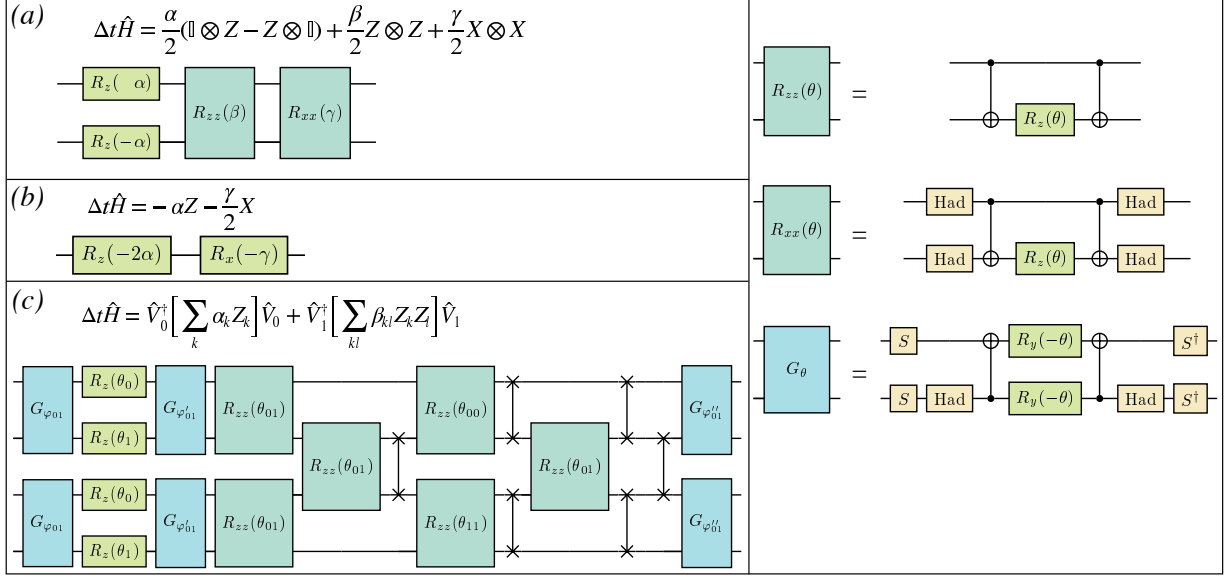


FIG. 6. Left: (a) quantum circuit to simulate a Trotter step of time evolution under the Hamiltonian of H<sub>2</sub> at STO-6G level in parity representation with two-qubit reduction (b) same as (a) but accounting for  $D_{\infty h}$  symmetry via reduction of a third qubit. (c) quantum circuit to simulate a Trotter step of time evolution under the Born-Oppenheimer Hamiltonian in a set of 2 spatial orbitals and Jordan-Wigner representation, using a low-rank decomposition with  $N_\gamma = 1$  term. Blue, teal and green blocks indicate Givens rotations, exponentials of  $Z \otimes Z$  and  $X \otimes X$  Pauli operators, and single-qubit  $Z$  rotations respectively. Angles  $\varphi_{kl}$  parametrize Givens rotations, and angles  $\theta_k$ ,  $\theta_{kl}$  are functions of the Hamiltonian coefficients  $\alpha_k$ ,  $\beta_{kl}$  respectively. Right: Implementation of the exponentials  $R_{zz}(\theta)$  (top),  $R_{xx}(\theta)$  (middle), and of a Givens rotation (bottom).

## B. Simulation of Hamiltonian dynamics

As discussed in Section II A 2, the simulation of Hamiltonian dynamics, i.e. the solution of the time-dependent Schrödinger equation, is a BQP-complete problem, and thus a natural application for a quantum computer.

In this Section, we present some important quantum algorithms for the simulation of Hamiltonian dynamics. Given a Hamiltonian  $\hat{H}$  acting on a set of  $n$  qubits, we say [162] that  $\hat{H}$  can be **efficiently simulated** (to an accuracy  $\varepsilon$ ) if one can produce a quantum circuit  $\hat{U}$  such that

$$\|\hat{U} - e^{-it\hat{H}}\| < \varepsilon \quad , \quad (20)$$

and  $\hat{U}$  comprises a number of gates scaling at most polynomially with  $n$ ,  $t$  and  $\varepsilon^{-1}$ . In the remainder of this Section, we will describe quantum algorithms to simulate the electronic structure Hamiltonian, in the sense of Eq. (20). These algorithms will be classified, according to the underlying mathematical formalism, into product formula [6, 7], quantum walk [163, 164] and linear combination of unitary operators (LCU) algorithms [165–168].

### 1. Product formula algorithms

Given a Hamiltonian operator  $\hat{H} = \sum_{\ell=1}^L \hat{h}_\ell$ , product formulas produce an approximation to  $e^{-it\hat{H}}$  using a product of exponential operators  $e^{-it\hat{h}_\ell}$ . This is achieved by dividing the time interval  $[0, t]$  into a large number  $n_T$  of steps,

$$\hat{U}(t) = e^{-it\hat{H}} = \prod_{i=0}^{n_T-1} \hat{U}(\Delta t) \quad , \quad \Delta t = \frac{t}{n_T} \quad , \quad (21)$$

and approximating each of the operators  $\hat{U}(\Delta t)$ . An important example is the primitive approximation [169, 170]

$$\hat{U}(\Delta t) = \prod_{\ell} e^{-i\Delta t \hat{h}_\ell} + \mathcal{O}(\Delta t^2) \quad , \quad \hat{U}_p(\Delta t) \equiv \prod_{\ell} e^{-i\Delta t \hat{h}_\ell} \quad . \quad (22)$$

The accuracy of the primitive approximation Eq. (22) can be estimated observing that

$$\|\hat{U}(t) - \hat{U}_p(\Delta t)^{n_T}\| = \gamma_p n_T \Delta t^2 + \mathcal{O}(t^3/n_T^2) , \quad \gamma_p = \frac{1}{2} \sum_{\ell < \ell'} \|[\hat{h}_\ell, \hat{h}_{\ell'}]\| . \quad (23)$$

Therefore, accuracy  $\varepsilon$  is attained for  $n_T = \mathcal{O}(\gamma_p t^2/\varepsilon)$ . More accurate approximations can be achieved relying on the Trotter-Suzuki formulas [169–172], which are defined recursively as

$$\begin{aligned} \hat{U}_{2k+2}(\Delta t) &= \hat{U}_{2k}^2(a_{2k}\Delta t) \hat{U}_{2k}((1-4a_{2k})\Delta t) \hat{U}_{2k}^2(a_{2k}\Delta t) , \\ \hat{U}_2(\Delta t) &= \left[ \prod_{\ell=L}^1 e^{-i\frac{\Delta t}{2}\hat{h}_\ell} \right] \left[ \prod_{\ell=1}^L e^{-i\frac{\Delta t}{2}\hat{h}_\ell} \right] , \quad a_{2k} = \frac{1}{4 - 4^{\frac{1}{2k+1}}} . \end{aligned} \quad (24)$$

Since  $\hat{U}_{2k}(\Delta t) = e^{-i\Delta t \hat{H}} + \mathcal{O}(\Delta t^{2k+1})$ , accuracy  $\varepsilon$  is achieved for  $n_T = t^{1+\frac{1}{2k}}\varepsilon^{-\frac{1}{2k}}$ . As seen, the cost of simulating Hamiltonian dynamics with product formulas has power-law scaling in  $t$  and  $\varepsilon^{-1}$ . To achieve efficient simulation, however, the number  $L$  of Hamiltonian terms and the cost of simulating  $e^{-i\Delta t \hat{h}_\ell}$  has to scale as  $\text{poly}(n)$ . This can be achieved, for example, mapping the electronic structure Hamiltonian Eq. (7) onto an  $M$ -qubit operator  $\hat{H} = \sum_{\ell=1}^L c_\ell \hat{P}_\ell$ , as outlined in Section IV A, and exponentiating individual  $M$ -qubit Pauli operators  $\hat{P}_\ell$  with the circuit presented in Section V, and exemplified in Fig. 6. The resulting scaling is between  $\tilde{\mathcal{O}}(M^4)$  and  $\mathcal{O}(M^5)$  per step [168, 173].

Alternative approaches exist, which can be used to lower the computational cost. In particular, Aharonov and Ta-Shma [174, 175] introduced an algorithm for the quantum simulation of  $d$ -sparse Hamiltonians, based on a combination of graph coloring and Trotter decomposition. More recently, various authors [173, 176–181] proposed product formulas based on low-rank representations of the electron-repulsion integral,  $(pr|qs) = \sum_{\gamma=1}^{N_\gamma} L_{pr}^\gamma L_{qs}^\gamma$ . Such representations can be efficiently computed from a density fitting approximation [182–190], a Cholesky decomposition [191–197], or a multi-unitary tensor hypercontraction representation [181, 198–201] and typically feature  $N_\gamma = \mathcal{O}(M)$  terms. In this framework, the electronic structure Hamiltonian is represented as

$$\hat{H} = E_0 + \hat{V}_0^\dagger \left[ \sum_p t_p \hat{n}_p \right] \hat{V}_0 + \sum_\gamma \hat{V}_\gamma^\dagger \left[ \sum_{pq} v_{pq}^\gamma \hat{n}_p \hat{n}_q \right] \hat{V}_\gamma , \quad \hat{V}_\gamma = e^{\sum_{pq} A_{pq}^\gamma \hat{a}_p^\dagger \hat{a}_q} , \quad (25)$$

and the time evolution operators  $e^{-i\Delta t \hat{H}}$  as

$$e^{-i\Delta t \hat{H}} \simeq \prod_\gamma \left[ \hat{V}_\gamma^\dagger \left( \prod_{pq} e^{-i\Delta t v_{pq}^\gamma \hat{n}_p \hat{n}_q} \right) \hat{V}_\gamma \right] \prod_p e^{-i\Delta t \hat{n}_p} . \quad (26)$$

Exponentials of one-body operators such as  $\hat{V}_\gamma$  can be decomposed into a product of up to  $\mathcal{O}(M^2)$  Givens transformations [178, 179] with standard linear algebra operations. Each of these Givens rotations can be implemented, in the JW representation, with a two-qubit gate acting on a pair of adjacent qubits. Exponentials of number and products of number operators can be implemented [178] with  $R_z(\varphi) = \exp(-i\varphi/2Z)$  and  $R_{zz}(\varphi) = \exp(-i\varphi/2 Z \otimes Z)$  gates, as exemplified in Fig. 6. The resulting scaling is  $\mathcal{O}(N_\gamma M^2) = \mathcal{O}(M^3)$  [173, 179]. Other approaches to implement time evolution with product formulas have explored alternatives to the high-order formulas Eq. (24) having a more favorable scaling with  $k$  [202], as well as grouping commuting Pauli terms [176] and divide-and-conquer strategies [203]. Recently, Childs and Su [204] revisited approaches based on product formulas, and demonstrated that their performance is more favorable than suggested by simple error bounds. Techniques of circuit recompilation aimed at generating optimal circuit are also intensely investigated [132, 205–207]. The design and improvement of product formulas, and the systematic assessment of their accuracy and computational cost for molecular problems, is thus an active and valuable research area at the interface between quantum computation and chemistry [15, 176, 208].

## 2. Quantum walks

Hamiltonian simulation by product formulas has cost scaling **super-linearly** with  $t$ . Such an observation leads to question of whether a better scaling can be achieved. For a general Hamiltonian, a scaling sub-linear in  $t$  cannot be achieved, due to the no-fast-forwarding theorem [175, 209]. On the other hand, a number of algorithms achieving linear scaling with  $t$  are known. The earliest example is represented by quantum walk algorithms [210–214].

In the context of Hamiltonian simulation by quantum walks, we consider a Hamiltonian operator  $\hat{H} = \sum_{\lambda} \lambda |\lambda\rangle\langle\lambda|$  acting on a Hilbert space  $\mathcal{H}$  and having eigenvalues  $\lambda \in [-1, 1]$ . Such a condition can always be satisfied by computing an upper bound  $\zeta \geq \|\hat{H}\|$  for the norm of  $\hat{H}$ , and rescaling the Hamiltonian and simulation time accordingly. Simulating Hamiltonian dynamics by a quantum walk consists in introducing a unitary operator  $\hat{W}$ , acting on an extended Hilbert space  $\mathcal{H}_e \supset \mathcal{H}$ , whose spectrum is connected with that of  $e^{-i\Delta t \hat{H}}$  by an invertible transformation. Such a unitary transformation has the form [212–214]

$$\hat{W} = i\hat{S} (2\hat{T}\hat{T}^\dagger - \mathbb{1}) \quad , \quad (27)$$

where  $\hat{T} : \mathcal{H} \rightarrow \mathcal{H}_e$  is an isometry,  $\hat{S} : \mathcal{H}_e \rightarrow \mathcal{H}_e$  a unitary operator such that  $\hat{S}^2 = \mathbb{1}$ , and

$$\hat{T}^\dagger \hat{S} \hat{T} = \hat{H} \quad . \quad (28)$$

Thanks to these properties, it can be proved [212, 214] that  $\hat{W}$  leaves a set of 2-dimensional subspaces

$$\mathcal{S}_{\lambda} = \text{span} \left\{ \hat{T}|\lambda\rangle, \hat{S}\hat{T}|\lambda\rangle \right\} \quad (29)$$

invariant, and has eigenvalues and eigenvectors

$$\hat{W}|\mu_{\pm}(\lambda)\rangle = \mu_{\pm}(\lambda)|\mu_{\pm}(\lambda)\rangle \quad , \quad \mu_{\pm}(\lambda) = \pm e^{\pm i \arcsin(\lambda)} \quad , \quad |\mu_{\pm}(\lambda)\rangle = \frac{1 + i\mu_{\pm}(\lambda)\hat{S}}{\sqrt{2(1 - \lambda^2)}} \hat{T}|\lambda\rangle \quad . \quad (30)$$

The operators  $\hat{S}$  and  $\hat{T}$  are constructed assuming the existence of an oracle, i.e. a unitary operator giving access to the binary representation of the matrix elements of  $\hat{H}$  in a suitable basis [212, 214], and the spectrum of  $\hat{W}$  is converted into that of  $e^{-it\hat{H}}$  using a subroutine based on the quantum phase estimation algorithm (see Section IV B 6). The quantum walk approach, though achieving linear scaling with  $t$ , retains algebraic scaling with  $\varepsilon$ , which was improved by LCU-based algorithms.

### 3. The linear combination of unitary operators: LCU lemma

Product formulas and quantum walks permit to approximate the time evolution operator by a sequence of unitary operations. A breakthrough in quantum simulation came from the realization that more accurate approximations can be achieved using **non-unitary approximations** [165–167, 215, 216]. In particular, such non-unitary approximations often take the form of linear combinations of unitary operations.

In order to describe several important quantum algorithms based on non-unitary approximations of the time evolution operator, in this section we present a theoretical result known as LCU lemma [166], showing how to apply linear combination of  $L$  unitary operators to a set of qubits prepared in a state  $|\Psi\rangle$ ,

$$|\Psi\rangle \mapsto \frac{\hat{X}|\Psi\rangle}{\|\hat{X}\Psi\|} \equiv |\Psi_X\rangle \quad , \quad \hat{X} = \sum_{\ell=0}^{L-1} \alpha_{\ell} \hat{U}_{\ell} \quad . \quad (31)$$

Since  $\hat{X}$  is not a unitary operator, it is not straightforward to represent the map (31) as a quantum circuit. On the other hand, such a representation is highly desirable, as it extends the reach of quantum computation to non-unitary operators. The LCU lemma provides a strategy for implementing the transformation (31) with probability  $p$ , based on the quantum circuit in Figure 7a. A register of  $n_A = \lceil \log_2(L) \rceil$  ancillary qubits is prepared in  $|0\rangle^{\otimes n_A}$  and coupled to a register of  $n$  qubits, prepared in the state  $|\Psi\rangle$ . The ancillae are manipulated with a preparation unitary

$$\hat{W}_p|0\rangle = \sum_{\ell=0}^{L-1} \sqrt{\frac{\alpha_{\ell}}{\alpha}} |\ell\rangle \quad , \quad \alpha = \sum_{\ell=0}^{L-1} \alpha_{\ell} \quad , \quad (32)$$

and coupled with the qubits of the main register by a selection unitary

$$\hat{W}_s = \sum_{\ell=0}^{L-1} \hat{U}_{\ell} \otimes |\ell\rangle\langle\ell| \quad . \quad (33)$$

The transformation  $\hat{W}_p$  is subsequently reversed, and the ancillae are measured. If the outcome of the measurement is  $(0 \dots 0)$ , which happens with probability  $p = \|\hat{X}\psi\|^2/\alpha^2$ , the qubits of the main register collapse onto the state  $|\Psi_X\rangle$ . The number of ancillae,  $n_A = \lceil \log_2(L) \rceil$  scales logarithmically with  $n$  provided that  $L = \text{poly}(n)$ . The unitary  $\hat{W}_p$  can require up to  $2^{n_A} = \text{poly}(n)$  gates [27]. Similarly, if every unitary  $\hat{U}_\ell$  can be controlled at cost  $c_\ell = \text{poly}(n)$ , then  $\hat{W}_s$  can be implemented at cost  $\text{poly}(n)$  [27]. The main limitation of the LCU algorithm is the success probability, which decays as  $1 - (1 - p)^k = 2^{-\mathcal{O}(k)}$  when the circuit in Fig. 7a is applied  $k$  times consecutively. When  $\hat{X}$  is a unitary operator [164], as in Hamiltonian evolution, the success probability  $p$  can be increased using the procedure called oblivious amplitude amplification (OAA) [215, 217, 218]. The OAA is described by the quantum circuit in Figure 7, where  $\hat{W}_{\text{LCU}} = \hat{W}_p^\dagger \hat{W}_s \hat{W}_p$  is the LCU unitary, and  $\hat{R} = \mathbb{1} \otimes (\mathbb{1} - 2|0\rangle\langle 0|)$  reflects ancillae around the state  $|0\rangle\langle 0|$ . The circuit  $\hat{A}^k \hat{W}_{\text{LCU}}$  leads to a state of the form

$$\hat{U}|0\rangle|\Psi\rangle = \sqrt{p_k} \frac{\hat{X}|\Psi\rangle}{\|\hat{X}\Psi\|} \otimes |0\rangle^{\otimes n_A} + \sqrt{1-p_k} |\Phi^\perp\rangle , \quad p_k = \sin^2((2k+1)\theta) , \quad \theta = \arcsin\sqrt{p} , \quad (34)$$

and  $p_k \geq 1 - \delta$  provided that  $k \geq \mathcal{O}(1/\sqrt{p})$ . We remark that, when  $\hat{X}$  is not a unitary operator, OAA gives Chebyshev polynomials of that operator [164].

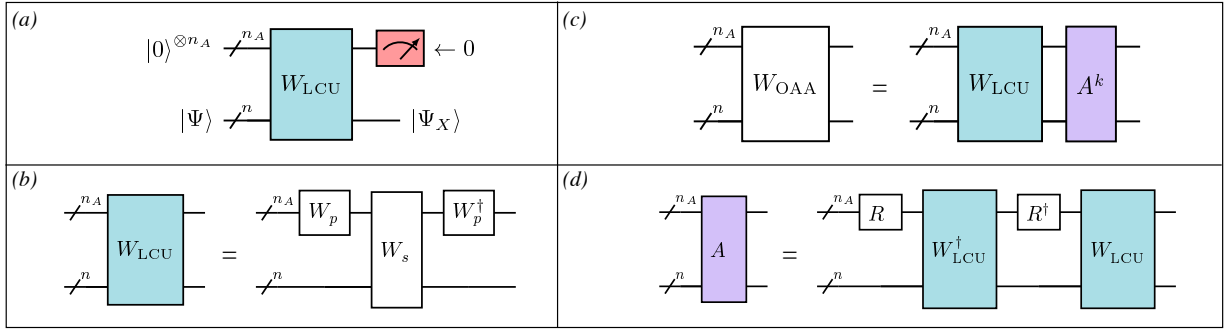


FIG. 7. Schematic representation of the algorithm for the probabilistic implementation of an LCU (a), structure of the LCU unitary (blue block) as composition of a preparation and a selection unitary (b), schematic representation of the OAA algorithm (c), and implementation of the OAA unitary (purple block) as a composition of the LCU unitary and a reflector unitary transformation (d). Slashes denote multi-qubit registers.

#### 4. LCU based algorithms

In 2014, Berry et al [166] introduced a method for Hamiltonian simulation, based on the Taylor series representation of the time evolution operator, to achieve a computational cost scaling linearly in  $t$  and logarithmically in  $\varepsilon^{-1}$  (i.e. exponentially better than product formulas and quantum walks). The algorithm focuses on Hamiltonian operators that can be written as LCUs,  $\hat{H} = \sum_{\ell=0}^{L-1} \alpha_\ell \hat{U}_\ell$ . For simplicity, we also assume that  $C = \sum_\ell \alpha_\ell = 1$ , which is equivalent to rescaling energy and time units,  $\hat{H} \rightarrow C^{-1}\hat{H}$  and  $t \rightarrow Ct$ . The time interval  $[0, t]$  is divided in  $r$  steps of duration  $\Delta t = t/r$ , and the operator  $e^{-i\Delta t \hat{H}}$  is expanded in Taylor series to order  $K$ ,

$$e^{-i\Delta t \hat{H}} \simeq \hat{V}_K(\Delta t) = \sum_{m=0}^K \frac{(-i\Delta t)^m}{m!} \hat{H}^m = \sum_{m=0}^K \sum_{\ell_0 \dots \ell_m=0}^{L-1} \frac{(-i\Delta t)^m}{m!} \alpha_{\ell_0} \dots \alpha_{\ell_m} \hat{U}_{\ell_0} \dots \hat{U}_{\ell_m} . \quad (35)$$

Eq. (35) is an LCU representation of  $e^{-i\Delta t \hat{H}}$ , which can be probabilistically applied relying on a particular implementation [166] of the LCU lemma presented in Section IV B 3, where  $K(1 + \log_2 L)$  ancillae are used, as shown in Fig. 8. The first  $K$  ancillae are prepared in the state  $\sum_m \sqrt{\Delta t^m/m!} |0\rangle^{K-m} |1\rangle^m$  using  $\mathcal{O}(K)$  controlled single-qubit rotations, and the remaining  $\log_2(L)$  groups of  $K$  ancillae are prepared in the normalized state  $\sum_\ell \sqrt{\alpha_\ell} |\ell\rangle$  using  $\mathcal{O}(KL)$  gates. The other basic component is the selection unitary, which maps states of the form  $|\psi\rangle |\ell_k\rangle \dots |\ell_1\rangle |k\rangle$  to  $(-i)^k \hat{U}_{\ell_1} \dots \hat{U}_{\ell_k} |\psi\rangle |\ell_k\rangle \dots |\ell_1\rangle |k\rangle$  at the cost of  $\mathcal{O}(L(n + \log_2 L)K)$  operations [166]. An important aspect of this

algorithm is the order  $K$  of the polynomial approximating  $e^{-i\Delta t \hat{H}}$  with accuracy  $\varepsilon/K$ , which scales as [166]

$$K = \mathcal{O}\left(\frac{\log\left(\frac{t}{\varepsilon}\right)}{\log\log\left(\frac{t}{\varepsilon}\right)}\right) . \quad (36)$$

The logarithmic dependence of the computational cost on  $\varepsilon^{-1}$  thus arises from the rapid convergence of the Taylor series, as well as on the specific use of ancillary qubits and controlled operations described in the previous paragraph.

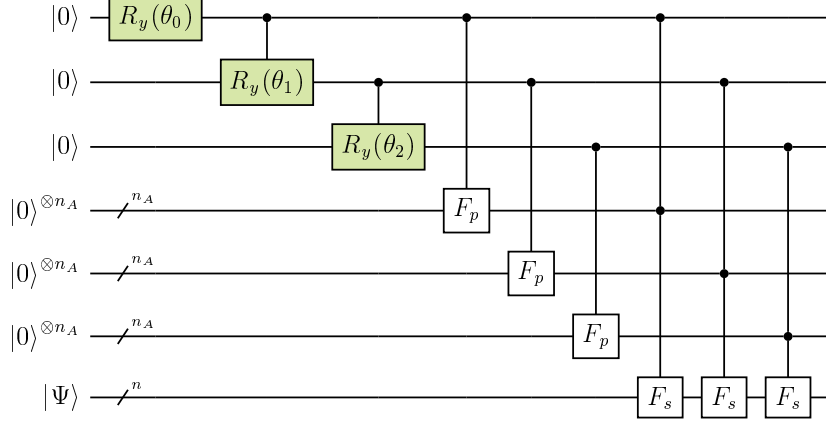


FIG. 8. Preparation ( $y$  rotations, multi-qubit gates  $c\hat{F}_p$ ) and selection (multi-qubit  $c\hat{F}_s$  gates) unitaries for Hamiltonian simulation based on a truncated Taylor series. Here  $K = 3$  and  $n_A = \log_2(L)$ . The angles in the  $y$  rotations are chosen to reproduce the state  $\sum_m \sqrt{\Delta t^m / m!} |0\rangle^{K-m} |1\rangle^m$ . The operation  $c\hat{F}_p$  is defined as  $c\hat{F}_p |0\rangle|k\rangle = V^k |0\rangle|k\rangle$ , with  $V|0\rangle = \sum_\ell \sqrt{\alpha_\ell} |\ell\rangle$ , and the operation  $c\hat{F}_s$  as  $c\hat{F}_s |\psi\rangle|\ell\rangle|k\rangle = (-i\hat{U}_\ell)^k |\psi\rangle|\ell\rangle|k\rangle$ .

### 5. Quantum signal processing and qubitization

The qubitization algorithm, developed by Low and Chuang [167], uses the LCU decomposition of the Hamiltonian and the quantum signal processing (QSP) technique [216, 219] to achieve a computational cost where the dependence on  $t$  and  $\log \varepsilon^{-1}$  is **additive rather than multiplicative**,  $\mathcal{O}(t + \log \varepsilon^{-1})$ , which is optimal in both accuracy and time [219].

Given a Hamiltonian operator  $\hat{H}$  acting on a Hilbert space  $\mathcal{H}$  and having norm  $\|\hat{H}\| \leq 1$ , the starting point of qubitization is the construction of a unitary operator  $\hat{W}_Q$ , called qubiterate. The qubiterate acts on an extended Hilbert space  $\mathcal{H}' \otimes \mathcal{H}$  and is an encoding for  $\hat{H}$ , in the sense that

$$\langle \phi | \langle g | \hat{U} | \psi \rangle | g \rangle = \langle \phi | \hat{H} | \psi \rangle \quad \text{for some } |g\rangle \in \mathcal{H}' \text{ and any } |\phi\rangle, |\psi\rangle \in \mathcal{H} . \quad (37)$$

Moreover, for any eigenvector of  $\hat{H}$ ,  $\hat{H} |\lambda\rangle = \lambda |\lambda\rangle$ , one has

$$\hat{W}_Q |g_\lambda\rangle = \lambda |g_\lambda\rangle - \sqrt{1 - \lambda^2} |g_\lambda^\perp\rangle , \quad \hat{W}_Q |g_\lambda^\perp\rangle = \lambda |g_\lambda^\perp\rangle + \sqrt{1 - \lambda^2} |g_\lambda\rangle , \quad (38)$$

where  $|g_\lambda\rangle = |\lambda\rangle|g\rangle$  and  $|g_\lambda^\perp\rangle$  is defined by the first of Eq. (38). In other words, the qubiterate leaves the two-dimensional subspaces  $\mathcal{S}_\lambda$  spanned by  $|g_\lambda\rangle$  and  $|g_\lambda^\perp\rangle$  invariant, so that its restriction to  $\bigoplus_\lambda \mathcal{S}_\lambda$  is a direct sum of  $Y$  rotations acting on the subspaces individually  $\mathcal{S}_\lambda$ ,

$$\hat{W}_Q = \bigoplus_\lambda e^{-i\theta_\lambda Y_\lambda} , \quad \theta_\lambda = \arccos(\lambda) . \quad (39)$$

The qubiterate is used to construct an operator  $\hat{V}_{\vec{\varphi}}$ , which in turn is used to approximate  $e^{-it\hat{H}}$ , by a QSP [216, 219]. The single-ancilla QSP is described by the quantum circuit in Fig. 9.

The operator  $\hat{V}_{\vec{\varphi}}$  has the form

$$\hat{V}_{\vec{\varphi}} = \prod_{m=0}^K \hat{U}_{\varphi_{2m+2} + \pi}^\dagger \hat{U}_{\varphi_{2m+1}} , \quad \hat{U}_\phi = [\mathbb{1} \otimes R_z(-\varphi) \text{ Had}] \mathbf{c}(iW_Q) [\mathbb{1} \otimes \text{Had} R_z(\varphi)] , \quad (40)$$

where  $c(iW_Q)$  is the controlled version of the gate  $iW_Q$ . It can be shown that [167]

$$\hat{V}_{\vec{\varphi}} = \sum_{\lambda, \pm} |\lambda_{\pm}\rangle\langle\lambda_{\pm}| \otimes u(\vec{\varphi}, \theta_{\lambda, \pm}) \quad , \quad (41)$$

where  $|\lambda_{\pm}\rangle$  is an eigenvector of  $\hat{W}_Q$  with eigenvalue  $e^{\pm i\theta_{\lambda}}$ , and  $u$  a single-qubit operator. Provided that the number of angles  $\vec{\varphi}$  is sufficiently large,  $K = \mathcal{O}(t + \log \varepsilon^{-1})$ , these angles can be set to values that are efficiently computable on a classical computer [167, 220–222] so that

$$\langle \chi | \langle g | (+| \hat{V}_{\vec{\varphi}} | \psi) | g \rangle | + \rangle \simeq \langle \chi | e^{-it\hat{H}} | \psi \rangle \quad (42)$$

with error bounded by  $\varepsilon$ . Qubitization is a systematic framework, that offers a concrete procedure to simulate Hamiltonian dynamics with optimal complexity with respect to  $t$  and  $\varepsilon$ . In recent years, its complexity with respect to the number of spin-orbitals was improved using low-rank [223] and tensor hypercontraction [224] techniques. Product formulas and Taylor series techniques allow simulation of Schrödinger equations with a time-dependent Hamiltonian  $\hat{H}(t)$ . On the other hand, the qubitization technique is formulated for time-independent Hamiltonians, and its extension to time-dependent Hamiltonians is an open and challenging research problem. An important consequence of this difference is that product formulas and Taylor series techniques allow simulation in the interaction picture of quantum mechanics. This is especially desirable for electronic structure problems, where the Born-Oppenheimer Hamiltonian can be written as the sum  $\hat{H} = \hat{T} + \hat{V}$  of a one-body operator and of a two-body operator, so that the unitary transformation

$$\Psi(t) \rightarrow \Psi_I(t) = e^{\frac{i}{\hbar}\hat{T}}\Psi_t \quad (43)$$

leads to a Schrödinger equation with a time-dependent Hamiltonian  $\hat{V}_I(t) = e^{\frac{i}{\hbar}\hat{T}}\hat{V}e^{-\frac{i}{\hbar}\hat{T}}$ . It is important to remark that, since  $\hat{T}$  is a one-body operator, the interaction term  $\hat{V}$ , and any other molecular property described by a  $k$ -body operator, can be exactly and efficiently transformed to the interaction picture,  $\hat{V} \rightarrow \hat{V}_I(t)$ .

## 6. Applications of Hamiltonian dynamics, and open problems

In the previous Section, we examined some emerging quantum algorithms for Hamiltonian dynamics simulation. Hamiltonian dynamics simulation is one of the most compelling applications for a quantum computer, as it lies in the complexity class BQP. The study, implementation and application of algorithms for Hamiltonian dynamics simulation is thus a relevant research area, and one that has significant potential to yield the first relevant quantum simulations of chemical systems [168]. Nevertheless, a careful consideration of the actual computational cost and of the accuracy of such algorithms, with particular attention to chemical problems, is a necessary requirement to understand, design and carry out such simulations.

While product formula algorithms have the highest asymptotic computational cost, compared against quantum walks and LCU (linear combination of unitary operators) based algorithms, the actual runtime of an algorithm for specific problems of interest is crucially determined by prefactors [225], as well as by other technical considerations, such as the amount of input and output data that need to be pre-computed and post-processed respectively, and moved between the classical and quantum computer [226], and the precise determination of the accuracy of quantum algorithms by tight numerical bounds as opposed to loose inequalities [204]. Furthermore, quantum walks and

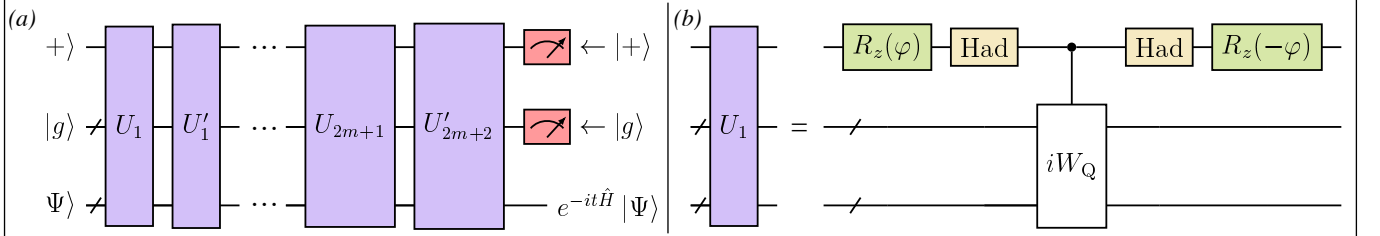


FIG. 9. Quantum circuit for single-ancilla quantum signal processing, where  $U_k = U_{\varphi_k}$  and  $U'_k = U_{\varphi_k+\pi}^\dagger$  for brevity (a) and structure of the gate  $\hat{U}_{\varphi}$  in terms of single-qubit operations and the qubiterate  $\hat{W}_Q$  (b).

LCU based algorithms require additional quantum resources, especially ancillae and controlled operations, which are challenging aspects when implementation on near-term quantum devices is considered.

In our view, such observations pinpoint the need of detailed comparative studies, conducted on a diverse range of chemical problems, with exhaustive cross-checks, validations and tests between classical and quantum algorithms. Such detailed comparisons can precisely establish by numerical studies the regime (i.e. the number of spin-orbitals  $M$ , simulation time  $t$ , and target accuracy  $\epsilon$ ) where quantum walks and LCU based algorithms become less expensive than product formulas, and of course of other algorithms for classical computers [225], and provide rigorous benchmarks for assessing the current state of the art in quantum simulation, for measuring its progress, and for developing new and improved techniques. We now describe some applications of algorithms for Hamiltonian dynamics simulation, that can represent occasions for such comparative studies.

Another important research direction aims at combining elements of each family of algorithms and fine-tuning their implementation for specific problems. Relevant examples are a procedure [164] to use LCU on the steps of the quantum walk described in Sec. IV B 2 and the observation [227, 228] that, for the purpose of estimating energies, the steps of the quantum walk Eq. (27) are sufficient, rather than the Hamiltonian evolution unitary constructed from the quantum walk.

*a. Time-dependent observables and correlation functions.* A natural application of the algorithms outlined in Section IV B is the calculation of time-dependent electrostatic properties, presented in Section III B. The monitoring and control of electronic motion in atoms and molecules in real time has been made possible by advances in laser technology [229–232], and can be addressed on classical computers by a variety of numerical methods [233–241]. Achieving this goal requires solving the time-dependent Schrödinger equation with  $\hat{H}(t) = \hat{H}_0 + \hat{\mathbf{d}} \cdot \mathbf{E}(t)$ , where  $\hat{\mathbf{d}}$  is the dipole operator and  $\mathbf{E}(t)$  is a time-dependent electric field, and computing electronic densities and polarizabilities over the time-evolved wavefunction.

Another important set of observables based on the simulation of Hamiltonian dynamics are time-dependent correlation functions, such as dipole-dipole correlation functions  $d_{\mu\nu}(t) = \langle \Psi_0 | \hat{d}_\mu(t) \hat{d}_\nu | \Psi_0 \rangle$ . The electronic structure Hamiltonian and the dipole operators are mapped onto linear combinations of Pauli operators,  $\hat{d}_\mu = \sum_j c_{j\mu} \hat{P}_j$ , reducing the computation of dipole-dipole correlation functions to that of Pauli operators. The quantum circuit [129, 130, 242] for the calculation of time-dependent correlation functions between unitary operators  $\hat{A}$ ,  $\hat{B}$  is shown in Fig. 10. The calculation of time-dependent correlation functions is also an important occasion to study, demonstrate, benchmark and improve the performance of quantum circuits comprising ancillae and controlled operations, an important and recurring theme in quantum simulation [201, 243–245].

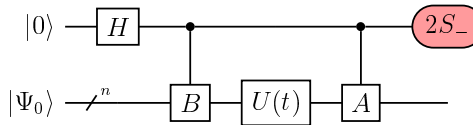


FIG. 10. Quantum circuit to measure the correlation function  $\langle \Psi_0 | \hat{U}^\dagger(t) \hat{A} \hat{U}(t) \hat{B} | \Psi_0 \rangle$  between unitaries  $\hat{A}$ ,  $\hat{B}$ , with  $S_- = \frac{X+iY}{2}$ .

*b. Quantum phase estimation (QPE).* QPE is one of the most important subroutines in quantum computation. It serves as a central building block for many quantum algorithms, and implements a measurement for essentially any Hermitian operator  $\hat{H}$ , most notably the Hamiltonian, through an algorithmic implementation of von Neumann's general measurement scheme [246]. Basic quantum-mechanical measurements are performed by decomposing  $\hat{H}$  into easily measurable terms, measuring each term separately, and collating results. QPE, on the other hand, prepares an eigenstate of the Hermitian operator to be measured in one register, and stores the corresponding eigenvalue in a second register. As such, QPE only requires a single shot and has the zero-variance property (if  $\Psi$  is an eigenfunction of  $\hat{H}$  with eigenvalue  $E_0$ , then the QPE measurement of  $\hat{H}$  returns  $E_0$  with probability 1).

More technically, QPE is used to estimate the eigenvalue  $u = e^{i2\pi\theta}$ ,  $0 < \theta < 1$ , corresponding to the eigenvector  $|u\rangle$  of a unitary  $\hat{U}$  [247, 248]. In the context of quantum simulation [131, 249–252]  $\hat{U}$  is a controllably accurate approximation of  $e^{-i\lambda\hat{H}}$  and  $\lambda$  a suitable rescaling factor, and QPE is thus used to compute eigenvalues corresponding to ground and excited state of  $\hat{H}$ . A simple but important observation is that eigenvalues of  $\hat{H}$  do not lie between 0 and  $2\pi$ , however one can scale and shift the Hamiltonian to an operator  $\hat{H}' = 2\pi(\hat{H} - E_1)/(E_2 - E_1)$ , where  $E_1/E_2$  is a lower/upper bound for the lowest/highest eigenvalue of  $\hat{H}$ , satisfying such a condition.

There are two main strategies for algorithmic QPE: the first makes use of the gate expensive inverse quantum Fourier transform (QFT) and, in an ideal quantum computer, could work with a single measurement, the second uses shallower circuits [248, 253, 254] but requires multiple measurements and classical post-processing. The former implementation of the QPE algorithm is described by the quantum circuit in Figure 11.

A register of qubits prepared in  $|u\rangle$  is coupled to  $t$  ancillae prepared in  $|0\rangle^{\otimes t}$ . Hadamard gates and controlled powers

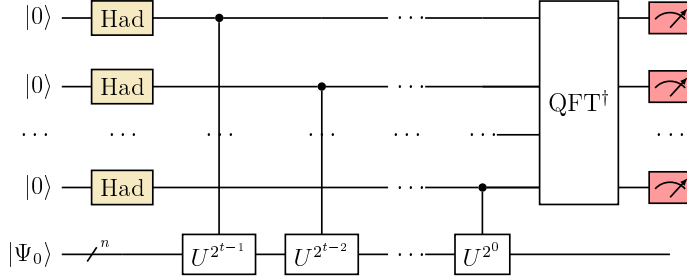


FIG. 11. Quantum circuit for the quantum phase estimation algorithm.

of  $\hat{U}$  are applied, and a subsequent inverse quantum Fourier transform [16, 19] leads to the final state

$$|\Psi\rangle = \sum_{z=0}^{2^t-1} \left( \sum_{k=0}^{2^t-1} \frac{e^{\frac{2\pi iz(2^t\theta-k)}{2^t}}}{2^t} \right) |z\rangle \otimes |u\rangle = \sum_{z=0}^{2^t-1} \Delta(z, \theta) |z\rangle \otimes |u\rangle . \quad (44)$$

If  $2^t\theta = k_0$  for some integer  $k_0 = 0 \dots 2^t - 1$ , then  $|\Psi\rangle = |k_0\rangle \otimes |\psi\rangle$ , and measuring the ancillae yields the binary representation of  $k_0 = 2^t\theta$  with probability 1. Otherwise, the probability distribution  $p(z) = |\Delta(z, \theta)|^2$  is concentrated around the integer  $k_0$  closest to  $2^t\theta$ ,  $p(k_0) \geq 4/\pi^2 \simeq 0.4$  [247].  $p(k_0)$  can be increased to  $1 - \varepsilon$  increasing the number of ancillae to  $t = \mathcal{O}(\log \varepsilon^{-1})$  [247].

A large body of work is dedicated to the optimization of QPE, from reducing the number of measurements needed to estimate eigenvalues in implementations not based on QFT [255], to methodologies for simultaneously determining multiple eigenvalues based on a classical time-series analysis [251, 256], to optimizing the implementation of QPE on contemporary quantum devices [252, 257].

c. *Adiabatic state preparation (ASP).* This technique approximates the ground state of an interacting system. The Hamiltonian is written as  $\hat{H} = \hat{H}_0 + \hat{H}_1$ , where the eigenvalues and eigenvectors of  $\hat{H}_0$  can be easily determined and encoded on a classical or a quantum computer (in chemistry, a natural choice is  $\hat{H}_0 = \hat{F} + \langle \Psi_{\text{HF}} | \hat{H} - \hat{F} | \Psi_{\text{HF}} \rangle$ , where  $\hat{F}$  is the Fock operator and  $\Psi_{\text{HF}}$  the Hartree-Fock state) and a curve of operators  $\hat{H}(s)$ ,  $0 \leq s \leq 1$ , with  $\hat{H}(s=0) = \hat{H}_0$  and  $\hat{H}(s=1) = \hat{H}$ , for example the segment  $\hat{H}(s) = \hat{H}_0 + s\hat{H}_1$ . The adiabatic theorem [258–263] states that, under opportune conditions, the solution of the Schrödinger equation

$$i \frac{d}{dt} |\Psi_t\rangle = \hat{H}(t/T) |\Psi_t\rangle , \quad 0 \leq t \leq T , \quad |\Psi_0\rangle = |\Phi_0(0)\rangle , \quad (45)$$

where  $|\Phi_0\rangle$  is the ground state of  $\hat{H}_0$ , converges to the ground state  $|\Phi_0(1)\rangle$  of  $\hat{H}$  in the large  $T$  limit,

$$\lim_{T \rightarrow \infty} |\Psi(T)\rangle = |\Phi_0(1)\rangle . \quad (46)$$

APS uses an operation suited for the quantum computer, the simulation of time evolution, to approximate Hamiltonian ground states. The method was originally proposed to address combinatorial optimization problems [264, 265] and later generalized to chemistry problems [266–268], as well as to a model of quantum computation, equivalent to the circuit model [38, 269, 270] and featuring interesting robustness properties against coherent and incoherent errors [271]. An important point is the following: the adiabatic theorem states that the time  $T$  to approximate the ground state with accuracy  $\varepsilon$  scales as  $\varepsilon^{-1} F(\gamma(s), f_1(s), f_2(s))$ , where  $F$  is a functional of the spectral gap  $\gamma(s)$  of  $\hat{H}(s)$ , and of the norms  $f_k(s) = \|\frac{d^k \hat{H}}{ds^k}\|(s)$  of the first and second derivative of  $\hat{H}$  along the adiabatic path [263]. The simulation time, and thus the computational cost of ASP, are especially connected with  $\gamma(s)$ : if such a quantity remains constant, or decreases as  $1/\text{poly}(M)$  where  $M$  is the number of spin-orbitals of the system, ASP is polynomially expensive [272, 273]. Otherwise, it can be exponentially expensive, in accordance with the QMA nature of the ground state problem.

### C. Simulation of Hamiltonian eigenstates

The problem of computing Hamiltonian eigenpairs,  $\hat{H} |\Phi_\mu\rangle = E_\mu |\Phi_\mu\rangle$  has enormous importance in chemistry (see e.g. the applications in Sections III A and IV B 6). This problem lies in the QMA complexity class, and thus

the existence of quantum algorithms outperforming their classical counterparts is not expected. However, heuristic quantum algorithms can, for certain structured problems, produce accurate approximations of ground and selected excited states at polynomial cost. In this Section, we review heuristic quantum algorithms for the computation of approximate Hamiltonian eigenstates and eigenvalues.

### 1. Variational quantum algorithms

Variational quantum algorithms (VQAs) have recently emerged as a widely used strategy to approximate Hamiltonian eigenstates/eigenvalues on quantum computers [15, 208, 274, 275], in part due to the fact that VQAs can be designed to operate within the limitations of contemporary quantum hardware. To define and implement a VQA, one first considers a parametrized wavefunction (or Ansatz) such as

$$|\Psi(\theta)\rangle = \hat{U}(\theta)|\Psi_0\rangle \quad , \quad \hat{U}(\theta) = \hat{u}_{n_g-1}(\theta_{n_g-1}) \dots \hat{u}_0(\theta_0) \quad , \quad (47)$$

where  $|\Psi_0\rangle$  is an initial wavefunction and the  $\{\hat{u}_k\}_k$  are parameterized unitaries. VQAs typically operate preparing the parametrized Ansatz (47) on a quantum computer, executing a circuit, measuring the obtained state, and updating the parameters  $\theta$  according to a classical optimization algorithm, based on the results of such measurements. The rather abstract structure of VQAs materializes in a wealth of particular implementations, which can be roughly classified in two families: variational quantum optimization (VQO) and variational quantum simulation (VQS) algorithms. The former approximate target states by minimizing a suitable cost function, and the latter approximate dynamical processes corresponding to curves in a Hilbert space by minimizing a suitable action functional.

### 2. The variational quantum eigensolver

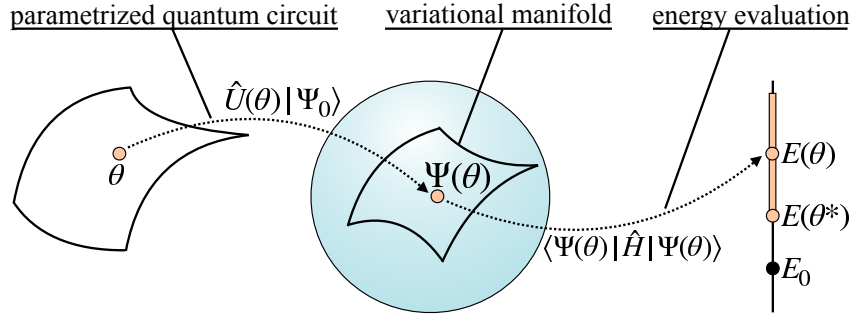


FIG. 12. Schematics of the VQE algorithm. A parametrized wavefunction is produced applying a parametrized unitary to an initial wavefunction. The set of wavefunctions accessible to the VQE algorithm is a manifold in the qubit Hilbert space, and the wavefunction minimizing the energy is chosen as an approximation of the ground state wavefunction.

A prominent example of a VQO is the variational quantum eigensolver (VQE) [276–279], schematized in Fig. 12, which approximates the ground-state energy and wavefunction of a Hamiltonian  $\hat{H}$  by minimizing the energy  $E(\theta) = \langle \Psi(\theta) | \hat{H} | \Psi(\theta) \rangle$  which, according to the variational principle, is an upper bound for the ground-state energy of  $\hat{H}$ . In the context of VQE, the quantum computer is used to efficiently evaluate  $E(\theta)$  and, in some implementations, its first and second derivatives [278, 280–283]. A simple and important aspect of VQO methods in general and VQE in particular, is that evaluating the energy on a quantum computer yields a statistical estimate,  $E(\theta) \sim \mu \pm \sigma$ , and thus optimizers used to update parameters have to take into account the statistical nature of quantum measurements [284]. Examples of such optimizers are the Simultaneous Perturbation Stochastic Approximation (SPSA) [285–287], ADaptive Moment estimation (ADAM) [288], and the Quantum Natural Gradient (QNG) [289]. SPSA is a stochastic optimization method where parameters are updated as  $\theta_{n+1} = \theta_n - a_n g(\theta_n)$ , where  $g(\theta_n)$  is an estimate of the gradient of the cost function obtained from random perturbation vectors of length  $c_n = c n^{-\gamma}$ , and the step length is defined as  $a_n = a n^{-1}$ . Careful optimization of the hyperparameters  $a, c, \gamma$  is key to an efficient optimization [290]. ADAM is a first-order gradient-based optimization of stochastic objective functions, based on adaptive estimates of lower-order moments, characterized by a simple implementation, modest memory requirements, and the ability to dynamically select a step size by maintaining a history of past gradients. Within QNG, the optimization dynamics is interpreted

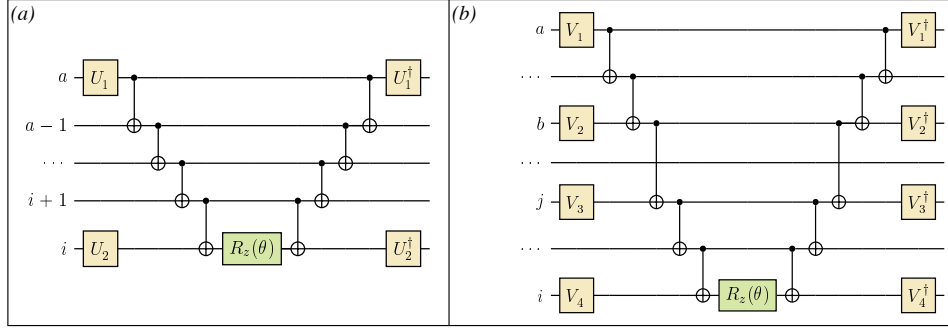


FIG. 13. Circuits for the exponentiation of the single (a) and double (b) excitation operators in Eq. (50). The repeated units across several qubits are shown in dashed lines, and the Clifford unitaries are  $(U_1, U_2) = \{(A_Y, A_X), (A_X, A_Y)\}$  and  $(V_1, V_2, V_3, V_4) = (A_X, A_X, A_Y, A_X), (A_Y, A_X, A_Y, A_Y), (A_X, A_Y, A_Y, A_Y), (A_X, A_X, A_X, A_Y), (A_Y, A_X, A_X, A_X), (A_X, A_Y, A_X, A_X), (A_Y, A_Y, A_Y, A_X), (A_Y, A_Y, A_X, A_Y)\}$  respectively.

as moving in the steepest descent direction with respect to the quantum information geometry, corresponding to the real part of the Fubini-Study metric tensor.

The accuracy and computational cost of VQE calculations are determined by the underlying Ansatz: on the one hand it should contain an accurate approximation to the ground state, on the other hand one desires circuits that can be easily executed on a quantum computer, with a well-behaved and rapidly convergent optimization of variational parameters [291, 292].

Two such Ansätze are reviewed in the following paragraphs.

*a. Quantum unitary coupled-cluster (q-UCC).* The ground state is approximated [250, 277, 279, 293–295] by an exponential Ansatz,

$$|\Psi\rangle = e^{\hat{T} - \hat{T}^\dagger} |\Psi_0\rangle \quad , \quad \hat{T} = \sum_{l=1}^k \hat{T}_l \quad , \quad \hat{T}_l = \sum_{a_0 \dots a_{l-1}} \sum_{i_0 \dots i_{l-1}} t_{i_0 \dots i_{l-1}}^{a_0 \dots a_{l-1}} \hat{a}_{a_0}^\dagger \dots \hat{a}_{a_{l-1}}^\dagger \hat{a}_{i_{l-1}} \dots \hat{a}_{i_0} \quad , \quad (48)$$

where  $|\Psi_0\rangle$  is a reference Slater determinant and  $\hat{T}$  is a linear combination of up to  $k$  particle-hole excitation operators that promote electrons from the hole (occupied) to the particle (unoccupied) orbitals of the reference state  $|\Psi_0\rangle$ . In many studies,  $\hat{T}$  is limited to single and double particle-hole excitations, defining the so-called q-UCCSD Ansatz. Standard coupled cluster theory is naturally implemented on a classical device, while its unitary variant is naturally implemented on a quantum device. Eq. (48) is factored into a product of exponentials of Pauli operators, using product formulas presented in Section IV B,

$$e^{\hat{T} - \hat{T}^\dagger} \simeq \prod_\mu e^{\theta_\mu (\hat{t}_\mu - \hat{t}_\mu^\dagger)} \quad . \quad (49)$$

Such a factorization is not unique, and optimal parameterization of fermionic wavefunctions via q-UCC has been recently explored [296]. For ease of implementation, Eq. (48) can be approximated [297] by a product of exponentials of individual one- and two-body operators,

$$e^{\hat{T} - \hat{T}^\dagger} \simeq \prod_{ia} e^{\theta_i^a (\hat{a}_a^\dagger \hat{a}_i - \hat{a}_i^\dagger \hat{a}_a)} \prod_{ijab} e^{\theta_{ij}^{ab} (\hat{a}_a^\dagger \hat{a}_b^\dagger \hat{a}_j \hat{a}_i - \hat{a}_i^\dagger \hat{a}_j^\dagger \hat{a}_b \hat{a}_a)} \quad . \quad (50)$$

In the JW representation, the exponentials in Eq. (50) are represented by the quantum circuits in Figure 13, each of which require  $\mathcal{O}(M)$  CNOT gates and have depth  $\mathcal{O}(M)$ . While the resulting quantum circuit has polynomial depth and number of gates, the  $\mathcal{O}(M^5)$  scaling of a basic implementation is sufficiently deep to limit implementations of q-UCCSD on today's quantum hardware.

Note that, when using a VQE solver, all Ansätze will give an energy that is above the true energy of the system provided that all the appropriate properties/symmetries (e.g. number of particles,  $S^2$ ,  $S_z$ ) are maintained.

*b. Hardware efficient Ansätze.* Hardware efficient Ansätze are typically designed to be experimentally feasible, because they are based on the realizable demands on connectivity and gate operations of a given chip. An example is shown in Fig. 14, and consists of alternating layers of arbitrary single-qubit gates and an entangling gate. While it is not guaranteed that such Ansätze contain good approximations to the state of interest, they enable important and conceptually insightful simulations on contemporary quantum devices.

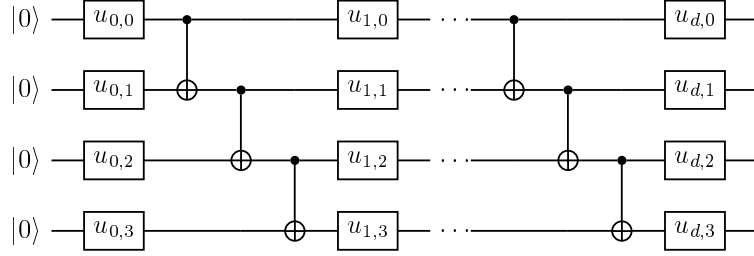


FIG. 14. Example of a hardware-efficient Ansatz for a 4-qubit problem, defined by layers of single-qubit gates  $u_{i,j}$  interspersed with CNOT gates acting on adjacent qubits on a device with linear connectivity.

It is worth emphasizing that some heuristic methods, epitomized by q-UCC, are based on hierarchies of increasingly more general (and therefore more accurate and expensive) Ansätze. As such, they offer the possibility to systematically converge results towards exact quantities, provided enough computational resources are available.

The design of compact Ansätze that join hardware efficiency and chemical insight is an active and valuable research area. An important progress in this regard was the development of schemes like qubit coupled-cluster [298] and ADAPT-VQE [299, 300]. In ADAPT-VQE, a pool of operators  $\{\hat{A}_i\}_i$  is chosen in advance, the ground state is approximated by the parametrized wavefunction  $|\Psi_\theta\rangle = \exp(\theta_n \hat{A}_{i_n}) \dots \exp(\theta_1 \hat{A}_{i_1}) |\Psi_0\rangle$ , where the angles are optimized variationally, and pool operators are appended to the circuit based on the value taken by the energy gradient  $g_i = \langle \Psi_\theta | [\hat{H}, \hat{A}_i] | \Psi_\theta \rangle$ . Numerical simulations showed ADAPT-VQE can improve over q-UCCSD in terms of the accuracy achievable for a given circuit depth.

### 3. Variational quantum simulation

Unlike VQO algorithms, which approximate a specific point of the Hilbert space by minimizing a cost function, VQS algorithms aim at approximating a curve in the Hilbert space of a system (corresponding to a dynamical process) by a curve of time-dependent parametrized wavefunctions,  $|\Psi_{\theta_t}\rangle$ . The flow of such a wavefunction is mapped to the evolution of the parameters  $\theta_t$ , which takes the form of a differential equation [301, 302]. For example, to variationally simulate Hamiltonian dynamics, parameters are evolved to make the vector

$$|\Delta\rangle = \frac{d}{dt} |\Psi_{\theta_t}\rangle + i\hat{H} |\Psi_{\theta_t}\rangle = \sum_k \frac{d\theta_k}{dt} |\Psi_{\theta_t}^k\rangle + i\hat{H} |\Psi_{\theta_t}\rangle \quad , \quad |\Psi_{\theta_t}^k\rangle = \frac{\partial}{\partial \theta_k} |\Psi_{\theta_t}\rangle \quad , \quad (51)$$

vanish. McLachlan's variational principle, i.e. minimization of  $\|\Delta\|^2$ , leads to the differential equation

$$b_r = \sum_k A_{rk} \frac{d\theta_k}{dt} \quad , \quad A_{rk} = \text{Re} (\langle \Psi_{\theta_t}^r | \Psi_{\theta_t}^k \rangle) \quad , \quad b_r = \text{Im} (\langle \Psi_{\theta_t}^r | \hat{H} | \Psi_{\theta_t}^k \rangle) \quad , \quad (52)$$

defining  $d\theta/dt$ . The quantities  $A, b$  are measured on the quantum computer [301, 302], and the classical computer uses such information to compute  $d\theta/dt$  and to update the parameters  $\theta$ . VQS algorithms are especially useful to carry out simulations of Hamiltonian dynamics on contemporary quantum hardware: while the Schrödinger equation can be solved by converting  $\exp(-it\hat{H})$  into a quantum circuit, as discussed in Section IV B, the depth of such a circuit generally increases polynomially with simulation time  $t$ . Like their VQO counterparts, VQS algorithms have heuristic nature, as they assume that the quantum state is represented by an Ansatz quantum circuit with fixed depth and structure at any time  $t$ . Depending on the problem of interest and the structure of the Ansatz, VQS algorithms may thus give inaccurate results.

### 4. Quantum diagonalization algorithms

In classical electronic structure, the search for ground and excited Hamiltonian eigenstates can be tackled relying on diagonalization methods. Given a Hamiltonian acting on a Hilbert space  $\mathcal{H}$  with dimension  $N$ , diagonalization methods are based on the synthesis of a collection of vectors  $\{|\mathbf{v}_a\rangle\}_{a=0}^{d-1}$  that form a basis for a  $d$ -dimensional subspace of  $\mathcal{H}$ . Once these vectors are available, the overlap and Hamiltonian matrices

$$S_{ab} = \langle \mathbf{v}_a | \mathbf{v}_b \rangle \quad , \quad H_{ab} = \langle \mathbf{v}_a | \hat{H} | \mathbf{v}_b \rangle \quad , \quad (53)$$

are computed, and the eigenvalue problem  $H\mathbf{c}_\mu = E_\mu S\mathbf{c}_\mu$  is solved, to determine approximate eigenvalues  $E_\mu$  and eigenvectors  $|\psi_\mu\rangle = \sum_a c_{a\mu} |\mathbf{v}_a\rangle$  of  $\hat{H}$  [303–305]. Recently, a number of quantum diagonalization algorithms have been conceived [306–313], that generate vectors  $|\mathbf{v}_a\rangle$  applying suitable operators to an initial state  $|\Psi_0\rangle$ ,

$$|\mathbf{v}_a\rangle = \hat{V}_a |\Psi_0\rangle \quad , \quad a = 0 \dots d - 1 \quad . \quad (54)$$

When the  $\hat{V}_a$  are unitary operators, the matrix elements Eq. (53) can be computed with the so-called Hadamard test circuit [130, 314], shown in Fig. 15. An alternative approach is to compile the operators  $\hat{V}_a^\dagger \hat{V}_b$  and  $\hat{V}_a^\dagger \hat{H} \hat{V}_b$  into linear combinations of Pauli operators, and measure them with the techniques described in Section II A, provided the number of Pauli operators grows polynomially with qubit number. Depending on the number and the nature of the vectors  $|\mathbf{v}_a\rangle$ , and on the structure of the problem at hand, quantum diagonalization algorithms can offer a polynomially expensive route to accurate approximation for ground and selected excited states. Examples of quantum diagonalization algorithms are briefly described in the remainder of this Section.

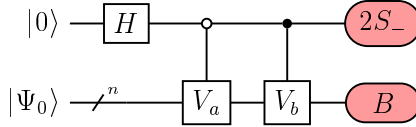


FIG. 15. Quantum circuit for the measurement of  $B_{ab} = \langle \mathbf{v}_a | \hat{B} | \mathbf{v}_b \rangle$ .

a. *Quantum subspace expansion (QSE).* In this algorithm, excited states are defined [306–308] by the Ansatz  $|\psi_\mu\rangle = \sum_a c_{a\mu} \hat{E}_a |\Psi_0\rangle$ , where  $\{\hat{E}_a\}_a$  is a set of pre-defined excitation operators. Common choices are Pauli operators of weight at most  $k$  and fermionic operators of rank at most  $k$ ,

$$\begin{aligned} P_k &= \left\{ \hat{\sigma}_{\mathbf{m}} = \hat{\sigma}_{m_{n-1}} \otimes \cdots \otimes \hat{\sigma}_{m_0} , \sigma_{m_i} \neq \mathbb{1} \text{ for at most } k \text{ indices} \right\} \quad , \\ F_k &= \left\{ \hat{a}_{i_0}^\dagger \dots \hat{a}_{i_{l-1}}^\dagger \hat{a}_{j_{l-1}} \dots \hat{a}_{j_0} , l \leq k \right\} \quad . \end{aligned} \quad (55)$$

b. *Quantum filter diagonalization (QFD).* This technique [201, 308, 311, 312] projects the Hamiltonian on a subspace spanned by a set of non-orthogonal quantum states generated via approximate time evolution,  $|\mathbf{v}_k\rangle = \exp(-ik\Delta t \hat{H}) |\Psi_0\rangle$ . QFD can be regarded as a quantum computational equivalent of classical filter diagonalization [315, 316], from which it inherits the connection with the Lanczos algorithm. Furthermore, it draws a profound connection between the two central problems of quantum simulation, namely BQP-complete Hamiltonian simulation and QMA-complete ground-state search. Finally, it provides a compelling framework to apply and test algorithms for approximate and variational time evolution, because QFD requires time evolution to generate a set of linearly independent states, a goal that can be achieved with less conservative approximations.

c. *Quantum equation of motion (q-EOM).* QSE computes total energies of ground and excited states, which can be subtracted to yield excitation energies. One route to compute excitation energies directly is the q-EOM method, well established in classical simulations and recently extended to quantum computation [310, 317–320]. In this framework, excitation energies are computed as

$$\Delta E_\mu = \frac{\langle \Psi_0 | [\hat{O}_\mu, \hat{H}, \hat{O}_\mu^\dagger] | \Psi_0 \rangle}{\langle \Psi_0 | [\hat{O}_\mu, \hat{O}_\mu^\dagger] | \Psi_0 \rangle} \quad , \quad (56)$$

where  $2[\hat{O}_\mu, \hat{H}, \hat{O}_\mu^\dagger] = [[\hat{O}_\mu, \hat{H}], \hat{O}_\mu^\dagger] + [\hat{O}_\mu, [\hat{H}, \hat{O}_\mu^\dagger]]$  and  $\hat{O}_\mu$  is an excitation operator expanded on a suitable basis. Commutators are introduced for several reasons. First, they can be used to compute energy differences directly rather than total energies: in fact, if  $\Psi_0$  is an eigenstate of  $\hat{H}$  with eigenvalue  $E_0$ , then  $\hat{H}\hat{O}_\mu^\dagger |\Psi_0\rangle = [\hat{H}, \hat{O}_\mu^\dagger] |\Psi_0\rangle + E_0 \hat{O}_\mu^\dagger |\Psi_0\rangle$  and thus  $\hat{O}_\mu^\dagger |\Psi_0\rangle$  is an eigenstate of  $\hat{H}$  with eigenvalue  $E_\mu$  if  $[\hat{H}, \hat{O}_\mu^\dagger] |\Psi_0\rangle = (E_\mu - E_0) \hat{O}_\mu^\dagger |\Psi_0\rangle = \Delta E_\mu \hat{O}_\mu^\dagger |\Psi_0\rangle$ . Second, they can project the Schrödinger equation onto a subspace of relevant electronic wavefunctions [317] and finally, the rank (number of electronic excitations) of a commutator is lower than the rank of a product, which has a beneficial impact on the computational cost. The variational problem of finding the stationary points of  $\Delta E_\mu$  leads to a generalized eigenvalue equation, the solutions of which are the excited-state energies.

d. *Quantum Lanczos (qLANCZOS).* In this algorithm, imaginary-time evolution (ITE)

$$|\mathbf{v}_k\rangle = \frac{e^{-k\Delta\tau \hat{H}} |\Psi_0\rangle}{\|e^{-k\Delta\tau \hat{H}} |\Psi_0\rangle\|} \quad , \quad k = 0 \dots d - 1 \quad , \quad (57)$$

is used to construct the subspace. QFD and qLANCZOS are examples of methods projecting the Schrödinger equation in a time series basis. ITE is a non-linear and non-unitary map, and thus is not naturally simulatable on a digital quantum computer. Various approaches to achieve this goal have been proposed, ranging from LCU-based to variational (see Sections IV B 4, IV C 3). Ref. [309] introduced an alternative approach to apply ITE on a quantum computer, termed quantum ITE or QITE, which is free from ancillae and controlled operations as well as from high-dimensional parameter optimizations. In the QITE method, a single step of ITE under a geometrically local term  $\hat{h}_m$  of the Hamiltonian is approximated by a unitary,  $e^{-\Delta\tau\hat{h}_m}|\Psi\rangle \propto e^{i\hat{A}_m}|\Psi\rangle$ , where  $\hat{A}_m = \sum_i x_{im}\hat{P}_{im}$ , the operators  $\hat{P}_{im}$  act on a neighborhood of the domain of  $\hat{h}_m$ , and the coefficients  $x_{im}$  are determined from local measurements [309]. While initial estimates in a limited set of problems show QITE to be resource-efficient compared to variational methods [245, 309, 321–324], an extensive numerical understanding of its performance and cost across different problems remains to be developed.

### 5. Applications of variational algorithms, and open problems

The design and improvement of heuristic algorithms for Hamiltonian eigenpair approximation is one of the most active research areas at the interface between quantum chemistry and quantum computation. Some of the directions of current and future research include: the creation of new Ansätze based on chemical notions, the extension of properties accessible to heuristic algorithms, and the economization of calculations.

The relationship between standard coupled-cluster  $e^{\hat{T}}|\Psi_0\rangle$  and unitary coupled-cluster Eq. (48) exemplifies how quantum computation can offer occasions to revive and reinterpret concepts and techniques from quantum chemistry. In both cases, the use of a cluster expansion is motivated by the qualitative accuracy of mean-field theory, and quantum computation provides a compelling framework to explore the theoretical and numerical differences between these theories [296, 325–327] especially in statically correlated situations. Circuits inspired by the q-UCCSD hierarchy but which directly substitute the fermionic field operators for spin ladder operators [298] have been suggested, as well as circuits based on the use of specific building blocks [181, 320, 328, 329] and symmetry preserving Ansätze [330].

The VQE algorithms has been extended to the calculation of excited states [331, 332] and the optimization of molecular orbitals [41, 333] by suitable modification of the cost function; to properties other than the ground-state energy [334, 335] by evaluation of suitable operators on the VQE wavefunction; and have been integrated in the workflow of solid-state chemistry [336, 337], transcorrelated Hamiltonian [43, 338] and quantum embedding [339–343] calculations. Modifying the VQE cost function has also been proposed as a technique to improve the quality or the convergence of ground-state simulations [344–346].

On the front of algorithm optimization, considerable effort has been devoted to reducing the measurement cost [347], for example by simultaneously measuring commuting subsets of the Pauli operators needed for the cost function [348–352], leveraging amplitude amplification [353], as well as adopting machine-learning techniques to extract more information from a given measurement dataset [354–356]. In the context of variational quantum algorithms for time evolution, important research directions are related with the simplification of the working equations (52), and the economization of the quantum measurement required by the simulation. For example, VQS techniques based on minimizing the distance (or maximizing the overlap) between states evolved in time exactly and variationally have been proposed [357, 358], along with techniques to economize quantum measurements introducing causal light-cone structure in the Ansatz [358–360]. Generalizing these techniques to chemical Hamiltonians is a compelling research direction, at the interface between quantum algorithms for physics and chemistry.

Furthermore, while molecular simulations generally require handling the N-electron wavefunction, recently proposed approaches have instead focused on the expression of the ground-state energy as a functional of the two-electron reduced density matrix [361, 362]. While recent results have indicated that they represent a promising direction for efficient molecular quantum simulations, additional research is needed to assess their full potential.

## V. ERROR MITIGATION TECHNIQUES FOR NEAR-TERM QUANTUM DEVICES

Until recently, executing quantum algorithms was only a theoretical possibility. Recent advances have made quantum computing devices available to the scientific community [363, 364], and computational packages to design and implement quantum algorithms [365–367].

Based on a broad range of architectures, such as superconducting [372, 373] and trapped ion [374, 375] qubits, such devices are capable of carrying out quantum computations of chemical systems on a limited scale, as exemplified in Table II, for a variety of technical reasons. In particular: (i) they comprise less than 100 qubits which, as seen in Section IV A, limits the number of electrons and orbitals that can be simulated, (ii) not all pairs of qubits are

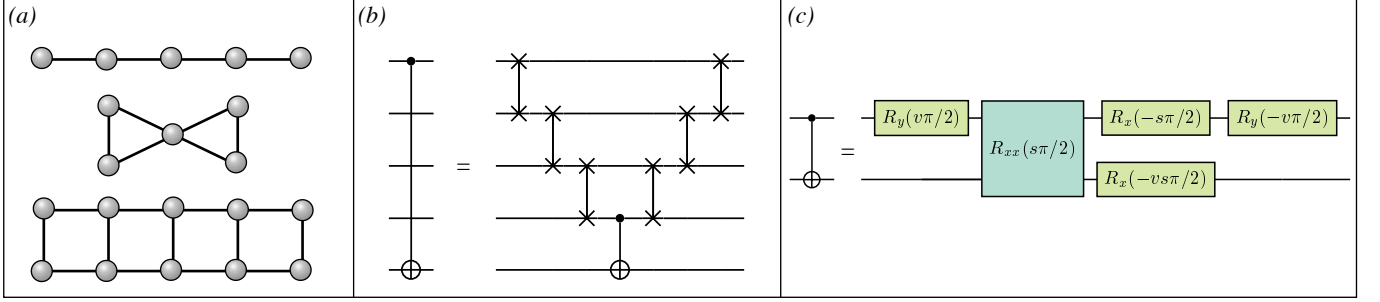


FIG. 16. Schematics (a) of chips with linear (top), bow-tie (middle) and ladder (bottom) topology. Implementation (b) of a CNOT gate between two non-adjacent qubits in a device with linear topology results in a significant overhead of SWAP gates. Implementation (c) of a CNOT gate on a device where native gates are single-qubit rotations and  $R_{xx}$  gates, with  $s, v = \pm 1$  (adapted from [368]).

reference	systems	number of qubits
[277]	$\text{HeH}^+$	2
[250, 290]	$\text{H}_2$	2
[290]	$\text{BeH}_2$	6
[290, 334]	$\text{LiH}$	4
[369]	$\text{H}_2\text{O}$	4
[370]	$\text{LiO}_2$ dimer	2
[371]	$\text{NaH}, \text{RbH}, \text{KH}$	4
[180]	$\text{H}_{12}$	12
[161]	$\text{H}_2\text{O}$	5

TABLE II. Some recent experiments on contemporary quantum hardware, aimed at simulating molecular systems .

physically connected, so that entangling gates have to be limited to adjacent qubits in the topology of the chip, or implemented incurring an overhead of SWAP gates, see Fig. 16, (iii) each device has a set of native gates, dictated by its architecture and manipulation techniques [376–378]; while such gates are universal (see Section II A 1), every gate in a quantum circuit has to be compiled into a product of native gates, (iv) quantum hardware is subject to decoherence and imperfect implementation of quantum operations. Errors occurring on a quantum device can be classified into coherent (unitary noise processes) and incoherent (non-unitary noise processes),

$$i\hbar \frac{d\rho_{\text{hw}}}{dt} = [\hat{H}_{\text{hw}}(t) + \hat{H}_c(t), \rho_{\text{hw}}] + \mathcal{L}_i(t, \rho_{\text{hw}}) \quad , \quad (58)$$

where  $\rho_{\text{hw}}$  is the density operator of the quantum hardware, and  $\hat{H}_c(t)$  and  $\mathcal{L}_i$  generate unitary and non-unitary evolution respectively. Coherent errors are exemplified by over- or under-rotation in qubit control pulses and qubit cross-talking, and examples of incoherent errors are the following single-qubit amplitude damping, phase damping and depolarization processes, respectively [16]

$$\mathcal{L}_a(\rho) = \gamma_a \mathcal{V}_{S_-}(\rho) \quad , \quad \mathcal{L}_p(\rho) = \gamma_p \mathcal{V}_Z(\rho) \quad , \quad \mathcal{L}_d(\rho) = \gamma_d \sum_m \mathcal{V}_{\sigma_m}(\rho) \quad , \quad (59)$$

where  $\mathcal{V}_A(\rho) = A\rho A^\dagger - A^\dagger A\rho - \rho A^\dagger A$ . Relaxation and dephasing processes occur on time scales  $T_1$  and  $T_2$  respectively, called qubit decoherence times. Deeper quantum circuits comprising more entangling gates have significantly larger biases and statistical uncertainties, due to the accumulation of coherent and incoherent errors, an effect that is especially pronounced when the execution time of the circuit is comparable with decoherence times of the qubits. Fully addressing the decoherence problem requires an advanced set of techniques, namely fault-tolerant quantum computation via quantum error correction [16, 379–382], which in turn requires extremely low error rates for qubit operations as well as a significant overhead of physical qubits [382, 383]. Enhancing the capabilities of near-term quantum computing hardware thus requires techniques to mitigate errors without requiring any additional quantum resources [275, 384, 385].

The emergent nature of quantum devices requires quantum chemists and quantum information scientists to conduct synergistic research, so that algorithmic implementations understand and leverage the nature, limitations and

features of quantum hardware, and the benchmarking and development of quantum hardware is driven by chemical applications. Conducting quantum simulations of chemical systems and designing algorithms for contemporary quantum hardware is also an important occasion to understand, characterize and mitigate errors induced by experimental imperfections. In the remainder of this section, we will describe some emerging techniques for mitigation of readout and gate errors.

*a. Readout error mitigation.* In theoretical considerations about quantum information protocols, a quantum device is often assumed to perform unbiased measurements. In practice, this assumption is often violated due to experimental imperfections and decoherence. Since measurements are a central part of any quantum simulation, this observation led to the development of readout error mitigation techniques.

Let us denote by  $\mathbf{p}_{\text{ideal}}$  the exact probability distribution for the outcomes of a quantum measurement, and  $\mathbf{p}_{\text{exp}}$  the probability distribution actually measured on the quantum hardware. The relationship between  $\mathbf{p}_{\text{ideal}}$  and  $\mathbf{p}_{\text{exp}}$  is in general captured by a complicated multidimensional function. However, if noise affecting measurements is weak, an accurate approximation can be obtained assuming the relation between the two probability distributions is given by a linear map,  $\mathbf{p}_{\text{exp}} = \Lambda \mathbf{p}_{\text{ideal}} + \Delta$ . The elements of  $\Lambda$  and  $\Delta$  can be estimated by choosing a set of calibration circuits  $\{c_k\}_k$  such that  $\mathbf{p}_{\text{ideal}}(k)$  can be computed analytically (e.g. circuits comprising a single layer of  $X$  gates), measuring the observable of interest over these circuits, obtaining probability distributions  $\mathbf{p}_{\text{exp}}(k)$ , and minimizing the distance  $\Lambda_0, \Delta_0 = \text{argmin}_{\Lambda, \Delta} \sum_k \|\mathbf{p}_{\text{exp}}(k) - \Lambda \mathbf{p}_{\text{ideal}}(k) - \Delta\|$ . The observable of interest is measured over a different state outside the calibration set, and the ideal probability distribution is reconstructed from the experimental one as  $\mathbf{p}_{\text{ideal}} \simeq \Lambda_0^{-1} [\mathbf{p}_{\text{exp}} - \Delta_0]$ . This method is solely based on classical post-processing and, although its cost scales exponentially with qubit number, suitable Ansätze on the structure of the pair  $\Lambda_0, \Delta_0$  can still give accurate maps at polynomial cost. Numerical studies have analyzed the impact of finite statistics (at the stage of estimation of probability distributions) on the protocol, and confirmed its approximate validity on a variety of publicly available prototypes of quantum chips [384–386].

*b. Gate error mitigation.* Recent work [386–388] has shown that the accuracy of computation based off expectation values of quantum observables, such as variational quantum algorithms, can be enhanced through an extrapolation of results from a collection of varying noisy experiments. Any quantum circuit can be expressed in terms of evolution under a time-dependent drive Hamiltonian  $\hat{H}_{\text{hw}}(t) = \sum_{\alpha} J_{\alpha}(t) \hat{P}_{\alpha}$  acting on the quantum hardware, where  $\hat{P}_{\alpha}$  represents some Hermitian operator of the quantum hardware and  $J_{\alpha}(t)$  the strength of the associated interaction. The expectation value  $B(\varepsilon)$  of an observable of interest over the state prepared by the drive  $\hat{H}_{\text{hw}}(t)$  in the presence of noise can be expressed as a power series around its zero-noise value,

$$B(\varepsilon) = b_0 + \sum_{k=1}^n b_k \varepsilon^k + \mathcal{O}(\varepsilon^{n+1}) , \quad (60)$$

where  $\varepsilon$  is a small noise parameter, and the coefficients in the expansion  $b_k$  are dependent on specific details of the noise model. The primary objective of gate error mitigation techniques is to experimentally obtain improved estimates to  $b_0$  despite using noisy quantum hardware. Assuming noise is time-translationally invariant a possible strategy [384], sketched in Fig. 17, is to perform a collection of experiments with stretched pulses,  $J_{\alpha}(t) \rightarrow c_i^{-1} J_{\alpha}(c_i^{-1} t)$  corresponding to noise strengths  $c_i \varepsilon$ , computing the corresponding expectation values  $B_i(\varepsilon) = B(c_i \varepsilon) = b_0 + \sum_k b_k (c_i \varepsilon)^k$ , and extracting  $b_0$  using a Richardson extrapolation [389]. This protocol, demonstrated for a variety of applications within and beyond molecular electronic structure [290], proved able to enhance the computational capabilities of quantum processors based on superconducting architectures, with no additional quantum resources or hardware modifications, which makes it very compelling for practical implementations on near-term hardware. It is important to notice that implementing the Richardson extrapolation protocol requires a profound understanding and control of the gates used in the circuit, which in turn motivated less general but more easily implementable schemes [334, 390]. Furthermore, unlike quantum error correction, gate error mitigation techniques do not allow for an indefinite extension of the computation time, and only provide corrections to expectation values, without correcting for the full quantum mechanical probability distributions.

There exist other gate error mitigation techniques, that achieve cancellation of errors, for example, by introducing quantum gates implementing unitary transformations generated by the symmetries of the system [391], or by resampling randomized circuits according to a quasi-probability distribution [386].

*c. Post-selection.* To mitigate the effect of hardware noise on the measurement results, one can also process hardware data by error-mitigation methods such as post-selection. When a Hamiltonian has  $\mathbb{Z}_2$  symmetries, as discussed in Sec. IV A 1, a wavefunction encoded on a quantum computer can be written as  $|\Psi\rangle = \hat{U}^\dagger \sum_s c_s |\Phi_s\rangle \otimes |\mathbf{s}\rangle$ , where the stabilizer parities  $\mathbf{s}$  label irreps of the symmetry group. In absence of noise, wavefunctions should have an intended stabilizer parity  $\mathbf{s}_0$ , to avoid mixing different irreps. However, during execution of the circuit, gate errors and qubit decoherence can induce nonzero overlap of the qubit state with subspaces of undesired parity. Post-selection can mitigate these undesirable effects by discarding measurement outcomes with the wrong parity [158, 159], as exemplified

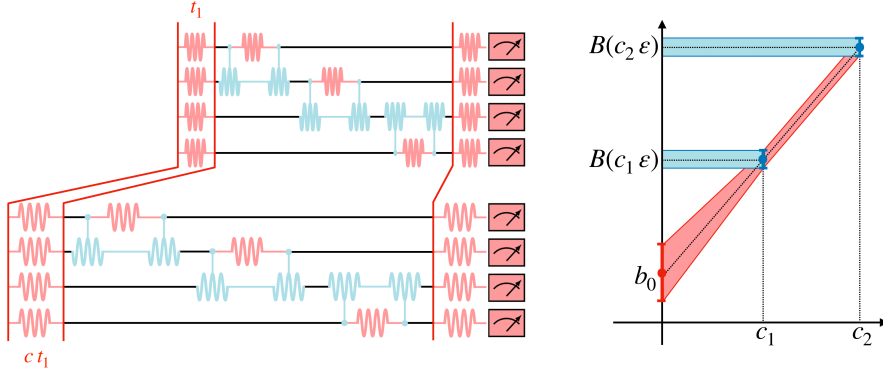


FIG. 17. Left: a measurement of the expectation value after rescaled state preparation is equivalent to a measurement under an amplified noise strength, if the noise is time-translation invariant. Right: illustration of gate error mitigation based on a first-order Richardson extrapolation to the zero-noise limit. This highlights that the variance of the mitigated estimate  $b_0$  is dependent on the variance of the unmitigated measurements, and the stretch factors  $c_i$ .

in Fig. 18. Compared against qubit reduction, post-selection requires more qubits, but typically retains the compact and efficient representation of fermionic and other operators as qubit operators, which the transformation  $\hat{U}$  typically undoes. In the context of molecular electronic structure, post-selection is particularly appealing when simulations are performed in the fermionic Fock space. While Fock space representations are often elected for ease of implementation, electronic structure wavefunctions have well-defined particle number and spin. When the JW representation is used in conjunction with low-rank decompositions of the Hamiltonian [201, 392], several such constants of motion quantities can be efficiently measured simultaneously with the one- and two-body contributions to the Hamiltonian, thereby projecting the electronic wavefunction into an eigenspace of constants of motion labeled by desired eigenvalues.

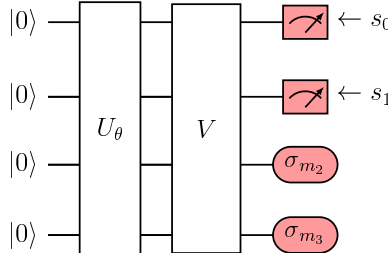


FIG. 18. Schematics of a post-selection procedure. The transformation  $\hat{V}$  achieves simultaneous measurement of the stabilizer generators, transformed to single-qubit operators acting on the first  $k = 2$  qubits, from which the stabilizer parities  $s_0, s_1$  are read. The other qubits are measured in  $X$ ,  $Y$  or  $Z$  basis depending on the Pauli string of interest, and measurement outcomes with the undesired parity are discarded.

## VI. CONCLUSION AND OUTLOOK

In this work, we explored emerging quantum computing algorithms for chemistry. In our discussion, we emphasized that quantum computers are special purpose machines, capable of solving certain structured problems with a polynomial amount of resources. These problems, exemplified by the simulation of Hamiltonian dynamics, can be projected to benefit from quantum algorithms. For other problems, exemplified by the simulation of Hamiltonian eigenpairs, quantum algorithms are based on heuristic approximation schemes.

We reviewed quantum algorithms for the simulation of Hamiltonian dynamics (product formulas, quantum walks, and LCU-based algorithms) and of Hamiltonian eigenstates (variational and diagonalization algorithms), highlighting some applications and open problems.

Given the emergent nature of quantum computation, a number of properties of quantum algorithms need to be characterized by systematic numerical studies over a set of diverse chemical problems, especially accuracy and computational cost. This characterization is needed for both heuristic (to help understand, establish and refine the underlying approximations) and non-heuristic algorithms (in order to determine when and how to apply them).

Chemists can contribute to this effort in many different ways. First, they can help design sets of chemical systems that interpolate between small, simple (e.g. H<sub>2</sub>) and large, realistic cases (e.g. enzymes). Achieving this goal can help demonstrate algorithms on today's devices, as well as lead to a more systematic understanding of their scalability and accuracy. Chemists can contribute also to the continuous development of new heuristics, by collaborating with quantum information scientists to optimally represent chemical wavefunctions and observables in terms of quantum circuits and measurements respectively.

#### ACKNOWLEDGMENT

We thank T. J. Lee, D. Maslov, H. Nakamura, A. Mezzacapo, and D. W. Berry for helpful feedback on the manuscript.

#### Appendix A: Glossary

acronym	meaning	acronym	meaning
2QR	two-qubit reduction	QITE	quantum imaginary-time evolution (ITE)
ADAM	adaptive moment estimation	qLANCZOS	quantum Lanczos
ASP	adiabatic state preparation	QMA	quantum Merlin-Arthur
BK	Bravyi-Kitaev	QM/MM	quantum mechanics / molecular mechanics approach
BQP	bounded-error quantum polynomial time	QNG	quantum natural gradient
CCSD	coupled-cluster (CC) with singles and doubles	QPE	quantum phase estimation
CCSD(T)	CCSD with perturbative estimate to connected triples	QSE	quantum subspace expansion
CI	configuration interaction	QSP	quantum signal processing
DFT	density functional theory	q-UCC	quantum unitary CC
FCI	full CI	q-UCCSD	q-UCC with singles and doubles
HF	Hartree-Fock	STO-6G	minimal basis where 6 primitive Gaussian orbitals are fit to a Slater-type orbital (STO)
JW	Jordan-Wigner	SPSA	simultaneous perturbation stochastic approximation
LCU	linear combination of unitaries	VQA	variational quantum (VQ) algorithm
OAA	oblivious amplitude amplification	VQE	VQ eigensolver
q-EOM	quantum equation of motion	VQO	VQ optimization
QFD	quantum filter diagonalization	VQS	VQ simulation
QFT	quantum Fourier transform		

TABLE III. Glossary of acronyms used throughout the present work.

- 
- [1] P. A. M. Dirac, The quantum theory of the electron, *Proc. Roy. Soc. London A, Math. Phys. Sci* **117**, 610 (1928).
  - [2] R. J. Bartlett and M. Musial, Coupled-cluster theory in quantum chemistry, *Rev. Mod. Phys* **79**, 291 (2007).
  - [3] T. Helgaker, S. Coriani, P. Jørgensen, K. Kristensen, J. Olsen, and K. Ruud, Recent advances in wave function-based methods of molecular-property calculations, *Chem. Rev* **112**, 543 (2012).
  - [4] T. Helgaker, P. Jørgensen, and J. Olsen, *Molecular electronic-structure theory* (John Wiley & Sons, 2014).
  - [5] R. P. Feynman, Simulating physics with computers, *Int. J. Theor. Phys* **21**, 467 (1982).
  - [6] S. Lloyd, Universal quantum simulators, *Science* **273**, 1073 (1996).
  - [7] D. S. Abrams and S. Lloyd, Simulation of many-body Fermi systems on a universal quantum computer, *Phys. Rev. Lett* **79**, 2586 (1997).
  - [8] I. M. Georgescu, S. Ashhab, and F. Nori, Quantum simulation, *Rev. Mod. Phys* **86**, 153 (2014).
  - [9] S. Mukamel, *Principles of nonlinear optical spectroscopy* (Oxford University Press, 1999).
  - [10] L. D. Barron, *Molecular light scattering and optical activity* (Cambridge University Press, 2009).
  - [11] G. Fleming, *Chemical applications of ultrafast spectroscopy* (Oxford University Press, 1986).
  - [12] C. Puzzarini, J. F. Stanton, and J. Gauss, Quantum-chemical calculation of spectroscopic parameters for rotational spectroscopy, *Int. Rev. Phys. Chem* **29**, 273 (2010).
  - [13] T. Helgaker, M. Jaszunski, and K. Ruud, Ab initio methods for the calculation of NMR shielding and indirect spin-spin coupling constants, *Chem. Rev* **99**, 293 (1999).

- [14] L. P. Hammett, Reaction rates and indicator acidities, *Chem. Rev.* **16**, 67 (1935).
- [15] B. Bauer, S. Bravyi, M. Motta, and G. Kim-Lic Chan, Quantum algorithms for quantum chemistry and quantum materials science, *Chem. Rev.* **120**, 12685 (2020).
- [16] M. A. Nielsen and I. L. Chuang, *Quantum computation and quantum information* (Cambridge University Press, 2010).
- [17] N. D. Mermin, *Quantum computer science: an introduction* (Cambridge University Press, 2007).
- [18] A. Y. Kitaev, A. Shen, M. N. Vyalyi, and M. N. Vyalyi, *Classical and quantum computation* (American Mathematical Society, 2002).
- [19] G. Benenti, G. Casati, D. Rossini, and G. Strini, *Principles of quantum computation and information: A Comprehensive Textbook* (World Scientific, 2019).
- [20] H.-K. Lo, T. Spiller, and S. Popescu, *Introduction to quantum computation and information* (World Scientific, 1998).
- [21] J. T. Seeley, M. J. Richard, and P. J. Love, The Bravyi-Kitaev transformation for quantum computation of electronic structure, *J. Chem. Phys.* **137**, 224109 (2012).
- [22] A. Y. Kitaev, Quantum computations: algorithms and error correction, *Rus. Math. Surv.* **52**, 1191 (1997).
- [23] A. W. Harrow, B. Recht, and I. L. Chuang, Efficient discrete approximations of quantum gates, *J. Math. Phys.* **43**, 4445 (2002).
- [24] C. M. Dawson and M. A. Nielsen, The Solovay-Kitaev algorithm, *Quant. Info. Comput.* **6**, 1 (2005).
- [25] V. Kliuchnikov, D. Maslov, and M. Mosca, Fast and efficient exact synthesis of single-qubit unitaries generated by Clifford and T gates, *Quant. Info. Comput.* **13**, 607–630 (2013).
- [26] N. J. Ross, Optimal ancilla-free Clifford+V approximation of z-rotations, *Quant. Info. Comput.* **15**, 932–950 (2015).
- [27] A. Barenco, C. H. Bennett, R. Cleve, D. P. DiVincenzo, N. Margolus, P. Shor, T. Sleator, J. A. Smolin, and H. Weinfurter, Elementary gates for quantum computation, *Phys. Rev. A* **52**, 3457 (1995).
- [28] M. Möttönen, J. J. Vartiainen, V. Bergholm, and M. M. Salomaa, Quantum circuits for general multiqubit gates, *Phys. Rev. Lett.* **93**, 130502 (2004).
- [29] V. V. Shende, S. S. Bullock, and I. L. Markov, Synthesis of quantum-logic circuits, *Trans. IEEE* **25**, 1000 (2006).
- [30] A. Daskin and S. Kais, Decomposition of unitary matrices for finding quantum circuits: application to molecular Hamiltonians, *J. Chem. Phys.* **134**, 144112 (2011).
- [31] D. Gottesman, The Heisenberg representation of quantum computers, quant-ph/9807006 (1998).
- [32] S. Aaronson and D. Gottesman, Improved simulation of stabilizer circuits, *Phys. Rev. A* **70**, 052328 (2004).
- [33] M. Nest, Classical simulation of quantum computation, the Gottesman-Knill theorem, and slightly beyond, *Quant. Info. Comput.* **10**, 3 (2008).
- [34] E. Bernstein and U. Vazirani, Quantum complexity theory, *SIAM J. Comput.* **26**, 1411 (1997).
- [35] J. Watrous, Quantum computational complexity, in *Encyclopedia of Complexity and Systems Science*, edited by R. A. Meyers (Springer New York, New York, NY, 2009) pp. 7174–7201.
- [36] R. P. Feynman, Quantum mechanical computers, *Found. Phys.* **16**, 507 (1986).
- [37] C. Zalka, Efficient simulation of quantum systems by quantum computers, *Progr. Phys.* **46**, 877 (1998).
- [38] J. Kempe, A. Kitaev, and O. Regev, The complexity of the local Hamiltonian problem, *SIAM J. Comput.* **35**, 1070 (2006).
- [39] M. Born and R. Oppenheimer, Zur Quantentheorie der Moleküle, *Ann. Phys.* **389**, 457 (1927).
- [40] A. Szabo and N. Ostlund, *Modern quantum chemistry: introduction to advanced electronic structure theory*, Dover Books on Chemistry (Dover Publications, 1989).
- [41] W. Mizukami, K. Mitarai, Y. O. Nakagawa, T. Yamamoto, T. Yan, and Y.-y. Ohnishi, Orbital optimized unitary coupled cluster theory for quantum computer, *Phys. Rev. Research* **2**, 033421 (2020).
- [42] T. Takeshita, N. C. Rubin, Z. Jiang, E. Lee, R. Babbush, and J. R. McClean, Increasing the representation accuracy of quantum simulations of chemistry without extra quantum resources, *Phys. Rev. X* **10**, 011004 (2020).
- [43] M. Motta, T. P. Gujarati, J. E. Rice, A. Kumar, C. Masteran, J. A. Latone, E. Lee, E. F. Valeev, and T. Y. Takeshita, Quantum simulation of electronic structure with a transcorrelated Hamiltonian: improved accuracy with a smaller footprint on the quantum computer, *Phys. Chem. Chem. Phys.* **22**, 24270 (2020).
- [44] M. Troyer and U. J. Wiese, Computational complexity and fundamental limitations to fermionic quantum Monte Carlo simulations, *Phys. Rev. Lett.* **94**, 170201 (2005).
- [45] N. Schuch and F. Verstraete, Computational complexity of interacting electrons and fundamental limitations of density functional theory, *Nat. Phys.* **5**, 732 (2009).
- [46] J. Paldus and X. Li, A critical assessment of coupled cluster method in quantum Chemistry, *Adv. Chem. Phys.* **110**, 1 (1999).
- [47] I. Shavitt and R. J. Bartlett, *Many-body methods in chemistry and physics* (Cambridge University Press, 2009).
- [48] S. R. White, Density matrix formulation for quantum renormalization groups, *Phys. Rev. Lett.* **69**, 2863 (1992).
- [49] S. R. White and R. L. Martin, Ab initio quantum chemistry using the density matrix renormalization group, *J. Chem. Phys.* **110**, 4127 (1999).
- [50] G. K.-L. Chan and M. Head-Gordon, Highly correlated calculations with a polynomial cost algorithm: a study of the density matrix renormalization group, *J. Chem. Phys.* **116**, 4462 (2002).
- [51] R. Olivares-Amaya, W. Hu, N. Nakatani, S. Sharma, J. Yang, and G. K.-L. Chan, The ab-initio density matrix renormalization group in practice, *J. Chem. Phys.* **142**, 034102 (2015).
- [52] G. K.-L. Chan, A. Keselman, N. Nakatani, Z. Li, and S. R. White, Matrix product operators, matrix product states, and ab initio density matrix renormalization group algorithms, *J. Chem. Phys.* **145**, 014102 (2016).
- [53] G. H. Booth, A. J. W. Thom, and A. Alavi, Fermion Monte Carlo without fixed nodes: a game of life, death, and annihilation in slater determinant space, *J. Chem. Phys.* **131**, 054106 (2009).

- [54] G. H. Booth, A. Gruneis, G. Kresse, and A. Alavi, Towards an exact description of electronic wavefunctions in real solids, *Nature* **493**, 365 (2013).
- [55] P. Reynolds, D. Ceperley, B. Alder, and J. Lester, Fixed-node quantum Monte Carlo for molecules, *J. Chem. Phys* **77**, 5593 (1982).
- [56] W. M. C. Foulkes, L. Mitas, R. J. Needs, and G. Rajagopal, Quantum Monte Carlo simulations of solids, *Rev. Mod. Phys* **73**, 33 (2001).
- [57] S. Zhang and H. Krakauer, Quantum Monte Carlo method using phase-free random walks with Slater determinants, *Phys. Rev. Lett* **90**, 136401 (2003).
- [58] M. Motta and S. Zhang, Ab initio computations of molecular systems by the auxiliary-field quantum Monte Carlo method, *WIREs Comput. Mol. Sci* **8**, e1364 (2018).
- [59] M. Motta, D. M. Ceperley, G. K.-L. Chan, J. A. Gomez, E. Gull, S. Guo, C. A. Jiménez-Hoyos, T. N. Lan, J. Li, F. Ma, *et al.*, Towards the solution of the many-electron problem in real materials: equation of state of the hydrogen chain with state-of-the-art many-body methods, *Phys. Rev. X* **7**, 031059 (2017).
- [60] R. M. Martin, *Electronic Structure: Basic theory and practical methods* (Cambridge University Press, 2004).
- [61] W. Kohn, Nobel lecture: Electronic structure of matter: wave functions and density functionals, *Rev. Mod. Phys* **71**, 1253 (1999).
- [62] S. Hammes-Schiffer, A conundrum for density functional theory, *Science* **355**, 28 (2017).
- [63] G. Knizia and G. K.-L. Chan, Density matrix embedding: a simple alternative to dynamical mean-field theory, *Phys. Rev. Lett* **109**, 186404 (2012).
- [64] G. Knizia and G. K.-L. Chan, Density matrix embedding: a strong-coupling quantum embedding theory, *J. Chem. Theory Comput* **9**, 1428 (2013).
- [65] S. Wouters, C. A. Jiménez-Hoyos, Q. Sun, and G. K.-L. Chan, A practical guide to density matrix embedding theory in quantum chemistry, *J. Chem. Theory Comput* **12**, 2706 (2016).
- [66] A. Georges, G. Kotliar, W. Krauth, and M. J. Rozenberg, Dynamical mean-field theory of strongly correlated fermion systems and the limit of infinite dimensions, *Rev. Mod. Phys.* **68**, 13 (1996).
- [67] D. Vollhardt, Dynamical mean-field theory for correlated electrons, *Ann. Phys* **524**, 1 (2012).
- [68] L. Hedin, New method for calculating the one-particle Green's function with application to the electron-gas problem, *Phys. Rev* **139**, A796 (1965).
- [69] K. Van Houcke, E. Kozik, N. Prokof'ev, and B. Svistunov, Diagrammatic Monte Carlo, *Phys. Proc* **6**, 95 (2010).
- [70] S. A. Kulagin, N. Prokof'ev, O. A. Starykh, B. Svistunov, and C. N. Varney, Bold diagrammatic Monte Carlo method applied to fermionized frustrated spins, *Phys. Rev. Lett* **110**, 070601 (2013).
- [71] T. Nguyen Lan, A. A. Kananenka, and D. Zgid, Rigorous ab initio quantum embedding for quantum chemistry using Green's function theory: Screened interaction, nonlocal self-energy relaxation, orbital basis, and chemical accuracy, *J. Chem. Theory Comput* **12**, 4856 (2016).
- [72] A. A. Kananenka, E. Gull, and D. Zgid, Systematically improvable multiscale solver for correlated electron systems, *Phys. Rev. B* **91**, 121111 (2015).
- [73] T. N. Lan, A. A. Kananenka, and D. Zgid, Communication: towards ab initio self-energy embedding theory in quantum chemistry, *J. Chem. Phys* **143**, 241102 (2015).
- [74] K. T. Williams, Y. Yao, J. Li, L. Chen, H. Shi, M. Motta, C. Niu, U. Ray, S. Guo, R. J. Anderson, *et al.*, Direct comparison of many-body methods for realistic electronic Hamiltonians, *Phys. Rev. X* **10**, 011041 (2020).
- [75] W. A. Al-Saidi, H. Krakauer, and S. Zhang, Auxiliary-field quantum Monte Carlo study of TiO and MnO molecules, *Phys. Rev. B* **73**, 075103 (2006).
- [76] W. Purwanto, S. Zhang, and H. Krakauer, An auxiliary-field quantum Monte Carlo study of the chromium dimer, *J. Chem. Phys* **142**, 064302 (2015).
- [77] W. Purwanto, S. Zhang, and H. Krakauer, Auxiliary-field quantum Monte Carlo calculations of the molybdenum dimer, *J. Chem. Phys* **144**, 244306 (2016).
- [78] J. Shee, B. Rudshteyn, E. J. Arthur, S. Zhang, D. R. Reichman, and R. A. Friesner, On achieving high accuracy in quantum chemical calculations of 3d transition metal-containing systems: a comparison of auxiliary-field quantum Monte Carlo with coupled cluster, density functional theory, and experiment for diatomic molecules, *J. Chem. Theory Comput* **15**, 2346 (2019).
- [79] J. Shee, M. Loipersberger, D. Hait, J. Lee, and M. Head-Gordon, Revealing the nature of electron correlation in transition metal complexes with symmetry breaking and chemical intuition, *J. Chem. Phys* **154**, 194109 (2021).
- [80] E. Rossi, G. L. Bendazzoli, S. Evangelisti, and D. Maynau, A full-configuration benchmark for the N<sub>2</sub> molecule, *Chem. Phys. Lett* **310**, 530 (1999).
- [81] K. D. Vogiatzis, D. Ma, J. Olsen, L. Gagliardi, and W. A. De Jong, Pushing configuration-interaction to the limit: Towards massively parallel mcscf calculations, *J. Chem. Phys* **147**, 184111 (2017).
- [82] E. I. Solomon, U. M. Sundaram, and T. E. Machonkin, Multicopper oxidases and oxygenases, *Chem. Rev* **96**, 2563 (1996).
- [83] N. Kitajima and Y. Moro-oka, Copper-dioxygen complexes. Inorganic and bioinorganic perspectives, *Chem. Rev* **94**, 737 (1994).
- [84] K. Samanta, C. A. Jiménez-Hoyos, and G. E. Scuseria, Exploring copper oxide cores using the projected Hartree-Fock method, *J. Chem. Theory Comput* **8**, 4944 (2012).
- [85] C. Gerdemann, C. Eicken, and B. Krebs, The crystal structure of catechol oxidase: new insight into the function of type-3 copper proteins, *Acc. Chem. Res* **35**, 183 (2002).

- [86] S. Sharma, K. Sivalingam, F. Neese, and G. K.-L. Chan, Low-energy spectrum of iron–sulfur clusters directly from many-particle quantum mechanics, *Nat. Chem.* **6**, 927 (2014).
- [87] Y. Kurashige, G. K.-L. Chan, and T. Yanai, Entangled quantum electronic wavefunctions of the Mn<sub>4</sub>CaO<sub>5</sub> cluster in photosystem II, *Nat. Chem.* **5**, 660 (2013).
- [88] Z. Li, S. Guo, Q. Sun, and G. K.-L. Chan, Electronic landscape of the P-cluster of nitrogenase as revealed through many-electron quantum wavefunction simulations, *Nat. Chem.* **11**, 1026–1033 (2019).
- [89] Z. Li, J. Li, N. S. Dattani, C. Umrigar, and G. K.-L. Chan, The electronic complexity of the ground-state of the FeMo cofactor of nitrogenase as relevant to quantum simulations, *J. Chem. Phys.* **150**, 024302 (2019).
- [90] V. G. Chilkuri, S. DeBeer, and F. Neese, Ligand field theory and angular overlap model based analysis of the electronic structure of homovalent iron-sulfur dimers, *Inorg. Chem.* **59**, 984 (2020).
- [91] L. Cao, O. Calderaru, and U. Ryde, Protonation and reduction of the FeMo cluster in nitrogenase studied by quantum mechanics/molecular mechanics (QM/MM) calculations, *J. Chem. Theory Comput.* **14**, 6653 (2018).
- [92] A. Damascelli, Z. Hussain, and Z.-X. Shen, Angle-resolved photoemission studies of the cuprate superconductors, *Rev. Mod. Phys.* **75**, 473 (2003).
- [93] A. Damascelli, Probing the electronic structure of complex systems by ARPES, *Phys. Scripta* **T109**, 61 (2004).
- [94] G. Onida, L. Reining, and A. Rubio, Electronic excitations: density-functional versus many-body Green's-function approaches, *Rev. Mod. Phys.* **74**, 601 (2002).
- [95] J. F. Stanton and R. J. Bartlett, The equation of motion coupled-cluster method. a systematic biorthogonal approach to molecular excitation energies, transition probabilities, and excited state properties, *J. Chem. Phys.* **98**, 7029 (1993).
- [96] A. L. Fetter and J. D. Walecka, *Quantum theory of many-particle systems* (Courier Corporation, 2012).
- [97] V. Barone, M. Biczysko, and C. Puzzarini, Quantum chemistry meets spectroscopy for astrochemistry: increasing complexity toward prebiotic molecules, *Acc. Chem. Res.* **48**, 1413 (2015).
- [98] J. M. Bowman, T. Carrington, and H.-D. Meyer, Variational quantum approaches for computing vibrational energies of polyatomic molecules, *Mol. Phys.* **106**, 2145 (2008).
- [99] T. J. Lee, J. M. Martin, and P. R. Taylor, An accurate ab initio quartic force field and vibrational frequencies for CH<sub>4</sub> and isotopomers, *J. Chem. Phys.* **102**, 254 (1995).
- [100] R. C. Fortenberry and T. J. Lee, Computational vibrational spectroscopy for the detection of molecules in space, in *Annu. Rep. Comput. Chem.*, Vol. 15 (Elsevier, 2019) pp. 173–202.
- [101] X. Huang, D. W. Schwenke, and T. J. Lee, What it takes to compute highly accurate rovibrational line lists for use in astrochemistry, *Acc. Chem. Res.* **54**, 1311 (2021).
- [102] K. Sadri, D. Lauvergnat, F. Gatti, and H.-D. Meyer, Numeric kinetic energy operators for molecules in polyspherical coordinates, *J. Chem. Phys.* **136**, 234112 (2012).
- [103] D. P. Tew, N. C. Handy, S. Carter, S. Irle, and J. Bowman, The internal coordinate path Hamiltonian; application to methanol and malonaldehyde, *Mol. Phys.* **101**, 3513 (2003).
- [104] A. Viel, M. D. Coutinho-Neto, and U. Manthe, The ground state tunneling splitting and the zero point energy of malonaldehyde: a quantum Monte Carlo determination, *J. Chem. Phys.* **126**, 024308 (2007).
- [105] M. Beck, A. Jäckle, G. Worth, and H.-D. Meyer, The multiconfiguration time-dependent Hartree (MCTDH) method: a highly efficient algorithm for propagating wavepackets, *Phys. Rep.* **324**, 1 (2000).
- [106] V. Vaida, Spectroscopy of photoreactive systems: Implications for atmospheric chemistry, *J. Phys. Chem. A* **113**, 5 (2008).
- [107] U. Heiter, K. Lind, M. Asplund, P. S. Barklem, M. Bergemann, L. Magrini, T. Masseron, Š. Mikolaitis, J. Pickering, and M. Ruffoni, Atomic and molecular data for optical stellar spectroscopy, *Phys. Scripta* **90**, 054010 (2015).
- [108] D. Smith, Formation and destruction of molecular ions in interstellar clouds, *Proc. Roy. Soc. London A, Math. Phys. Sci.* **324**, 257 (1988).
- [109] P. Schilke, D. Benford, T. Hunter, D. Lis, and T. Phillips, A line survey of Orion-KL from 607 to 725 GHz, *Astrophys. J., Suppl. Ser.* **132**, 281 (2001).
- [110] M. Agúndez, J. Cernicharo, J. Pardo, M. Guélin, and T. Phillips, Tentative detection of phosphine in IRC+ 10216, *Astron. Astrophys.* **485**, L33 (2008).
- [111] M. Agúndez, J. Cernicharo, and M. Guélin, New molecules in IRC+ 10216: confirmation of C<sub>5</sub>S and tentative identification of MgCCH, NCCP, and SiH<sub>3</sub>CN, *Astron. Astrophys.* **570**, A45 (2014).
- [112] J. A. Pople, Nobel lecture: Quantum chemical models, *Rev. Mod. Phys.* **71**, 1267 (1999).
- [113] S. R. Hartshorn, *Aliphatic nucleophilic substitution* (Cambridge University Press, 1973).
- [114] L. G. Wade, *Organic chemistry* (Pearson, 2013).
- [115] C. J. Cramer and D. G. Truhlar, Implicit solvation models: equilibria, structure, spectra, and dynamics, *Chem. Rev.* **99**, 2161 (1999).
- [116] A. Klamt, The COSMO and COSMO-RS solvation models, *WIREs Comput. Mol. Sci.* **1**, 699 (2011).
- [117] B. Mennucci, Polarizable continuum model, *WIREs Comput. Mol. Sci.* **2**, 386 (2012).
- [118] H. M. Senn and W. Thiel, QM/MM methods for biomolecular systems, *Angew. Chem., Int. Ed. Engl.* **48**, 1198 (2009).
- [119] J. Bernstein, *Polymorphism in Molecular Crystals* (International Union of Crystal, 2020).
- [120] S. L. Price, D. E. Braun, and S. M. Reutzel-Edens, Can computed crystal energy landscapes help understand pharmaceutical solids?, *Chem. Comm.* **52**, 7065 (2016).
- [121] G. M. Day, W. S. Motherwell, and W. Jones, A strategy for predicting the crystal structures of flexible molecules: the polymorphism of phenobarbital, *Phys. Chem. Chem. Phys.* **9**, 1693 (2007).
- [122] F. Lombardo, P. V. Desai, R. Arimoto, K. E. Desino, H. Fischer, C. E. Keefer, C. Petersson, S. Winiwarter, and F. Broccatelli, In silico absorption, distribution, metabolism, excretion, and pharmacokinetics (ADME-PK): utility and

- best practices, *J. Med. Chem.* **60**, 9097 (2017).
- [123] K. Kamat, R. Guo, S. M. Reutzel-Edens, S. L. Price, and B. Peters, Diabat method for polymorph free energies: Extension to molecular crystals, *J. Chem. Phys.* **153**, 244105 (2020).
- [124] G. J. Beran, Modeling polymorphic molecular crystals with electronic structure theory, *Chem. Rev.* **116**, 5567 (2016).
- [125] L.-A. Wu and D. Lidar, Qubits as parafermions, *J. Math. Phys.* **43**, 4506 (2002).
- [126] C. D. Batista and G. Ortiz, Algebraic approach to interacting quantum systems, *Adv. Phys.* **53**, 1 (2004).
- [127] S. B. Bravyi and A. Y. Kitaev, Fermionic quantum computation, *Ann. Phys.* **298**, 210 (2002).
- [128] P. Jordan and E. P. Wigner, Über das paulische äquivalenzverbot, in *The Collected Works of Eugene Paul Wigner* (Springer, 1993) pp. 109–129.
- [129] G. Ortiz, J. E. Gubernatis, E. Knill, and R. Laflamme, Quantum algorithms for fermionic simulations, *Phys. Rev. A* **64**, 022319 (2001).
- [130] R. Somma, G. Ortiz, J. E. Gubernatis, E. Knill, and R. Laflamme, Simulating physical phenomena by quantum networks, *Phys. Rev. A* **65**, 042323 (2002).
- [131] A. Aspuru-Guzik, A. D. Dutoi, P. J. Love, and M. Head-Gordon, Simulated quantum computation of molecular energies, *Science* **309**, 1704 (2005).
- [132] J. D. Whitfield, J. Biamonte, and A. Aspuru-Guzik, Simulation of electronic structure Hamiltonians using quantum computers, *Mol. Phys.* **109**, 735 (2011).
- [133] S. Bravyi, J. M. Gambetta, A. Mezzacapo, and K. Temme, Tapering off qubits to simulate fermionic Hamiltonians, *arXiv preprint arXiv:1701.08213* (2017).
- [134] K. Setia, R. Chen, J. E. Rice, A. Mezzacapo, M. Pistoia, and J. D. Whitfield, Reducing qubit requirements for quantum simulations using molecular point group symmetries, *J. Chem. Theory Comput.* **16**, 6091 (2020).
- [135] P. Faist, S. Nezami, V. V. Albert, G. Salton, F. Pastawski, P. Hayden, and J. Preskill, Continuous symmetries and approximate quantum error correction, *Phys. Rev. X* **10**, 041018 (2020).
- [136] M. Steudtner and S. Wehner, Fermion-to-qubit mappings with varying resource requirements for quantum simulation, *New J. Phys.* **20**, 063010 (2018).
- [137] D. Gottesman, *Stabilizer codes and quantum error correction*, Ph.D. thesis, California Institute of Technology (1997).
- [138] M. P. Fisher, P. B. Weichman, G. Grinstein, and D. S. Fisher, Boson localization and the superfluid-insulator transition, *Phys. Rev. B* **40**, 546 (1989).
- [139] M. H. Levitt, *Spin dynamics: basics of nuclear magnetic resonance* (John Wiley & Sons, 2013).
- [140] E. B. Wilson, J. C. Decius, and P. C. Cross, *Molecular vibrations: the theory of infrared and Raman vibrational spectra* (Courier Corporation, 1980).
- [141] N. J. Turro, *Modern molecular photochemistry* (University science books, 1991).
- [142] Y. Hong, Y. Wu, S. Wu, X. Wang, and J. Zhang, Overview of computational simulations in quantum dots, *Isr. J. Chem.* **59**, 661 (2019).
- [143] L. Veis, J. Višňák, H. Nishizawa, H. Nakai, and J. Pittner, Quantum chemistry beyond Born-Oppenheimer approximation on a quantum computer: A simulated phase estimation study, *Int. J. Quantum Chem.* **116**, 1328 (2016).
- [144] S. Joshi, A. Shukla, H. Katiyar, A. Hazra, and T. Mahesh, Estimating Franck-Condon factors using an NMR quantum processor, *Phys. Rev. A* **90**, 022303 (2014).
- [145] A. Teplukhin, B. K. Kendrick, and D. Babikov, Calculation of molecular vibrational spectra on a quantum annealer, *J. Chem. Theory Comput.* **15**, 4555 (2019).
- [146] S. McArdle, A. Mayorov, X. Shan, S. Benjamin, and X. Yuan, Digital quantum simulation of molecular vibrations, *Chem. Sci.* **10**, 5725 (2019).
- [147] N. P. Sawaya and J. Huh, Quantum algorithm for calculating molecular vibronic spectra, *J. Phys. Chem. Lett.* **10**, 3586 (2019).
- [148] A. Macridin, P. Spentzouris, J. Amundson, and R. Harnik, Electron-phonon systems on a universal quantum computer, *Phys. Rev. Lett.* **121**, 110504 (2018).
- [149] A. Macridin, P. Spentzouris, J. Amundson, and R. Harnik, Digital quantum computation of fermion-boson interacting systems, *Phys. Rev. A* **98**, 042312 (2018).
- [150] C. Sabín, Digital quantum simulation of linear and nonlinear optical elements, *Quantum Rep.* **2**, 208 (2020).
- [151] A. Di Paolo, P. K. Barkoutsos, I. Tavernelli, and A. Blais, Variational quantum simulation of ultrastrong light-matter coupling, *Phys. Rev. Research* **2**, 033364 (2020).
- [152] N. P. Sawaya, T. Menke, T. H. Kyaw, S. Johri, A. Aspuru-Guzik, and G. G. Guerreschi, Resource-efficient digital quantum simulation of  $d$ -level systems for photonic, vibrational, and spin- $s$  Hamiltonians, *npj Quantum Inf.* **6**, 1 (2020).
- [153] N. P. Sawaya, F. Paesani, and D. P. Tabor, Near-and long-term quantum algorithmic approaches for vibrational spectroscopy, *arXiv preprint arXiv:2009.05066* (2020).
- [154] R. Ball, Fermions without fermion fields, *Phys. Rev. Lett.* **95**, 176407 (2005).
- [155] F. Verstraete and J. I. Cirac, Mapping local Hamiltonians of fermions to local Hamiltonians of spins, *J. Stat. Mech.* **2005**, P09012 (2005).
- [156] V. Havlíček, M. Troyer, and J. D. Whitfield, Operator locality in the quantum simulation of fermionic models, *Phys. Rev. A* **95**, 032332 (2017).
- [157] K. Setia, S. Bravyi, A. Mezzacapo, and J. D. Whitfield, Superfast encodings for fermionic quantum simulation, *Phys. Rev. Research* **1**, 033033 (2019).

- [158] X. Bonet-Monroig, R. Sagastizabal, M. Singh, and T. O'Brien, Low-cost error mitigation by symmetry verification, *Phys. Rev. A* **98**, 062339 (2018).
- [159] S. McArdle, X. Yuan, and S. Benjamin, Error-mitigated digital quantum simulation, *Phys. Rev. Lett* **122**, 180501 (2019).
- [160] V. E. Elfving, M. Millaruelo, J. A. Gámez, and C. Gogolin, Simulating quantum chemistry in the seniority-zero space on qubit-based quantum computers, *Phys. Rev. A* **103**, 032605 (2021).
- [161] A. Eddins, M. Motta, T. P. Gujarati, S. Bravyi, A. Mezzacapo, C. Hadfield, and S. Sheldon, Doubling the size of quantum simulators by entanglement forging, *arXiv preprint arXiv:2104.10220* (2021).
- [162] A. M. Childs, *Quantum information processing in continuous time*, Ph.D. thesis, Massachusetts Institute of Technology (2004).
- [163] A. M. Childs, Universal computation by quantum walk, *Phys. Rev. Lett* **102**, 180501 (2009).
- [164] D. W. Berry, A. M. Childs, and R. Kothari, Hamiltonian simulation with nearly optimal dependence on all parameters, in *Proc. FOCS* (IEEE, 2015) pp. 792–809.
- [165] G. H. Low and I. L. Chuang, Optimal Hamiltonian simulation by quantum signal processing, *Phys. Rev. Lett* **118**, 010501 (2017).
- [166] D. W. Berry, A. M. Childs, R. Cleve, R. Kothari, and R. D. Somma, Simulating Hamiltonian dynamics with a truncated Taylor series, *Phys. Rev. Lett* **114**, 090502 (2015).
- [167] G. H. Low and I. L. Chuang, Hamiltonian simulation by qubitization, *Quantum* **3**, 163 (2019).
- [168] A. M. Childs, D. Maslov, Y. Nam, N. J. Ross, and Y. Su, Toward the first quantum simulation with quantum speedup, *Proc. Natl. Acad. Sci. USA* **115**, 9456 (2018).
- [169] H. F. Trotter, On the product of semi-groups of operators, *Proc. AMS* **10**, 545 (1959).
- [170] M. Suzuki, Generalized Trotter's formula and systematic approximants of exponential operators and inner derivations with applications to many-body problems, *Comm. Math. Phys* **51**, 183 (1976).
- [171] M. Suzuki, General theory of fractal path integrals with applications to many-body theories and statistical physics, *J. Math. Phys* **32**, 400 (1991).
- [172] A. M. Childs, Y. Su, M. C. Tran, N. Wiebe, and S. Zhu, Theory of Trotter error with commutator scaling, *Phys. Rev. X* **11**, 011020 (2021).
- [173] M. Motta, E. Ye, J. R. McClean, Z. Li, A. J. Minnich, R. Babbush, and G. K.-L. Chan, Low rank representations for quantum simulation of electronic structure, *npj Quantum Inf* **7**, 1 (2021).
- [174] D. Aharonov and A. Ta-Shma, Adiabatic quantum state generation and statistical zero knowledge, in *Proc. ACM* (2003) pp. 20–29.
- [175] D. W. Berry, G. Ahokas, R. Cleve, and B. C. Sanders, Efficient quantum algorithms for simulating sparse Hamiltonians, *Comm. Math. Phys* **270**, 359 (2007).
- [176] D. Poulin, M. B. Hastings, D. Wecker, N. Wiebe, A. C. Doberty, and M. Troyer, The Trotter step size required for accurate quantum simulation of quantum chemistry, *Quant. Info. Comput* **15**, 361–384 (2015).
- [177] R. Babbush, N. Wiebe, J. McClean, J. McClain, H. Neven, and G. K.-L. Chan, Low-depth quantum simulation of materials, *Phys. Rev. X* **8**, 011044 (2018).
- [178] Z. Jiang, K. J. Sung, K. Kechedzhi, V. N. Smelyanskiy, and S. Boixo, Quantum algorithms to simulate many-body physics of correlated fermions, *Phys. Rev. Appl* **9**, 044036 (2018).
- [179] I. D. Kivlichan, J. McClean, N. Wiebe, C. Gidney, A. Aspuru-Guzik, G. K.-L. Chan, and R. Babbush, Quantum simulation of electronic structure with linear depth and connectivity, *Phys. Rev. Lett* **120**, 110501 (2018).
- [180] F. Arute *et al.*, Hartree-Fock on a superconducting qubit quantum computer, *Science* **369**, 1084 (2020).
- [181] Y. Matsuzawa and Y. Kurashige, Jastrow-type decomposition in quantum chemistry for low-depth quantum circuits, *J. Chem. Theory Comput* **16**, 944 (2020).
- [182] J. L. Whitten, Coulombic potential-energy integrals and approximations, *J. Chem. Phys* **58**, 4496 (1973).
- [183] B. I. Dunlap, J. W. D. Connolly, and J. R. Sabin, Applicability of LCAO-X $\alpha$  methods to molecules containing transition-metal atoms – nickel atom and nickel hydride, *Int. J. Quantum Chem. Symp* **12**, 81 (1977).
- [184] B. I. Dunlap, J. W. D. Connolly, and J. R. Sabin, On some approximations in applications of X $\alpha$  theory, *J. Chem. Phys* **71**, 3396 (1979).
- [185] M. Feyereisen, G. Fitzgerald, and A. Komornicki, Use of approximate integrals in ab initio theory. An application in MP2 calculations, *Chem. Phys. Lett* **208**, 359 (1993).
- [186] A. Komornicki and G. Fitzgerald, Molecular gradients and Hessians implemented in density functional theory, *J. Chem. Phys* **98**, 1398 (1993).
- [187] O. Vahtras, J. Almlöf, and M. W. Feyereisen, Integral approximations for LCAO-SCF calculations, *Chem. Phys. Lett* **213**, 514 (1993).
- [188] A. P. Rendell and T. J. Lee, Coupled-cluster theory employing approximate integrals: An approach to avoid the input/output and storage bottlenecks, *J. Chem. Phys* **101**, 400 (1994).
- [189] R. A. Kendall and H. A. Fruchtl, The impact of the resolution of the identity approximate integral method on modern ab initio algorithm development, *Theor. Chem. Acc* **97**, 158 (1997).
- [190] F. Weigend, A fully direct RI-HF algorithm: implementation, optimized auxiliary basis sets, demonstration of accuracy and efficiency, *Phys. Chem. Chem. Phys* **4**, 4285 (2002).
- [191] N. H. F. Beebe and J. Linderberg, Simplifications in the generation and transformation of two-electron integrals in molecular calculations, *Int. J. Quantum Chem* **12**, 683 (1977).
- [192] I. Roeggen and E. Wisloff-Nilssen, On the Beebe-Linderberg 2-electron integral approximation, *Chem. Phys. Lett* **132**, 154 (1986).

- [193] H. Koch, A. S. de Meras, and T. B. Pedersen, Reduced scaling in electronic structure calculations using Cholesky decompositions, *J. Chem. Phys.* **118**, 9481 (2003).
- [194] F. Aquilante, T. B. Pedersen, and R. Lindh, Low-cost evaluation of the exchange Fock matrix from Cholesky and density fitting representations of the electron repulsion integrals, *J. Chem. Phys.* **126**, 194106 (2007).
- [195] F. Aquilante, L. Gagliardi, T. B. Pedersen, and R. Lindh, Atomic Cholesky decompositions: a route to unbiased auxiliary basis sets for density fitting approximation with tunable accuracy and efficiency, *J. Chem. Phys.* **130**, 154107 (2009).
- [196] M. Motta, J. Shee, S. Zhang, and G. K.-L. Chan, Efficient ab initio auxiliary-field quantum Monte Carlo calculations in Gaussian bases via low-rank tensor decomposition, *J. Chem. Theory Comput.* **15**, 3510 (2019).
- [197] B. Peng and K. Kowalski, Highly efficient and scalable compound decomposition of two-electron integral tensor and its application in coupled cluster calculations, *J. Chem. Theory Comput.* **13**, 4179 (2017).
- [198] E. G. Hohenstein, R. M. Parrish, and T. J. Martínez, Tensor hypercontraction density fitting I: quartic scaling second-and third-order Møller-Plesset perturbation theory, *J. Chem. Phys.* **137**, 044103 (2012).
- [199] R. M. Parrish, E. G. Hohenstein, T. J. Martínez, and C. D. Sherrill, Tensor hypercontraction II: least-squares renormalization, *J. Chem. Phys.* **137**, 224106 (2012).
- [200] R. M. Parrish, E. G. Hohenstein, N. F. Schunck, C. D. Sherrill, and T. J. Martínez, Exact tensor hypercontraction: a universal technique for the resolution of matrix elements of local finite-range  $N$ -body potentials in many-body quantum problems, *Phys. Rev. Lett.* **111**, 132505 (2013).
- [201] J. Cohn, M. Motta, and R. M. Parrish, Quantum filter diagonalization with double-factorized Hamiltonians, *arXiv preprint arXiv:2104.08957* (2021).
- [202] G. H. Low, V. Kliuchnikov, and N. Wiebe, Well-conditioned multiproduct Hamiltonian simulation, *arXiv preprint arXiv:1907.11679* (2019).
- [203] J. Haah, M. Hastings, R. Kothari, and G. H. Low, Quantum algorithm for simulating real time evolution of lattice Hamiltonians, in *Proc. FOCS* (IEEE, 2018) pp. 350–360.
- [204] A. M. Childs and Y. Su, Nearly optimal lattice simulation by product formulas, *Phys. Rev. Lett.* **123**, 050503 (2019).
- [205] M. B. Hastings, D. Wecker, B. Bauer, and M. Troyer, Improving quantum algorithms for quantum chemistry, *Quantum Inf. Comput.* **15**, 1–21 (2015).
- [206] A. M. Childs, A. Ostrander, and Y. Su, Faster quantum simulation by randomization, *Quantum* **3**, 182 (2019).
- [207] E. Campbell, Random Compiler for Fast Hamiltonian Simulation, *Phys. Rev. Lett.* **123**, 070503 (2019).
- [208] Y. Cao, J. Romero, J. P. Olson, M. Degroote, P. D. Johnson, M. Kieferová, I. D. Kivlichan, T. Menke, B. Peropadre, N. P. Sawaya, *et al.*, Quantum chemistry in the age of quantum computing, *Chem. Rev.* **119**, 10856 (2019).
- [209] A. M. Childs and R. Kothari, Limitations on the simulation of non-sparse Hamiltonians, *Quant. Info. Comput.* **10** (2009).
- [210] J. Kempe, Quantum random walks: an introductory overview, *Contemp. Phys.* **44**, 307 (2003).
- [211] S. E. Venegas-Andraca, Quantum walks: a comprehensive review, *Quantum Inf. Process.* **11**, 1015 (2012).
- [212] D. W. Berry and A. M. Childs, Black-box Hamiltonian simulation and unitary implementation, *Quant. Info. Comput.* **10** (2009).
- [213] A. M. Childs and R. Kothari, Simulating sparse Hamiltonians with star decompositions, in *Theory of Quantum Computation, Communication, and Cryptography* (Springer, 2010) pp. 94–103.
- [214] A. M. Childs, On the relationship between continuous-and discrete-time quantum walks, *Comm. Math. Phys.* **294**, 581 (2010).
- [215] D. W. Berry, A. M. Childs, R. Cleve, R. Kothari, and R. D. Somma, Exponential improvement in precision for simulating sparse Hamiltonians, in *Proc. ACM* (2014) pp. 283–292.
- [216] G. H. Low, T. J. Yoder, and I. L. Chuang, Methodology of resonant equiangular composite quantum gates, *Phys. Rev. X* **6**, 041067 (2016).
- [217] G. Brassard and P. Hoyer, An exact quantum polynomial-time algorithm for Simon’s problem, in *Proc. ISTCS* (IEEE, 1997) pp. 12–23.
- [218] L. K. Grover, Quantum computers can search rapidly by using almost any transformation, *Phys. Rev. Lett.* **80**, 4329 (1998).
- [219] G. H. Low and I. L. Chuang, Hamiltonian simulation by uniform spectral amplification, *arXiv preprint arXiv:1707.05391* (2017).
- [220] Y. Dong, X. Meng, K. B. Whaley, and L. Lin, Efficient phase-factor evaluation in quantum signal processing, *Phys. Rev. A* **103**, 042419 (2021).
- [221] J. M. Martyn, Z. M. Rossi, A. K. Tan, and I. L. Chuang, A grand unification of quantum algorithms, *arXiv preprint arXiv:2105.02859* (2021).
- [222] R. Chao, D. Ding, A. Gilyen, C. Huang, and M. Szegedy, Finding angles for quantum signal processing with machine precision, *arXiv preprint arXiv:2003.02831* (2020).
- [223] D. W. Berry, C. Gidney, M. Motta, J. R. McClean, and R. Babbush, Qubitization of arbitrary basis quantum chemistry leveraging sparsity and low rank factorization, *Quantum* **3**, 208 (2019).
- [224] J. Lee, D. Berry, C. Gidney, W. J. Huggins, J. R. McClean, N. Wiebe, and R. Babbush, Even more efficient quantum computations of chemistry through tensor hypercontraction, *arXiv preprint arXiv:2011.03494* (2020).
- [225] V. E. Elfving, B. W. Broer, M. Webber, J. Gavartin, M. D. Halls, K. P. Lorton, and A. Bochevarov, How will quantum computers provide an industrially relevant computational advantage in quantum chemistry?, *arXiv preprint arXiv:2009.12472* (2020).
- [226] V. von Burg, G. H. Low, T. Häner, D. S. Steiger, M. Reiher, M. Roetteler, and M. Troyer, Quantum computing enhanced computational catalysis, *arXiv preprint arXiv:2007.14460* (2020).

- [227] D. W. Berry, M. Kieferová, A. Scherer, Y. R. Sanders, G. H. Low, N. Wiebe, C. Gidney, and R. Babbush, Improved techniques for preparing eigenstates of fermionic hamiltonians, *npj Quantum Inf* **4**, 1 (2018).
- [228] D. Poulin, A. Kitaev, D. S. Steiger, M. B. Hastings, and M. Troyer, Quantum algorithm for spectral measurement with a lower gate count, *Phys. Rev. Lett* **121**, 010501 (2018).
- [229] M. Hentschel, R. Kienberger, C. Spielmann, G. A. Reider, N. Milosevic, T. Brabec, P. Corkum, U. Heinzmann, M. Drescher, and F. Krausz, Attosecond metrology, *Nature* **414**, 509 (2001).
- [230] R. Kienberger, M. Hentschel, M. Uiberacker, C. Spielmann, M. Kitzler, A. Scrinzi, M. Wieland, T. Westerwalbesloh, U. Kleineberg, U. Heinzmann, *et al.*, Steering attosecond electron wave packets with light, *Science* **297**, 1144 (2002).
- [231] P. H. Bucksbaum, Ultrafast control, *Nature* **421**, 593 (2003).
- [232] A. Föhlisch, P. Feulner, F. Hennies, A. Fink, D. Menzel, D. Sánchez-Portal, P. M. Echenique, and W. Wurth, Direct observation of electron dynamics in the attosecond domain, *Nature* **436**, 373 (2005).
- [233] T. Klamroth, Laser-driven electron transfer through metal-insulator-metal contacts: Time-dependent configuration interaction singles calculations for a jellium model, *Phys. Rev. B* **68**, 245421 (2003).
- [234] P. Saalfrank, T. Klamroth, C. Huber, and P. Krause, Laser-driven electron dynamics at interfaces, *Isr. J. Chem* **45**, 205 (2005).
- [235] P. Krause, T. Klamroth, and P. Saalfrank, Time-dependent configuration-interaction calculations of laser-pulse-driven many-electron dynamics: Controlled dipole switching in lithium cyanide, *J. Chem. Phys* **123**, 074105 (2005).
- [236] P. Krause, T. Klamroth, and P. Saalfrank, Molecular response properties from explicitly time-dependent configuration interaction methods, *J. Chem. Phys* **127**, 034107 (2007).
- [237] M. Nest, T. Klamroth, and P. Saalfrank, The multiconfiguration time-dependent Hartree–Fock method for quantum chemical calculations, *J. Chem. Phys* **122**, 124102 (2005).
- [238] A. J. Daley, C. Kollath, U. Schollwöck, and G. Vidal, Time-dependent density-matrix renormalization-group using adaptive effective Hilbert spaces, *J. Stat. Mech* **2004**, P04005 (2004).
- [239] U. Schollwöck, The density-matrix renormalization group in the age of matrix product states, *Ann. Phys* **326**, 96 (2011).
- [240] X. Xie, Y. Liu, Y. Yao, U. Schollwöck, C. Liu, and H. Ma, Time-dependent density matrix renormalization group quantum dynamics for realistic chemical systems, *J. Chem. Phys* **151**, 224101 (2019).
- [241] N. E. Dahlen and R. van Leeuwen, Solving the Kadanoff-Baym equations for inhomogeneous systems: application to atoms and molecules, *Phys. Rev. Lett* **98**, 153004 (2007).
- [242] R. Somma, G. Ortiz, E. Knill, and J. Gubernatis, Quantum Simulations of Physics Problems, *Proc. SPIE* **5105**, 96 (2003).
- [243] A. Chiesa, F. Tacchino, M. Grossi, P. Santini, I. Tavernelli, D. Gerace, and S. Carretta, Quantum hardware simulating four-dimensional inelastic neutron scattering, *Nat. Phys.* **15**, 455 (2019).
- [244] A. Francis, J. K. Freericks, and A. F. Kemper, Quantum computation of magnon spectra, *Phys. Rev. B* **101**, 014411 (2020).
- [245] S.-N. Sun, M. Motta, R. N. Tazhigulov, A. T. Tan, G. K.-L. Chan, and A. J. Minnich, Quantum computation of finite-temperature static and dynamical properties of spin systems using quantum imaginary time evolution, *Phys. Rev. X Quantum* **2**, 010317 (2021).
- [246] J. von Neumann, *Mathematical Foundations of Quantum Mechanics* (Princeton University Press, 1955).
- [247] R. Cleve, A. Ekert, C. Macchiavello, and M. Mosca, Quantum algorithms revisited, *Proc. Roy. Soc. London A, Math. Phys. Sci* **454**, 339 (1998).
- [248] A. Y. Kitaev, Quantum measurements and the Abelian stabilizer problem, *arXiv quant-ph/9511026* (1995).
- [249] B. P. Lanyon, J. D. Whitfield, G. G. Gillett, M. E. Goggin, M. P. Almeida, I. Kassal, J. D. Biamonte, M. Mohseni, B. J. Powell, M. Barbieri, *et al.*, Towards quantum chemistry on a quantum computer, *Nat. Chem* **2**, 106 (2010).
- [250] P. J. O’Malley, R. Babbush, I. D. Kivlichan, J. Romero, J. R. McClean, R. Barends, J. Kelly, P. Roushan, A. Tranter, N. Ding, *et al.*, Scalable quantum simulation of molecular energies, *Phys. Rev. X* **6**, 031007 (2016).
- [251] T. E. O’Brien, B. Tarasinski, and B. M. Terhal, Quantum phase estimation of multiple eigenvalues for small-scale (noisy) experiments, *New J. Phys* **21**, 023022 (2019).
- [252] P. M. Cruz, G. Catarina, R. Gautier, and J. Fernández-Rossier, Optimizing quantum phase estimation for the simulation of Hamiltonian eigenstates, *Quant. Sci. Tech* **5**, 044005 (2020).
- [253] R. B. Griffiths and C.-S. Niu, Semiclassical Fourier transform for quantum computation, *Phys. Rev. Lett* **76**, 3228 (1996).
- [254] M. Dobšíček, G. Johansson, V. Shumeiko, and G. Wendin, Arbitrary accuracy iterative quantum phase estimation algorithm using a single ancillary qubit: A two-qubit benchmark, *Phys. Rev. A* **76**, 030306 (2007).
- [255] K. M. Svore, M. B. Hastings, and M. Freedman, Faster phase estimation, *Quant. Info. Comput* **14** (2013).
- [256] R. D. Somma, Quantum eigenvalue estimation via time series analysis, *New J. Phys* **21**, 123025 (2019).
- [257] H. Mohammadbagherpoor, Y.-H. Oh, P. Dreher, A. Singh, X. Yu, and A. J. Rindos, An improved implementation approach for quantum phase estimation on quantum computers, in *Proc. ICRC* (IEEE, 2019) pp. 1–9.
- [258] M. Born and V. Fock, Beweis des adiabatensatzes, *Zeit. Phys* **51**, 165 (1928).
- [259] T. Kato, On the adiabatic theorem of quantum mechanics, *J. Phys. Soc. Jpn* **5**, 435 (1950).
- [260] A. Messiah, *Quantum mechanics: volume II* (North-Holland Publishing Company Amsterdam, 1962).
- [261] J. E. Avron and A. Elgart, Adiabatic theorem without a gap condition, *Comm. Math. Phys* **203**, 445 (1999).
- [262] S. Teufel, *Adiabatic perturbation theory in quantum dynamics* (Springer, 2003).
- [263] S. P. Jordan, *Quantum computation beyond the circuit model*, Ph.D. thesis, Massachusetts Institute of Technology (2008).
- [264] E. Farhi, J. Goldstone, S. Gutmann, and M. Sipser, Quantum computation by adiabatic evolution, *arXiv quant-ph/0001106* (2000).

- [265] E. Farhi, J. Goldstone, S. Gutmann, J. Lapan, A. Lundgren, and D. Preda, A quantum adiabatic evolution algorithm applied to random instances of an NP-complete problem, *Science* **292**, 472 (2001).
- [266] J. Du, N. Xu, X. Peng, P. Wang, S. Wu, and D. Lu, Nmr implementation of a molecular hydrogen quantum simulation with adiabatic state preparation, *Phys. Rev. Lett* **104**, 030502 (2010).
- [267] R. Babbush, P. J. Love, and A. Aspuru-Guzik, Adiabatic quantum simulation of quantum chemistry, *Sci. Rep* **4**, 6603 (2014).
- [268] L. Veis and J. Pittner, Adiabatic state preparation study of methylene, *J. Chem. Phys* **140**, 214111 (2014).
- [269] D. Nagaj and S. Mozes, New construction for a QMA complete three-local Hamiltonian, *J. Math. Phys* **48**, 072104 (2007).
- [270] D. Aharonov, W. Van Dam, J. Kempe, Z. Landau, S. Lloyd, and O. Regev, Adiabatic quantum computation is equivalent to standard quantum computation, *SIAM Rev* **50**, 755 (2008).
- [271] A. M. Childs, E. Farhi, and J. Preskill, Robustness of adiabatic quantum computation, *Phys. Rev. A* **65**, 012322 (2001).
- [272] W. Van Dam, M. Mosca, and U. Vazirani, How powerful is adiabatic quantum computation?, in *Proc. FOCS* (IEEE, 2001) pp. 279–287.
- [273] S. Jansen, M.-B. Ruskai, and R. Seiler, Bounds for the adiabatic approximation with applications to quantum computation, *J. Math. Phys* **48**, 102111 (2007).
- [274] M. Cerezo, A. Arrasmith, R. Babbush, S. C. Benjamin, S. Endo, K. Fujii, J. R. McClean, K. Mitarai, X. Yuan, L. Cincio, et al., Variational quantum algorithms, *Nat. Rev. Phys* , 1 (2021).
- [275] K. Bharti, A. Cervera-Lierta, T. H. Kyaw, T. Haug, S. Alperin-Lea, A. Anand, M. Degroote, H. Heimonen, J. S. Kottmann, T. Menke, et al., Noisy intermediate-scale quantum (nisq) algorithms, *arXiv preprint arXiv:2101.08448* (2021).
- [276] E. Farhi, J. Goldstone, and S. Gutmann, A quantum approximate optimization algorithm, *arXiv preprint arXiv:1411.4028* (2014).
- [277] A. Peruzzo, J. McClean, P. Shadbolt, M.-H. Yung, X.-Q. Zhou, P. J. Love, A. Aspuru-Guzik, and J. L. O’Brien, A variational eigenvalue solver on a photonic quantum processor, *Nat. Commun* **5**, 4213 (2014).
- [278] J. R. McClean, J. Romero, R. Babbush, and A. Aspuru-Guzik, The theory of variational hybrid quantum-classical algorithms, *New J. Phys* **18**, 023023 (2016).
- [279] J. Romero, R. Babbush, J. R. McClean, C. Hempel, P. J. Love, and A. Aspuru-Guzik, Strategies for quantum computing molecular energies using the unitary coupled cluster Ansatz, *Quantum Sci. Technol.* **4**, 014008 (2018).
- [280] R. M. Parrish, E. G. Hohenstein, P. L. McMahon, and T. J. Martinez, Hybrid quantum/classical derivative theory: analytical gradients and excited-state dynamics for the multistate contracted variational quantum eigensolver, *arXiv preprint arXiv:1906.08728* (2019).
- [281] M. Schuld, V. Bergholm, C. Gogolin, J. Izaac, and N. Killoran, Evaluating analytic gradients on quantum hardware, *Phys. Rev. A* **99**, 032331 (2019).
- [282] K. Mitarai, Y. O. Nakagawa, and W. Mizukami, Theory of analytical energy derivatives for the variational quantum eigensolver, *Phys. Rev. Research* **2**, 013129 (2020).
- [283] J. S. Kottmann, A. Anand, and A. Aspuru-Guzik, A feasible approach for automatically differentiable unitary coupled-cluster on quantum computers, *Chem. Sci* **12**, 3497 (2021).
- [284] G. G. Guerreschi and M. Smelyanskiy, Practical optimization for hybrid quantum-classical algorithms, *arXiv preprint arXiv:1701.01450* (2017).
- [285] J. C. Spall, *Introduction to stochastic search and optimization: estimation, simulation, and control* (John Wiley & Sons, 2005).
- [286] T. Hirokami, Y. Maeda, and H. Tsukada, Parameter estimation using simultaneous perturbation stochastic approximation, *Electr. Eng. Jpn* **154**, 30 (2006).
- [287] S. Bhatnagar, H. Prasad, and L. Prashanth, *Stochastic recursive algorithms for optimization: simultaneous perturbation methods* (Springer, 2013).
- [288] D. P. Kingma and J. Ba, Adam: A method for stochastic optimization, *arXiv preprint arXiv:1412.6980* (2014).
- [289] J. Stokes, J. Izaac, N. Killoran, and G. Carleo, Quantum natural gradient, *Quantum* **4**, 269 (2020).
- [290] A. Kandala, A. Mezzacapo, K. Temme, M. Takita, M. Brink, J. M. Chow, and J. M. Gambetta, Hardware-efficient variational quantum eigensolver for small molecules and quantum magnets, *Nature* **549**, 242 (2017).
- [291] J. R. McClean, S. Boixo, V. N. Smelyanskiy, R. Babbush, and H. Neven, Barren plateaus in quantum neural network training landscapes, *Nat. Commun* **9**, 1 (2018).
- [292] V. Akshay, H. Philathong, M. Morales, and J. Biamonte, Reachability deficits in quantum approximate optimization, *Phys. Rev. Lett* **124**, 090504 (2020).
- [293] R. J. Bartlett, S. A. Kucharski, and J. Noga, Alternative coupled-cluster Ansätze II. The unitary coupled-cluster method, *Chem. Phys. Lett* **155**, 133 (1989).
- [294] N. Moll, P. Barkoutsos, L. S. Bishop, J. M. Chow, A. Cross, D. J. Egger, S. Filipp, A. Fuhrer, J. M. Gambetta, M. Ganzhorn, A. Kandala, A. Mezzacapo, P. Müller, W. Riess, G. Salis, J. Smolin, I. Tavernelli, and K. Temme, Quantum optimization using variational algorithms on near-term quantum devices, *Quantum Sci. Technol.* **3**, 030503 (2018).
- [295] T. Albash and D. A. Lidar, Adiabatic quantum computation, *Rev. Mod. Phys* **90**, 015002 (2018).
- [296] F. A. Evangelista, G. K.-L. Chan, and G. E. Scuseria, Exact parameterization of fermionic wave functions via unitary coupled cluster theory, *J. Chem. Phys* **151**, 244112 (2019).
- [297] P. K. Barkoutsos, J. F. Gonthier, I. Sokolov, N. Moll, G. Salis, A. Fuhrer, M. Ganzhorn, D. J. Egger, M. Troyer, A. Mezzacapo, S. Filipp, and I. Tavernelli, Quantum algorithms for electronic structure calculations: particle-hole Hamiltonian and optimized wave-function expansions, *Phys. Rev. A* **98**, 022322 (2018).

- [298] I. G. Ryabinkin, T.-C. Yen, S. N. Genin, and A. F. Izmaylov, Qubit coupled cluster method: a systematic approach to quantum chemistry on a quantum computer, *J. Chem. Theory Comput.* **14**, 6317 (2018).
- [299] H. R. Grimsley, S. E. Economou, E. Barnes, and N. J. Mayhall, An adaptive variational algorithm for exact molecular simulations on a quantum computer, *Nat. Commun.* **10**, 3007 (2019).
- [300] H. L. Tang, V. Shkolnikov, G. S. Barron, H. R. Grimsley, N. J. Mayhall, E. Barnes, and S. E. Economou, Qubit-ADAPT-VQE: an adaptive algorithm for constructing hardware-efficient Ansätze on a quantum processor, *Phys. Rev. X Quantum* **2**, 020310 (2021).
- [301] S. McArdle, T. Jones, S. Endo, Y. Li, S. C. Benjamin, and X. Yuan, Variational Ansatz-based quantum simulation of imaginary time evolution, *npj Quantum Inf.* **5**, 1 (2019).
- [302] X. Yuan, S. Endo, Q. Zhao, Y. Li, and S. C. Benjamin, Theory of variational quantum simulation, *Quantum* **3**, 191 (2019).
- [303] C. Lanczos, An iteration method for the solution of the eigenvalue problem of linear differential and integral operators, *J. Res. Natl. Bur. Stand.* **45**, 2133 (1950).
- [304] E. R. Davidson, The iterative calculation of a few of the lowest eigenvalues and corresponding eigenvectors of large real-symmetric matrices, *J. Comp. Phys.* **17**, 87 (1975).
- [305] R. B. Morgan and D. S. Scott, Generalizations of Davidson's method for computing eigenvalues of sparse symmetric matrices, *SIAM J. Sci. Comput.* **7**, 817 (1986).
- [306] J. R. McClean, M. E. Kimchi-Schwartz, J. Carter, and W. A. De Jong, Hybrid quantum-classical hierarchy for mitigation of decoherence and determination of excited states, *Phys. Rev. A* **95**, 042308 (2017).
- [307] J. I. Colless, V. V. Ramasesh, D. Dahmen, M. S. Blok, M. Kimchi-Schwartz, J. McClean, J. Carter, W. De Jong, and I. Siddiqi, Computation of molecular spectra on a quantum processor with an error-resilient algorithm, *Phys. Rev. X* **8**, 011021 (2018).
- [308] W. J. Huggins, J. Lee, U. Baek, B. O'Gorman, and K. B. Whaley, A non-orthogonal variational quantum eigensolver, *New J. Phys.* **22**, 073009 (2020).
- [309] M. Motta, C. Sun, A. T. Tan, M. J. O'Rourke, E. Ye, A. J. Minnich, F. G. Brandão, and G. K.-L. Chan, Determining eigenstates and thermal states on a quantum computer using quantum imaginary time evolution, *Nat. Phys.* **16**, 205 (2020).
- [310] P. J. Ollitrault, A. Kandala, C.-F. Chen, P. K. Barkoutsos, A. Mezzacapo, M. Pistoia, S. Sheldon, S. Woerner, J. M. Gambetta, and I. Tavernelli, Quantum equation of motion for computing molecular excitation energies on a noisy quantum processor, *Phys. Rev. Research* **2**, 043140 (2020).
- [311] R. M. Parrish and P. L. McMahon, Quantum filter diagonalization: quantum eigendecomposition without full quantum phase estimation, *arXiv preprint arXiv:1909.08925* (2019).
- [312] N. H. Stair, R. Huang, and F. A. Evangelista, A multireference quantum Krylov algorithm for strongly correlated electrons, *J. Chem. Theory Comput.* **16**, 2236 (2020).
- [313] F. Jamet, A. Agarwal, C. Lupo, D. E. Browne, C. Weber, and I. Runger, Krylov variational quantum algorithm for first principles materials simulations, *arXiv preprint arXiv:2105.13298* (2021).
- [314] D. Aharonov, V. Jones, and Z. Landau, A polynomial quantum algorithm for approximating the Jones polynomial, *Algorithmica* **55**, 395 (2009).
- [315] D. Neuhauser, Bound state eigenfunctions from wave packets: Time-energy resolution, *J. Chem. Phys.* **93**, 2611 (1990).
- [316] D. Neuhauser, Circumventing the Heisenberg principle: a rigorous demonstration of filter-diagonalization on a LiCN model, *J. Chem. Phys.* **100**, 5076 (1994).
- [317] D. J. Rowe, Equations-of-Motion Method and the Extended Shell Model, *Rev. Mod. Phys.* **40**, 153 (1968).
- [318] M. Ganzhorn, D. Egger, P. Barkoutsos, P. Ollitrault, G. Salis, N. Moll, M. Roth, A. Fuhrer, P. Mueller, S. Woerner, I. Tavernelli, and S. Filipp, Gate-efficient simulation of molecular eigenstates on a quantum computer, *Phys. Rev. Appl.* **11**, 044092 (2019).
- [319] Q. Gao, G. O. Jones, M. Motta, M. Sugawara, H. C. Watanabe, T. Kobayashi, E. Watanabe, Y.-y. Ohnishi, H. Nakamura, and N. Yamamoto, Applications of quantum computing for investigations of electronic transitions in phenylsulfonyl-carbazole TADF emitters, *npj Comput. Mater.* **7**, 1 (2021).
- [320] S. Barison, D. E. Galli, and M. Motta, Quantum simulations of molecular systems with intrinsic atomic orbitals, *arXiv preprint arXiv:2011.08137* (2020).
- [321] K. Yeter Aydeniz, G. Siopsis, and R. C. Pooser, Scattering in the ising model with the quantum Lanczos algorithm, *New J. Phys.* **23**, 043033 (2021).
- [322] N. Gomes, F. Zhang, N. F. Berthelsen, C.-Z. Wang, K.-M. Ho, P. P. Orth, and Y. Yao, Efficient step-merged quantum imaginary time evolution algorithm for quantum chemistry, *J. Chem. Theory Comput.* **16**, 6256–6266 (2020).
- [323] K. Yeter-Aydeniz, R. C. Pooser, and G. Siopsis, Practical quantum computation of chemical and nuclear energy levels using quantum imaginary time evolution and Lanczos algorithms, *npj Quantum Inf.* **6**, 63 (2020).
- [324] H. Kamakari, S.-N. Sun, M. Motta, and A. J. Minnich, Digital quantum simulation of open quantum systems using quantum imaginary time evolution, *arXiv preprint arXiv:2104.07823* (2021).
- [325] B. Cooper and P. J. Knowles, Benchmark studies of variational, unitary and extended coupled cluster methods, *J. Chem. Phys.* **133**, 234102 (2010).
- [326] G. Harsha, T. Shiozaki, and G. E. Scuseria, On the difference between variational and unitary coupled cluster theories, *J. Chem. Phys.* **148**, 044107 (2018).
- [327] J. Lee, W. J. Huggins, M. Head-Gordon, and K. B. Whaley, Generalized unitary coupled cluster wave functions for quantum computation, *J. Chem. Theory Comput.* **15**, 311 (2018).

- [328] B. O'Gorman, W. J. Huggins, E. G. Rieffel, and K. B. Whaley, Generalized swap networks for near-term quantum computing, *arXiv preprint arXiv:1905.05118* (2019).
- [329] G.-L. R. Anselmetti, D. Wierichs, C. Gogolin, and R. M. Parrish, Local, expressive, quantum-number-preserving VQE Ansätze for fermionic systems, *arXiv preprint arXiv:2104.05695* (2021).
- [330] B. T. Gard, L. Zhu, G. S. Barron, N. J. Mayhall, S. E. Economou, and E. Barnes, Efficient symmetry-preserving state preparation circuits for the variational quantum eigensolver algorithm, *npj Quantum Inf* **6**, 1 (2020).
- [331] O. Higgott, D. Wang, and S. Brierley, Variational quantum computation of excited states, *Quantum* **3**, 156 (2019).
- [332] Y. Ibe, Y. O. Nakagawa, N. Earnest, T. Yamamoto, K. Mitarai, Q. Gao, and T. Kobayashi, Calculating transition amplitudes by variational quantum deflation, *arXiv preprint arXiv:2002.11724* (2020).
- [333] I. O. Sokolov, P. K. Barkoutsos, P. J. Ollitrault, D. Greenberg, J. Rice, M. Pistoia, and I. Tavernelli, Quantum orbital-optimized unitary coupled cluster methods in the strongly correlated regime: can quantum algorithms outperform their classical equivalents?, *J. Chem. Phys* **152**, 124107 (2020).
- [334] J. E. Rice, T. P. Gujarati, M. Motta, T. Y. Takeshita, E. Lee, J. A. Latone, and J. M. Garcia, Quantum computation of dominant products in lithium–sulfur batteries, *J. Chem. Phys* **154**, 134115 (2021).
- [335] I. O. Sokolov, P. K. Barkoutsos, L. Moeller, P. Suchsland, G. Mazzola, and I. Tavernelli, Microcanonical and finite-temperature ab initio molecular dynamics simulations on quantum computers, *Phys. Rev. Research* **3**, 013125 (2021).
- [336] K. Choudhary, Quantum computation for predicting electron and phonon properties of solids, *J. Phys Cond. Mat* **33**, 385501 (2021).
- [337] H. Ma, M. Govoni, and G. Galli, Quantum simulations of materials on near-term quantum computers, *npj Comput. Mater* **6**, 1 (2020).
- [338] S. McArdle and D. P. Tew, Improving the accuracy of quantum computational chemistry using the transcorrelated method, *arXiv preprint arXiv:2006.11181* (2020).
- [339] N. C. Rubin, A hybrid classical/quantum approach for large-scale studies of quantum systems with density matrix embedding theory, *arXiv preprint arXiv:1610.06910* (2016).
- [340] D. Dhawan, M. Metcalf, and D. Zgid, Dynamical self-energy mapping (DSEM) for quantum computing, *arXiv preprint arXiv:2010.05441* (2020).
- [341] M. Metcalf, N. P. Bauman, K. Kowalski, and W. A. De Jong, Resource-efficient chemistry on quantum computers with the variational quantum eigensolver and the double unitary coupled-cluster approach, *J. Chem. Theory Comput* **16**, 6165 (2020).
- [342] Y. Kawashima, M. P. Coons, Y. Nam, E. Lloyd, S. Matsuura, A. J. Garza, S. Johri, L. Huntington, V. Senicourt, A. O. Maksymov, *et al.*, Efficient and accurate electronic structure simulation demonstrated on a trapped-ion quantum computer, *arXiv preprint arXiv:2102.07045* (2021).
- [343] M. Rossmannek, P. K. Barkoutsos, P. J. Ollitrault, and I. Tavernelli, Quantum hf/dft-embedding algorithms for electronic structure calculations: scaling up to complex molecular systems, *J. Chem. Phys* **154**, 114105 (2021).
- [344] N. H. Stair and F. A. Evangelista, Simulating many-body systems with a projective quantum eigensolver, *Phys. Rev. X Quantum* **2**, 030301 (2021).
- [345] K. Kuroiwa and Y. O. Nakagawa, Penalty methods for a variational quantum eigensolver, *Phys. Rev. Research* **3**, 013197 (2021).
- [346] I. G. Ryabinkin, S. N. Genin, and A. F. Izmaylov, Constrained variational quantum eigensolver: Quantum computer search engine in the fock space, *J. Chem. Theory Comput* **15**, 249 (2018).
- [347] J. F. Gonthier, M. D. Radin, C. Buda, E. J. Doskocil, C. M. Abuan, and J. Romero, Identifying challenges towards practical quantum advantage through resource estimation: the measurement roadblock in the variational quantum eigensolver, *arXiv preprint arXiv:2012.04001* (2020).
- [348] D. Wecker, M. B. Hastings, and M. Troyer, Progress towards practical quantum variational algorithms, *Phys. Rev. A* **92**, 042303 (2015).
- [349] A. Jena, S. Genin, and M. Mosca, Pauli partitioning with respect to gate sets, *arXiv preprint arXiv:1907.07859* (2019).
- [350] A. F. Izmaylov, T.-C. Yen, R. A. Lang, and V. Verteletskyi, Unitary partitioning approach to the measurement problem in the variational quantum eigensolver method, *J. Chem. Theory Comput* **16**, 190 (2019).
- [351] J. M. Kübler, A. Arrasmith, L. Cincio, and P. J. Coles, An adaptive optimizer for measurement-frugal variational algorithms, *Quantum* **4**, 263 (2020).
- [352] A. Zhao, A. Tranter, W. M. Kirby, S. F. Ung, A. Miyake, and P. J. Love, Measurement reduction in variational quantum algorithms, *Phys. Rev. A* **101**, 062322 (2020).
- [353] G. Wang, D. E. Koh, P. D. Johnson, and Y. Cao, Minimizing estimation runtime on noisy quantum computers, *Phys. Rev. X Quantum* **2**, 010346 (2021).
- [354] G. Torlai, G. Mazzola, G. Carleo, and A. Mezzacapo, Precise measurement of quantum observables with neural-network estimators, *Phys. Rev. Research* **2**, 022060 (2020).
- [355] C. Hadfield, S. Bravyi, R. Raymond, and A. Mezzacapo, Measurements of quantum hamiltonians with locally-biased classical shadows, *arXiv preprint arXiv:2006.15788* (2020).
- [356] S. Hillmich, C. Hadfield, R. Raymond, A. Mezzacapo, and R. Wille, Decision diagrams for quantum measurements with shallow circuits, *arXiv preprint arXiv:2105.06932* (2021).
- [357] S. Barison, F. Vicentini, and G. Carleo, An efficient quantum algorithm for the time evolution of parameterized circuits, *arXiv preprint arXiv:2101.04579* (2021).
- [358] M. Benedetti, M. Fiorentini, and M. Lubasch, Hardware-efficient variational quantum algorithms for time evolution, *Phys. Rev. Research* **3**, 033083 (2021).

- [359] M. Foss-Feig, D. Hayes, J. M. Dreiling, C. Figgatt, J. P. Gaebler, S. A. Moses, J. M. Pino, and A. C. Potter, Holographic quantum algorithms for simulating correlated spin systems, *Phys. Rev. Research* **3**, 033002 (2021).
- [360] J. Kattemölle and J. van Wezel, Variational quantum eigensolver for the heisenberg antiferromagnet on the kagome lattice, *arXiv preprint arXiv:2108.02175* (2021).
- [361] J.-N. Boyn, A. O. Lykhin, S. E. Smart, L. Gagliardi, and D. A. Mazziotti, Quantum-classical hybrid algorithm for the simulation of all-electron correlation, *arXiv preprint arXiv:2106.11972* (2021).
- [362] D. A. Mazziotti, S. E. Smart, and A. R. Mazziotti, Quantum simulation of molecules without fermionic encoding of the wave function, *arXiv preprint arXiv:2101.11607* (2021).
- [363] IBM Quantum, Quantum computing services, <https://www.ibm.com/quantum-computing/> (2020).
- [364] Rigetti computing, Quantum cloud services, <https://qcs.rigetti.com/dashboard> (2020).
- [365] R. S. Smith, M. J. Curtis, and W. J. Zeng, A practical quantum instruction set architecture, *arXiv preprint arXiv:1608.03355* (2016).
- [366] H. Abraham *et al.*, *Qiskit: An open-source framework for quantum computing* (2019).
- [367] J. R. McClean, N. C. Rubin, K. J. Sung, I. D. Kivlichan, X. Bonet-Monroig, Y. Cao, C. Dai, E. S. Fried, C. Gidney, B. Gimby, *et al.*, Openfermion: the electronic structure package for quantum computers, *Quant. Sci. Tech* **5**, 034014 (2020).
- [368] D. Maslov, Basic circuit compilation techniques for an ion-trap quantum machine, *New J. Phys* **19**, 023035 (2017).
- [369] Y. Nam, J.-S. Chen, N. C. Pisenti, K. Wright, C. Delaney, D. Maslov, K. R. Brown, S. Allen, J. M. Amini, J. Apisdorf, *et al.*, Ground-state energy estimation of the water molecule on a trapped-ion quantum computer, *npj Quantum Inf* **6**, 1 (2020).
- [370] Q. Gao, H. Nakamura, T. P. Gujarati, G. O. Jones, J. E. Rice, S. P. Wood, M. Pistoia, J. M. Garcia, and N. Yamamoto, Computational investigations of the lithium superoxide dimer rearrangement on noisy quantum devices, *J. Phys. Chem. A* **125**, 1827 (2021).
- [371] A. J. McCaskey, Z. P. Parks, J. Jakowski, S. V. Moore, T. D. Morris, T. S. Humble, and R. C. Pooser, Quantum chemistry as a benchmark for near-term quantum computers, *npj Quantum Inf* **5**, 1 (2019).
- [372] P. Krantz, M. Kjaergaard, F. Yan, T. P. Orlando, S. Gustavsson, and W. D. Oliver, A quantum engineer's guide to superconducting qubits, *Appl. Phys. Rev* **6**, 021318 (2019).
- [373] M. H. Devoret, A. Wallraff, and J. M. Martinis, Superconducting qubits: A short review, *cond-mat/0411174* (2004).
- [374] C. D. Bruzewicz, J. Chiaverini, R. McConnell, and J. M. Sage, Trapped-ion quantum computing: Progress and challenges, *Appl. Phys. Rev* **6**, 021314 (2019).
- [375] K. R. Brown, J. Chiaverini, J. M. Sage, and H. Häffner, Materials challenges for trapped-ion quantum computers, *Nat. Rev. Mater.*, 1 (2021).
- [376] C. Rigetti and M. Devoret, Fully microwave-tunable universal gates in superconducting qubits with linear couplings and fixed transition frequencies, *Phys. Rev. B* **81**, 134507 (2010).
- [377] J. M. Chow, A. D. Corcoles, J. M. Gambetta, C. Rigetti, B. R. Johnson, J. A. Smolin, J. R. Rozen, G. A. Keefe, M. B. Rothwell, M. B. Ketchen, *et al.*, Simple all-microwave entangling gate for fixed-frequency superconducting qubits, *Phys. Rev. Lett* **107**, 080502 (2011).
- [378] F. Yan, P. Krantz, Y. Sung, M. Kjaergaard, D. L. Campbell, T. P. Orlando, S. Gustavsson, and W. D. Oliver, Tunable coupling scheme for implementing high-fidelity two-qubit gates, *Phys. Rev. Appl* **10**, 054062 (2018).
- [379] A. Peres, Reversible logic and quantum computers, *Phys. Rev. A* **32**, 3266 (1985).
- [380] P. W. Shor, Scheme for reducing decoherence in quantum computer memory, *Phys. Rev. A* **52**, R2493 (1995).
- [381] A. M. Steane, Error correcting codes in quantum theory, *Phys. Rev. Lett* **77**, 793 (1996).
- [382] A. G. Fowler, M. Mariantoni, J. M. Martinis, and A. N. Cleland, Surface codes: towards practical large-scale quantum computation, *Phys. Rev. A* **86**, 032324 (2012).
- [383] J. Preskill, Quantum computing in the NISQ era and beyond, *Quantum* **2**, 79 (2018).
- [384] A. Kandala, K. Temme, A. D. Corcoles, A. Mezzacapo, J. M. Chow, and J. M. Gambetta, Extending the computational reach of a noisy superconducting quantum processor, *Nature* **567**, 491 (2018).
- [385] F. B. Maciejewski, Z. Zimborás, and M. Oszmaniec, Mitigation of readout noise in near-term quantum devices by classical post-processing based on detector tomography, *Quantum* **4**, 257 (2020).
- [386] K. Temme, S. Bravyi, and J. M. Gambetta, Error mitigation for short-depth quantum circuits, *Phys. Rev. Lett* **119**, 180509 (2017).
- [387] Y. Li and S. C. Benjamin, Efficient variational quantum simulator incorporating active error minimization, *Phys. Rev. X* **7**, 021050 (2017).
- [388] S. Endo, S. C. Benjamin, and Y. Li, Practical quantum error mitigation for near-future applications, *Phys. Rev. X* **8**, 031027 (2018).
- [389] L. F. Richardson, The approximate arithmetical solution by finite differences with an application to stresses in masonry dams, *Philos. Trans. Royal Soc. A* **210**, 307 (1911).
- [390] E. F. Dumitrescu, A. J. McCaskey, G. Hagen, G. R. Jansen, T. D. Morris, T. Papenbrock, R. C. Pooser, D. J. Dean, and P. Lougovski, Cloud quantum computing of an atomic nucleus, *Phys. Rev. Lett* **120**, 210501 (2018).
- [391] M. C. Tran, Y. Su, D. Carney, and J. M. Taylor, Faster digital quantum simulation by symmetry protection, *Phys. Rev. X Quantum* **2**, 010323 (2021).
- [392] W. J. Huggins, J. R. McClean, N. C. Rubin, Z. Jiang, N. Wiebe, K. B. Whaley, and R. Babbush, Efficient and noise resilient measurements for quantum chemistry on near-term quantum computers, *npj Quantum Inf* **7**, 1 (2021).